Corrosion and Tarnish of Dental Alloys

Revised by Spiro Megremis, American Dental Association
Clifton M. Carey, American Dental Association Foundation

DENTAL ALLOY DEVICES serve to restore or align lost or misaligned teeth so that normal biting function and aesthetics can prevail. Alloys are used for direct fillings, crowns, inlays, onlays, bridges, fixed and removable partial dentures, full denture bases, implanted support structures, and wires and brackets for the controlled movement of teeth. In addition to applications calling for cast or wrought alloys, other uses of alloys include soldered assemblies, porcelain fused to metal, and resin bonded to metal restorations.

Dental Alloy Compositions and Properties

Dental Alloy Compositions. The compositions of alloys used to fulfill the diverse applications germane to dentistry include the following elements: Au, Pd, Pt, Ag, Cu, Co, Cr, Ni, Fe, Mo, W, Ti, Zn, In, Ir, Rh, Sn, Ga, Ru, Si, Mn, Be, B, Al, V, C, Ta, Zr, and others. Figures 1 to 6 show a number of typical restorations and appliances fabricated from alloys containing some of these metals.

Compositions for direct filling restorations usually consist of silver-tin-copper-zinc amalgams, although this is rapidly changing with the continued improvement of polymer composites. Pure gold in the form of cohesive foil, mat, or powder is used only in very limited applications.

Alloys for all-alloy cast crown and bridge restorations are usually gold-, silver-, or nickel-base compositions, although iron-base and other alloys have also been used. The gold-base alloys contain silver and copper as principal alloying elements, with smaller additions of palladium, platinum, zinc, indium, and other noble metals as grain refiners. The silver-base alloys contain palladium as a major alloying element, with additions of copper, gold, zinc, indium, and grain refiners. The nickel-base alloys are alloyed with chromium, iron, molybdenum, and other elements.

Alloys for porcelain fused to alloy restorations are gold-, palladium-, nickel-, or cobalt-base compositions. The gold-base alloys are divided into gold-platinum-palladium, gold-palladium-silver, and gold-palladium types. The palladium-base alloys are palladium-silver alloys or palladium-gallium alloys with additions from either copper or cobalt. The nickel- and cobalt-base alloys are alloyed primarily with chromium and with minor additions of molybdenum and other elements. In contrast to alloys for crown and bridge use, alloys fused to porcelain contain low concentrations of oxidizable elements, such as tin; indium; iron; gallium for the noble metal containing alloys; and aluminum, vanadium, and others for the base metal alloys. During the heating cycle, these elements form oxides on the surface of the alloy and combine with the porcelain at the firing temperatures to promote chemical bonding.

Alloys for removable partial dentures are primarily nickel- and cobalt-base compositions and are similar to alloys used for porcelain fused to alloy applications. However, carbon is present in amounts up to 0.3 to 0.4% with the partial denture alloys. Carbon is not added to alloys to be used for porcelain bonding.

Alloys that have found applications for support structures implanted in the lower or upper jaws are composed of cobalt-chromium, nickel-chromium, stainless steel, and titanium and its alloys. Wrought orthodontic wires are composed of stainless steel, cobalt-chromium-nickel, nickel-titanium, and β-titanium alloys. Silver- and gold-alloy solders are used for the joining of components. High-temperature brazing alloys are used for the joining of a number of high fusing temperature alloys. Additional information on noble metals is available in the article "Corrosion of Precious Metals and Alloys" in *Corrosion,* Vol 13B, of the *ASM Handbook*.

Properties. The diversity in available alloys exists so that alloys with specific properties can be used when needed. For example, the mechanical property requirements of alloys used for crown and bridge applications are different from the requirements of alloys used for porcelain fused to alloy restorations. Even though crown and bridge alloys must possess sufficient hardness and rigidity when used in stress-bearing restorations, excessively high strength is a disadvantage for grinding, polishing, and burnishing. Also, excessive wear of the occluding teeth

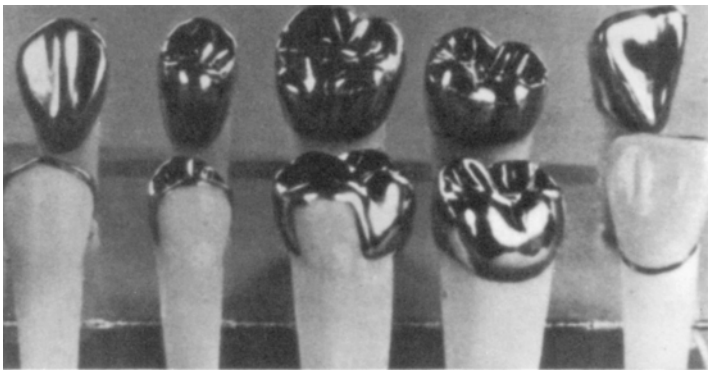

Fig. 1 Various types of crowns. Source: Ref 1

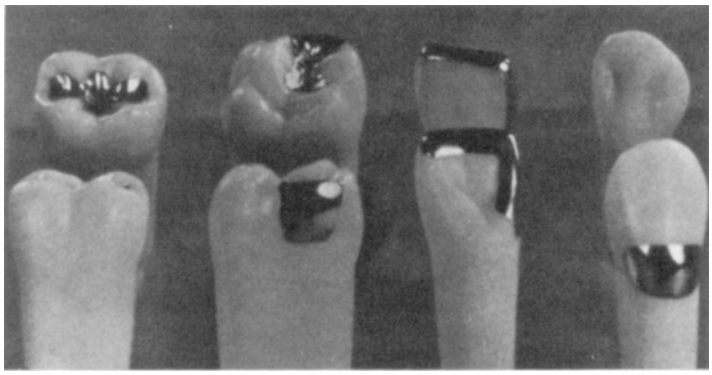

Fig. 2 Various types of inlays. Source: Ref 1

is also likely to occur. Alloys used with porcelain fused to metal restorations are used as substrates for the overlaying porcelain. In this case, the high strength and rigidity of the alloys more closely matches the properties of the porcelain. Also, a higher sag resistance of the alloy at temperatures used for firing the porcelain means less distortion and less retained residual stresses.

Similarly, alloys used for partial denture and implant applications must possess increased mechanical properties for resistances to failures. However, clasps contained within removable partial denture devices are often fabricated from a more ductile alloy, such as a gold-base alloy, than from cobalt-chromium or nickel-chromium alloys. This ensures that the clasps possess suficient ductility for adjustments without breakage from brittle fractures.

Other properties required in specific systems include the matching of the thermal expansion coefficients between porcelain and substrate alloy, negligible setting contractions with the direct filling amalgams, and specific modulus to yield strength ratios with orthodontic wires. Tarnish and corrosion of all dental alloy systems have been and will remain of prime importance.

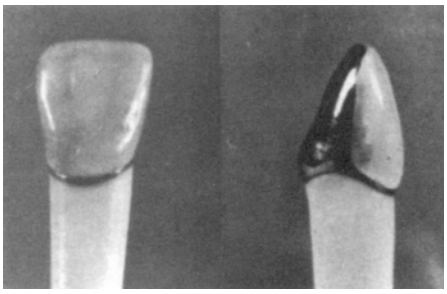

Fig. 3 Porcelain veneer fused to alloy. Source: Ref 1

Tarnish and Corrosion Resistance

Dental alloy devices must possess acceptable corrosion resistance primarily because of safety and efficacy. Aesthetics is also a consideration.

Safety

Dental alloys are required to have acceptable corrosion resistance so that biocompatibility is maintained during the time the metallic components are used (Ref 5–7). No harmful ions or corrosion products can be generated such that toxicological conditions result. The effects of the dental alloys on the oral environment have the capabilities for producing local, remote, or systematic changes that may be short term, long term, or repetitive (tissue sensitization) in nature (Ref 8). Dental alloy-oral environment interactions have the potential for generating such conditions as metallic taste, discoloration of teeth, galvanic pain, oral lesions, cariogenesis, allergic hypersensitive reactions, dermatitis and stomatitis, endodontic failures, dental implant rejection, tumorgenisis, and carcinogenisis. Figure 7 shows a schematic of useful dental anatomy.

Metallic Taste. The symptom of metallic taste has been reported and related to the presence of metallic materials in the mouth (Ref 9). In addition, the release of ions and the formation of products through corrosion, wear, and abrasion can occur simultaneously, which can accelerate the process. Therefore, patients with metallic restorations and with an inclination toward bruxism (the unconscious gritting or grinding of the teeth) are likely to be more susceptible to metallic taste. Although this condition is not as prevalent as it once was when metallic materials with lower corrosion resistances were more often used, metallic taste is still known to occur on occasion.

Discoloration of teeth has occurred mainly with amalgam fillings (Ref 10) and with base alloy screwposts (Ref 11). With amalgams, tin and zinc concentrations have been identified in the dentinal tubules of the discolored areas, while with the screwposts, copper and zinc were

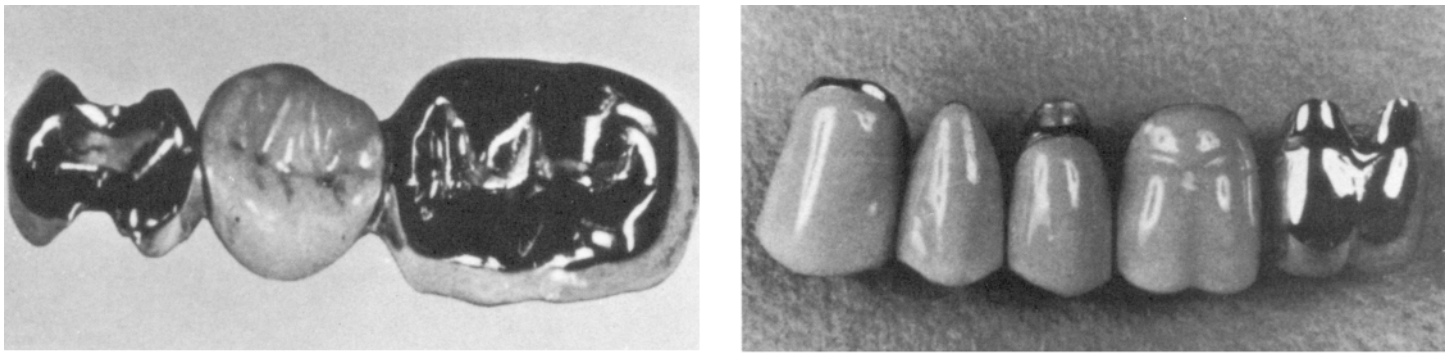

(a) (b)

Fig. 4 Fixed bridges. (a) Three-unit bridge consisting of inlay (left member), onlay (right member), and porcelain fused to alloy pontic (center member). Source: Ref 2. (b) Five-unit bridge consisting of four porcelain fused to alloy members and one crown. Source: Ref 1

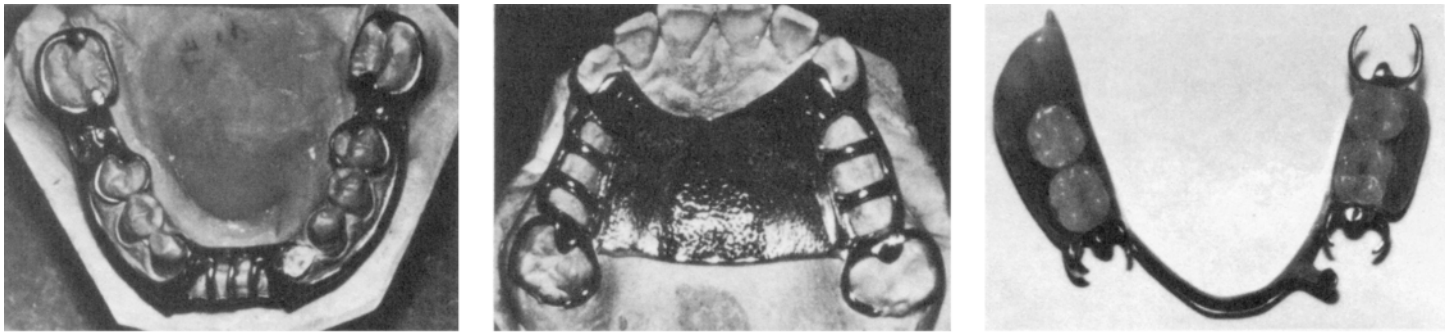

(a) (b) (c)

Fig. 5 Removable partial dentures, (a) lower and (b) upper cobalt-chromium frameworks, and (c) a completed unit in. Source: Ref 3

detached in both the dentin and enamel and the surrounding soft connective tissue. Discoloration is not, however, a definite indicator of the presence of metallic ions.

Galvanic pain has been reported from the contact of dissimilar-alloy restorations, either continuously or intermittently (Ref 9, 12). An electrochemical circuit occurring between the two dissimilar-alloy restorations is short circuited by the contact. In the case of intermittent contact, instantaneous current flows through the external circuit, which is the oral tissues, and may cause pain. The placement of dissimilar-alloy restorations in direct contact is ill advised.

Oral lesions resulting from the metallic prosthesis contacting tissue can be due to physical factors alone (Ref 9). An irritation in the opposing tissues of the oral mucosa can be generated because of the shape and location in the mouth of the prosthesis, as well as its metallurgical properties, such as surface finish, grain size, and microstructural features. Tarnish and corrosion can change the nature of the alloy surface and add to the irritation in the opposing tissues. Microgalvanic currents due to chemical differences of microstructural constituents must also be considered as possible causative factors in traumatizing and damaging tissue. However, no data have related *in vivo* galvanic currents from dental restorations to tissue damage. The released metallic ions from corrosion reactions can interact with the oral tissues to generate redness, swelling, and infection. Oral lesions can then occur. These reactions are discussed in the section "Allergic Hypersensitive Reactions" in this article.

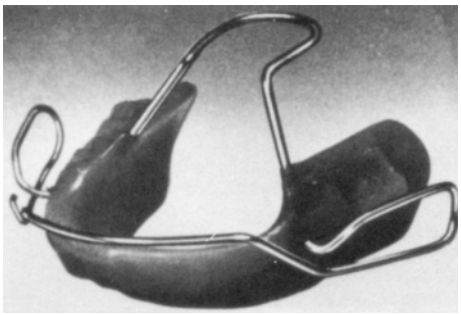

Fig. 6 Removable orthodontic appliance. Source: Ref 4

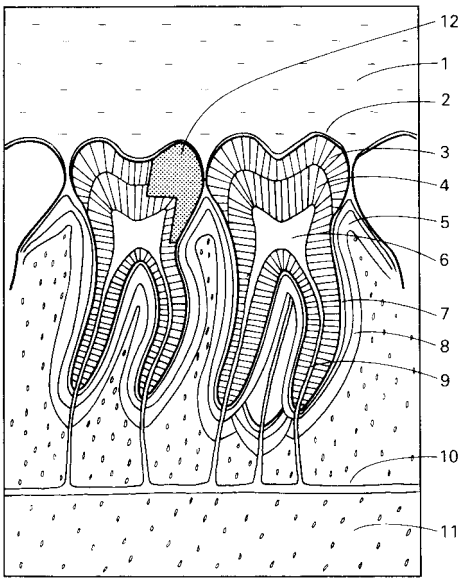

Fig. 7 Useful dental anatomy. 1, saliva; 2, integument; 3, enamel; 4, dentin; 5, gingiva; 6, pulp; 7, cementum; 8, periodontal ligament; 9, root canal; 10, artery; 11, alveolar bone; 12, restoration—amalgam filling

Cariogenesis corresponds to the ability for released metallic ions and formed corrosion products to affect the resistance of either dentin or enamel to decay (caries). The mechanisms involved with caries formation (Ref 13–15), which include the fermentation of carbohydrate by microorganisms and the production of acid, are likely to become altered when metallic ions and products from corrosion reactions are included. This may be indicated by the reports that show tin and zinc concentrations (originating from amalgam corrosion) in softened, demineralized dentin and enamel (Ref 16–18).

Allergic Hypersensitive Reactions. With allergic hypersensitive contact reactions, some people can become sensitized to particular foreign substances, such as ions or products from the corrosion of dental alloys (Ref 9, 19). The metallic ions or products combine with proteins in the skin or mucosa to form complete antigens. Upon first exposure to the foreign substance by the oral mucosa, sensitization of the host may occur in times of up to several weeks and with no adverse reactions. Thereafter, any new exposures to the foreign substance will lead to biological reactions, such as swelling, redness, burning sensation, vesiculation, ulceration, and necrosis. Abstinence from the foreign substance leads to healing. Identification and avoidance are the means for controlling these allergic hypersensitive reactions. Exposure of the oral mucosa to the foreign substance can lead not only to allergic stomatitis reactions (of the oral mucosa), but also to allergic dermatitis reactions (of the skin) at sites well away from the contact site with the oral mucosa. However, because the oral mucosa is more resistant to allergic reactions than the skin, the reverse process usually does not occur.

Of the currently used metals contained in dental alloys, nickel, cobalt, chromium, mercury, beryllium, and cadmium need to be considered as inducing possible allergic or cytotoxic reactions. Nickel is the primary alloying element in nickel-chromium casting alloys (up to 80%), in nickel-titanium wires (up to 50%) and in lower concentrations in some cobalt-chromium alloys, and in austenitic stainless steels. Nickel from dental alloy is known to react with the oral tissues in some individuals to produce allergic sensitization reactions (Ref 20). About 9% of women and 1% of men are estimated to be allergic to nickel. It is recommended that individuals be screened for possible nickel allergies prior to dental treatments. If an allergy arises from a nickel-containing dental restoration, it is recommended that the individual be tested for allergies to nickel and, if so indicated by the test results, have the restoration replaced with a nickel-free alloy.

Cobalt, also a component of some dental alloys, has been known to react with the oral mucosa and cause allergic reactions (Ref 20). However, the occurrences of such allergies are less than 1% of the population and mainly affect women. If reactions to cobalt from cobalt-containing materials are suspected, then testing for cobalt allergies should be performed. Contact allergic reactions to chromium from dental alloys are also reported (Ref 20), but the occurrences of such reactions are rare.

Mercury is contained in amalgam fillings, which contain microstructural phases composed of silver-mercury and tin-mercury. Mercury ions may be released from microstructural phases through corrosion. However, the concentrations are low and not relatable to toxicological ramifications. Mercury vapors released from amalgam surfaces may also occur. Again, because of the low concentrations emitted, amalgam mercury vapors are not related to toxicity. Allergic reactions to mercury contained in dental amalgams have been reported (Ref 20). If mercury allergic reactions are suspected from the amalgam, it is recommended that testing for mercury allergies be conducted.

Beryllium is contained in some nickel-chromium casting alloys in concentrations up to about 2 wt%. There are only a few cases of transient contact dermatitis that have been reported among dental professionals (Ref 21, 22). More of a health hazard is posed to the dental personnel doing the actual melting and finishing of the alloy than to individuals having a prosthesis made from a beryllium-containing alloy. For instance, the Occupational Safety and Health Administration (OSHA) has posted a Hazard Information Bulletin titled "Preventing Adverse Health Effects from Exposure to Beryllium in Dental Laboratories" expressing its concern about reports of chronic beryllium disease among dental laboratory technicians that are exposed to dust from melting, grinding, polishing, and finishing beryllium-containing alloys (Ref 23). As a result of safety concerns about beryllium, the American Dental Association (ADA) Council on Scientific Affairs recommends that dentists "use alloys that do not contain beryllium in the fabrication of dental prostheses" (Ref 24). Furthermore, the European Committee for Standardisation passed a resolution in February 2002 recommending that all standards pertaining to dental alloys permit a maximum beryllium content of only 0.02% wt%, which essentially excludes its use as an alloying element (Ref 25).

Cadmium is contained in some dental gold and silver solders of up to 15% (Ref 26). No biological reactions have been related to the cadmium contained in these materials; however,

precautions should be taken in fusing solders containing cadmium.

Additional information on the biocompatibility of metals and acceptable exposure limits is available in the article "Toxicity of Metals" in *Properties and Selection: Nonferrous Alloys and Special-Purpose Materials,* Vol 2, of the *ASM Handbook* (refer to pages 1233 to 1269).

Endodontic Failures. Root canals obturated with silver cones (or points) have occasionally been associated with corrosion (Ref 27). Figure 8 shows examples of restored teeth including two cases of endodontically treated teeth. Development of a fluid-tight seal at the apex of the root canal is the primary objective of endodontic therapy. Corrosion of the silver points is known to lead to failure by allowing the penetration of fluids along the silver cone/root canal interface. Figure 8(b) shows a schematic of a tooth with cones.

Dental Implant Rejection. Dental implants, which are used for permanently attaching bridges, and so on, extend through or up to the maxillary or mandibular bones and must function in both hard and soft tissues, as well as within a wide range of applied stresses (Ref 28, 29). Depending on the chemical inertness of the materials used for these devices, the thickness of the tissue connecting implant to bone varies. Released ions can infiltrate thick membranes surrounding loosely held implants, which can lead to an early rejection of the implant through immune response.

Tumorgenisis and Carcinogenisis. Even though dental alloy devices have not been implicated with tumorgenisis and carcinogenisis, their possible formation must never be ruled out and should always be considered as potential biological reactions, especially with new, untried alloys (Ref 29).

Efficacy

The oral environment must not induce changes in physical, mechanical, chemical, optical, and other properties of the dental alloy, such that inferior functioning and/or aesthetics result. The effect of the oral environment on the alloy has the potential for altering dimensions, weight, stress versus strain behavior, bonding strengths with other alloys and with nonmetals, appearances, and creating or enhancing crevices. In combination with mechanical forces, the oral environment is capable of generating premature failure through stress corrosion and corrosion fatigue and of generating increased surface deterioration by fretting, abrasion, and wear.

Dimensions, Weight, Mechanical Properties, and Crevices. At least in theory, corrosion of precision castings and attachments, which rely on accurate and close tolerance for proper fit and functioning, can alter their dimensions, thus changing the fit and functionality of the restorations. Similarly, corrosion of margins on crowns and other cast restorations can lead to decreased dimensions and to enhanced crevice conditions. The increased seepage of oral secretions into the crevices created between restoration and tooth can lead to microorganism invasion, generation of acidic conditions, and the operation of differential aeration cells. Under these conditions, the bonding of the restoration to the dentinal walls through the underlying cement is likely to become weakened. In combination with biting stresses, microcrack formation along the interface is likely to occur; this will cause the penetration of the crevice even further beneath the restoration. Eventually, the loosening of the entire restoration may occur.

With amalgam restorations, however, a slight amount of corrosion on these surfaces adjacent to the cavity walls may actually be beneficial because corrosion product buildup increases dimensions and adaptability. The crevice between an amalgam and the cavity is reduced in width, which leads to a decreased seepage of fluids. Additionally, the corrosion surface may inhibit bacterial growth, thus reducing bacterial invasion of small crevices. On the other hand, corrosion of the amalgam deteriorates its subsurface structure; this is likely to lead to an increased occurrence of marginal fracture, a known problem with amalgams, through corrosion fatigue mechanisms with stresses generated from biting (Ref 30).

The loss of sufficient material from any dental alloy through corrosion can lead to a reduction in mechanical strength. This can lead to a direct failure of the alloy or reduced rigidity resulting in unacceptable stains. For silver-soldered wires, corrosion of the solder leads to a weakening of the entire joint (Ref 31). Loosening of crowns and bridges because of corrosion-induced fractures of posts and pins is also known to occur (Ref 32), as shown in Fig. 8(a) and (c). Still other possibilities of the effects of corrosion include the reduction in bond strengths of metal brackets bonded to teeth, as well as the degradation of porcelain fused to metal restorations.

Appearance. Because of the various optical properties of corrosion products, the appearance of tarnished and corroded surfaces can become unacceptable. A degradation in surface appearance, without a loss in the properties of the appliance, can be taken to be either acceptable or unacceptable, depending on individual preferences. If, however, the tarnished surface promotes additional consequences, such as the attachment of plaque and bacteria or a greater irritation to opposing tissue, then tarnishing must be deemed unacceptable.

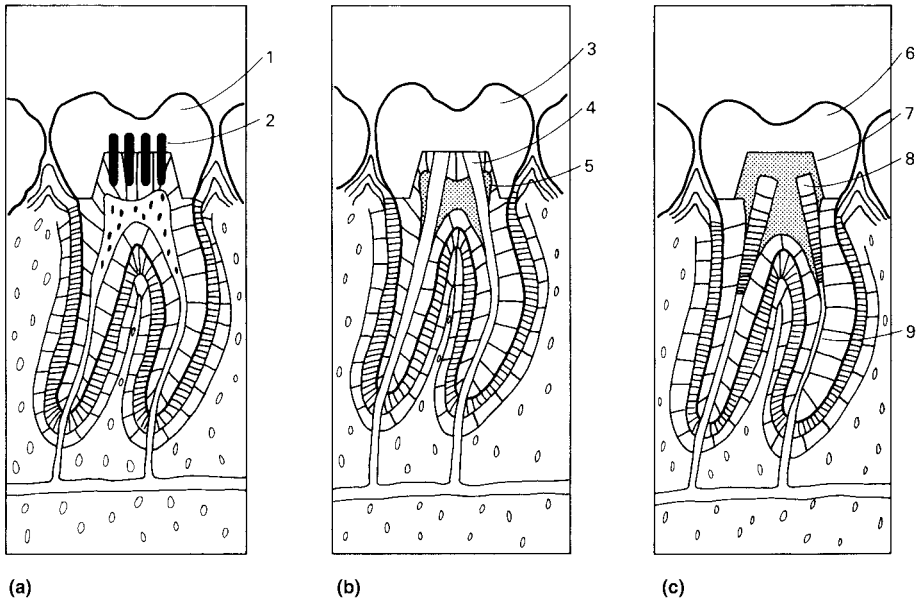

Fig. 8 Typical restored teeth. (a) Pin restored amalgam filling on vital tooth. (b) Cast metal crown restoration on endodontically treated tooth with silver cones and cement to seal root canals. (c) Cast metal crown restoration on endodontically treated tooth with cement core buildup and screwposts. 1, amalgam filling; 2, stainless steel pins; 3, metal crown; 4, silver cones; 5, cement; 6, metal crown; 7, cement core; 8, screw posts; 9, gutta-percha or similar sealing material

Interstitial versus Oral Fluid Environments and Artificial Solutions

In order to select and/or develop dental alloys, an understanding of the environment to which these materials will be exposed is imperative. This section defines and compares interstitial fluid and oral fluid environments. In addition, artificial solutions developed for testing and evaluation of dental materials also are discussed.

Interstitial Fluid

Applications of metallic materials to oral rehabilitation are confronted with a number of

environmental conditions that differentiate most dental uses from other biomedical uses (Ref 33). The one major exception is dental implants because interstitial fluids (the fluids in direct contact with tissue cells) are encountered by both dental and other types of surgical implants (see, for example, the article "Corrosion Effects on the Biocompatibility of Metallic Materials and Implants" in this Volume). As discussed later in this article, other exceptions occur because restorations in teeth have their interior surfaces in direct contact with the dentinal and bone fluids, which are more similar to interstitial fluids in composition than to saliva.

Other types of extracellular fluids, such as lymph and blood plasma, contain similar inorganic contents and are also likely to come into contact with dental implants, particularly with plasma during and shortly after surgery. Table 1 presents a composition of blood plasma. The inorganic content is similar to the inorganic content of interstitial and other types of extracellular fluids, while the protein concentration for plasma is higher than for other biofluids. For plasma, the major proteins are albumin, globulins, and fibrinogen. For all extracellular fluids, the inorganic contents are characterized by high sodium (Na) and chloride (Cl^-) and moderate bicarbonate (HCO_3^-) contents. Considerable variations in pH, p_{O_2}, and p_{CO_2} can occur in the vicinity of an implant. In crevices formed between plates and screws, some extreme values ranging between 5 to 7 in pH, and <8 to 110 and <10 to 300 mm Hg, respectively, have been determined (Ref 35). Similar corrosive conditions are expected regardless of the extracellular fluid, provided the effects of the protein and cellular contents are minimal.

Tissue cells and other types of cellular matter can also directly contact implant material, with the possibility of intracellular fluid permeating through the cell membrane and effecting corrosion of the alloy. Separation by shearing of biological cells from alloy surfaces almost always generates cohesive failures through the cell instead of adhesive failures along the alloy/cell interface (Ref 36). In these situations, intracellular fluids can gain direct access to the surface of the alloy. In contrast to extracellular fluids, intracellular fluids contain high potassium and organic anion contents. The sodium is replaced by potassium and Cl^- by orthophosphate (HPO_4^{2-}). The effectiveness of intracellular fluids in corroding implant surfaces will be governed by the ability of the larger organic anions to pass through cell membranes, which are usually very restricted. Extracellular fluids are, therefore, the fluids interacting with the implant in most cases, although the possible effects from intracellular fluids must not be dismissed.

Table 1 Mean human adult blood plasma composition

Compound	mg/100 mL
Inorganic	
Na^+	325
K^+	16
Ca^{2+}	9.8
Mg^{2+}	2.1
Cl^-	369
HCO_3^-	146–189
PO_4^{3-}	3.1–4.9
Si^-	0.8
SO_4^{2-}	3.7
Nonprotein organic	
Urea	33
Uric acid	4.9
Carbohydrates	260
Fructose	7.5
Glucosamine	81
Glucose	97
Glycogen	6.8
Polysaccharides (nonglucosamine)	129
Organic acids	19
Citric	2.2
Lactic	36
Other organic acids	5
Lipids	530
Fatty acids	316
Amino acids	37.1
Major proteins	
Albumin	4800
Globulins	2300
Fibrinogen	300

Source: Ref 34

Oral Fluids

Whole mixed saliva is produced by the paratid, submandibular, and sublingual glands, together with the minor accessory glands of the cheeks, lips, tongue, and hard and soft palates from the oral mucosa. Gingival or crevicular fluid is also produced, as well as fluid transport between the hard tissues of the teeth and saliva. The composition of the secretion from each gland is different and varies with flow rate and with the intensity and duration of the stimulus. Saliva composition varies from individual to individual and in the same individual under different circumstances, such as time of day and emotional state.

Although about 1 L of saliva is produced per day in response to stimulation accompanying chewing and eating, for the greater part of the day, the flow rate is at very low levels (0.25 to 0.5 mL/min) (Ref 37, 38). During sleep, there is virtually no flow from the major glands. At low flow rates, the concentrations of sodium, Cl^-, and HCO_3^- are reduced notably; the concentration of calcium is elevated slightly; and the concentrations of magnesium, phosphate (PO_4^{3-}), and urea are elevated decidedly when compared with stimulated flow rates (Ref 39). It is therefore impossible to define specific compositions and concentrations that are universally applicable. However, compilations of data encompassing large statistical populations have been made by a number of researchers. One typical analysis for the composition of human saliva is shown in Table 2.

The inorganic ions readily detectable in saliva are Na^+, K^+, Ca^{2+}, Mg^{2+}, Cl^-, PO_4^{3-}, HCO_3^-, thiocyanate (SCN^-), and sulfate (SO_4^{2-}). Minute traces of F^-, I^-, Br^-, Fe^{2+}, Sn^{2+}, and nitrite (NO_2^-) are also found, and on occasion, Zn^{2+}, Pb^{2+}, Cu^{2+}, and Cr^{3+} are found in trace quantities. Figure 9 shows the Cl^- and HCO_3^- variations in concentration as saliva is stimulated to a flow rate of 1.5 mL/min. The O_2 and N_2 contents of saliva are 0.18 to 0.25 and 0.9 vol%, respectively. The carbon dioxide (CO_2) content varies greatly with flow rate, being about 20 vol% when unstimulated and up to about 150 vol% when vigorously

Table 2 Mean whole unstimulated human saliva composition

Compound	mg/100 mL
Inorganic	
Na^+	23.2
K^+	80.3
Ca^{2+}	5.8
Mg^{2+}	1.4
Cl^-	55
HCO_3^-	39
PO_4^{3-}	14.9
SCN^-	13.4
Nonprotein organic	
Urea	12.7
Uric acid	1.5
Amino acids	4
Citrate	1.1
Lactate	1.7
Ammonia	0.4
Sugars	19.6
Carbohydrates	73
Lipids	2
Protein	
Glycoproteins	45
Amylase	42
Lysozyme	14
Mucins	250
Albumin	2
Gamma-globulin	5

Source: Ref 34

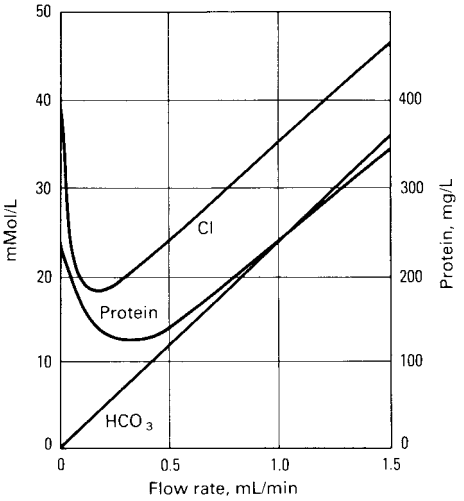

Fig. 9 Variations in the concentrations of Cl^-, HCO_3^-, and protein in human saliva as a function of the flow rate of saliva. Source: Ref 38

stimulated. The buffering capacity is chiefly due to the CO_2/HCO_3 system, with that of the PO_4^{3-} system only having a small, limited part. The redox potential of saliva indicates it to possess reducing properties, which is likely due to bacteria reductions, carbohydrate splitoffs from glycoproteins, and nitrates. The normal pH of unstimulated saliva is in the 6 to 7 range and increases with flow rate.

The clearance of saliva involves its movement toward the back of the mouth and its eventual introduction into the stomach. Saliva is continually being secreted and replenished, especially during active times. A volume of about 1 L/d is considered average for saliva production. Chemical analysis of human mouth air showed hydrogen sulfide (H_2S), methyl mercaptan, and dimethyl sulfide to be some of the most important constituents (Ref 39).

Organic. Human saliva is composed of nonprotein organic and protein contents, as shown in Table 2. The largest contributions from the nonprotein ingredients are from the carbohydrates, while smaller amounts are from urea, organic acids, amino acids, ammonia, sugars, lipids, blood group substances, water-soluble vitamins, and others. Some of the lipids include the fatty acids, glycerides, and cholesterol. At least 18 amino acids have been identified, with glycine being the main constituent. Many of these components are produced directly by the salivary glands, while others, such as some carbohydrates and amino acids, are the result of the dissociation of glycoproteins and proteins by bacterial enzymes. Still others are derived from blood plasma. The protein content of human saliva is primarily of salivary gland origin, with a very small amount derived from blood plasma. The protein content may vary from less than 1 to more than 6 g/L. Detailed information on protein and glycoproteins that have been identified to be in saliva can be found in Ref 40 to 42.

Chemicals in Food, Drink, and Air. All of the ingredients found in food and drink are capable of becoming incorporated into saliva. However, most of the foods are ingested before the breakdown into basic chemicals occurs. Some foods and beverages, though, contain chemicals that are reactive by themselves, without any reductions, and may become dissolved in saliva and affect the tarnish and corrosion of metallic materials. Some of these include various organic acids, such as lactic, tartaric, oleic, ascorbic, fumaric, maleic, and succinic, as well as sulfates, chlorides, nitrates, sulfides, acetates, bichromates, formaldehyde, sulfoxylates, urea, and the nutrients themselves of lipids, carbohydrates, proteins, vitamins, and minerals (Ref 43).

The components found in atmospheric air and pollutants, coupled with the human respiratory function, have the potential of exposing the oral environment to additional aggressive chemical species. Some of the species known to be in atmospheric air and pollutants are O_2, CO_2, NO_2, carbon monoxide (CO), sulfur dioxide (SO_2), Cl_2, hydrogen chloride (HCl), hydrogen sulfide (H_2S), ammonia (NH_3), formaldehyde, formic acid, acetic acid, Cl^- salts, ammonium salts of sulfate and nitrate, and dust (Ref 44).

Because the volume of lung ventilation is of the order of 8.5 L/min, the amount of potentially hazardous and corrosive material possibly coming into contact with the oral environment is significant. In approximately 2 h, 1 m^3 of air (for a mouth breather) will have been used during respiration, with the potential uptake of sulfur dioxide in the normal urban area being 0.11 to 2.3 mg. Sulfur dioxide can be involved in many interactions, accelerating the tarnish and corrosion of metals. Fortunately, the proteins in saliva combine with most of the aggressive external stimuli coming into contact with saliva; therefore, most of the aforementioned hazardous species are rendered inactive before they can cause tarnish and corrosion. However, the pathway from the atmosphere to the surfaces of dental alloys are certainly potential sources for introducing corrosive species.

A comparison between interstitial and oral fluids shows differences in both inorganic and organic contents. One important difference is the approximately sevenfold higher Cl^- concentration in interstitial fluid. Even though interstitial fluids do undergo variations in pH and p_{O2}, especially at the site of the implant, saliva is more susceptible to variations in composition. This comes about because the composition of saliva depends to a large degree on flow rate, which in turn depends on a number of physical and emotional factors. Saliva is also subjected to exposures from chemicals contained in the air, food, drink, pharmaceuticals, as well as temperature variations of 0 to 60 °C (32 to 140 °F) and microbiological involvement with the production of acid and plaque.

Artificial Solutions. Numerous solutions simulating human saliva have been formulated and used for testing the tarnish and corrosion susceptibility of dental alloys (Ref 45–50). Modifications to these solutions have also been made and used (Ref 51–56). Some of the solutions contain only inorganics (Ref 48–50, Ref 52–54), while others include the addition of an organic component consisting mostly of mucin (Ref 45–47, 51–53). Some researchers also purge a $CO_2/O_2/N_2$ gas mixture through the solution to simulate pH control and buffering capacity controlled by the CO_2/HCO_3^- redox reaction. All compositions contain mostly chlorides (Na, K, and Ca) and various forms (mono-, di-, or tri-basic, pyro) of phosphates in smaller amounts. Additional ingredients include bicarbonate, thiocyanate, sulfide, carbonate, organic acids, citrate, hydroxide, and urea.

Table 3 presents the composition for an artificial saliva that corresponds very well to human saliva, with regard to the anodic polarization of dental alloys. Ringer's physiological saline solution used to simulate interstitial fluid is also included in Table 3. Both solutions are entirely inorganic. The Cl^- concentration of Ringer's is about seven times higher than that of the saliva. The anionic content of Ringer's is entirely chloride, while the artificial saliva also contains phosphate and sulfide. Urea is also a constituent of the artificial saliva. Sodium, potassium, and calcium constitute the cationic content of both solutions.

A number of additional artificial physiological solutions, some of which are named Hanks, Tyrod, Locke, and Krebs, appear in the literature and have been used to simulate the interstitial fluids. Basically, these solutions contain small additions of modifying ingredients, such as magnesium chloride, glucose, lactate, amino acids, and organic anions. The Ringer's solution presented in this article, after the National Formulary Designation, does not contain sodium bicarbonate ($NaHCO_3^-$). Some solutions, however, referred to in the literature as Ringer's, do contain bicarbonate.

Effect of Saliva Composition on Alloy Tarnish and Corrosion

Chloride/Orthophosphate/Bicarbonate/Thiocyanate. The interactions of the various salts contained in saliva are complex. The effects from the combined saliva solutions are not simply the additive effects from the isolated individual salts. This synergistic behavior is discussed for the corrosion of an amalgam in the $Cl^-/HPO_4^{2-}/HCO_3^-/SCN^-$ system in Ref 50. Chloride alone produces a powdery, finely crystalline corrosion product in heaps around the sites of attack, such as porosities and pits. The addition of HPO_4^{2-}, which by itself produced very little effect, caused the corrosion products to become organized in conical structures, the bases being over the sites of corrosion. The addition of HCO_3^- to the Cl^-/HPO_4^{2-} system generated increased microstructural corrosion. On the contrary, addition of SCN^- to the Cl^-/HPO_4^{2-} system suppressed the microstructural corrosion. By adding all four salts together, an even more corrosion-resistant system was obtained. Corrosion was much reduced and more localized.

Artificial Salivas. The effect on alloy corrosion from different artificial saliva solutions has been studied (Ref 49). The polarization behavior of a number of dental alloys, including gold-base alloys, nickel-chromium, and cobalt-chromium, in artificial salivas without HCO_3^- and SCN^-, but with protein, provided the best correlation with the behavior observed with human saliva in both aerated and deaerated conditions. The

Table 3 Composition of artificial solutions

	Composition, mg/100 ml	
Compound	Artificial saliva	Ringer's solution
NaCl	40	82–90
KCl	40	2.5–3.5
$CaCl_2 \cdot 2H_2O$	79.5	3.0–3.6
$NaH_2PO_4 \cdot H_2O$	69	. . .
$Na_2S \cdot 9H_2O$	0.5	. . .
Urea	100	. . .

Source: Ref 49

artificial salivas containing HCO_3^- and SCN^-, but no proteins, constantly shortened the passivation range of the alloys. The specific contributions from Cl^- and SCN^- shortened the passivation range of the gold-base alloy, but phosphate increased the passivation range of all alloys.

Lowering the pH shifted the amalgam polarization curve to increased currents and potentials, while buffering capacity, which was increased by protein content, influenced corrosion behavior under localized corrosion conditions (Ref 57). In sulfide solution, the polarization curves of amalgams indicated increased corrosion (Ref 47, 58). Dissolved O_2 generated both inhibition and acceleration, as reflected by the formation of anodic films and the consumption of electrons by cathodic depolarization. The particular alloy-environment combination determines whether corrosion is inhibited or accelerated.

Chloride and Organic Content. Anodic polarization of amalgams in human saliva compared with Ringer's solution was shown to be shifted by up to several orders of magnitude to lower currents at constant potentials, depending on the amalgam system (Ref 59). These differences were related to the Cl^- concentration of the solutions. The effect of Cl^- on amalgam polarization is well documented (Ref 55, 60, 61). Pretreatment of gold-base alloys in human saliva prior to galvanic coupling with amalgams in a protein-free artificial saliva reduced the corrosion on some of the amalgams studied (Ref 62). Pretreatment of the amalgams had little effect.

Significant reductions in the weight gains of amalgams stored in artificial saliva with mucin as compared with mucin-free saliva have been reported (Ref 47). Anodic polarization of amalgams in artificial saliva or diluted Ringer's solution, with and without additions of mucin or albumin, was, however, shown to be very similar (Ref 47, 60). Proteins in artificial saliva on silver-palladium and nickel-chromium alloy polarizations were also reported to have little effect (Ref 57). For a copper-aluminum crown and bridge alloy, anodic polarization differences were detected in an artificial saliva with and without additions of a human salivary dialysate (Ref 63). The total accumulated anodic charge passed from corrosion potentials to $+0.3$ V versus saturated calomel electrode (SCE) was significantly reduced in protein-containing saliva. Similarly, the polarization resistance of the alloy was more than doubled by progressively adding up to 1.6 mg dialysate/mL to saliva initially free of proteins.

Microorganisms. The tarnishing of dental alloys by three microorganisms likely to be found in the mouth has been reported (Ref 64). Some specificity between the degree of tarnish and the type of microorganism was obtained. A likely tarnishing mechanism was due to the organic acids generated by the fermentation of carbohydrate by the bacteria. The effect of microorganisms on accelerating corrosion is discussed in the section "Oral Corrosion Processes" in this article.

Oral Corrosion Pathways and Electrochemical Properties

The electrochemical properties of dental alloy restorations vary widely. Electrochemical potentials, current pathways, and resistances depend on whether there is no contact, intermittent contact, or continuous contact between alloy restorations. This section examines the effects of restoration contact on electrochemical parameters and reviews concentration cells developed by dental alloy-environment electrochemical reactions.

Noncontacting Alloy Restorations

Isolated. The total liquid environment of a restoration includes, in addition to saliva, fluids contained within the interior of dentin and enamel, which are more like extracellular fluids in composition than saliva. Figure 10 shows a schematic of a likely current path for a single metallic restoration. The current path encompasses a route that includes the restoration, enamel, dentin, membranes such as the periodontal ligament, soft tissues, and saliva (see Fig. 7). The conduction of current through hard tissues, including enamel, dentin, and bone, occurs through the extracellular fluids, which are compositionally similar in all hard and soft tissues. However, the current through these different hard tissues will take pathways of least resistances. For example, the resistance of dentin in a direction parallel to the tubules is about 18 times lower than in a perpendicular direction due to the calcification of the tubule walls. Structural details, including imperfections, orientations, and so on, control the actual resistances for particular hard tissue structures.

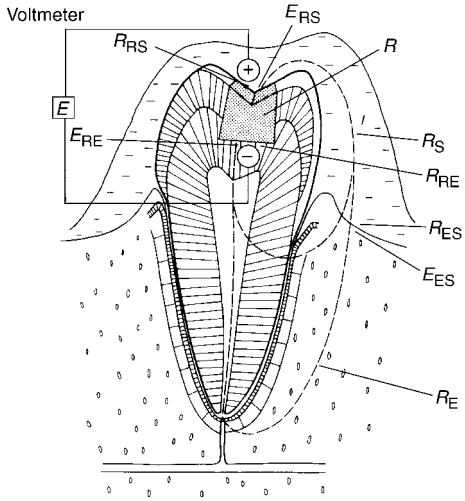

Fig. 10 Schematic of a single metallic restoration (R) showing two possible current (I) paths between external surface exposed to saliva and interior surface exposed to dentinal fluids. Because the dentinal fluids contain a higher Cl^- concentration than saliva, it is assumed the electrode potential of interior surface exposed to dentinal fluids is more active and is therefore given a negative sign (−). The potential difference between the two surfaces is represented by E.

The restoration (R) develops electrochemical potentials with the extracellular fluids, E_{RE}, and with saliva E_{RS}, while a liquid junction potential occurs between extracellular fluids and saliva, E_{ES}. Contact resistances occur between restoration and extracellular fluids, R_{RE}, and between restoration and saliva, R_{RS}. In general, these potentials generated at interfaces are caused by the materials and/or liquids existing at different energy levels. Resistances of the extracellular fluids, R_E, extracellular fluid-saliva junction, R_{ES}, and of saliva, R_S, also occur. Figure 11 shows an electrical schematic for this system. Summing electromotive forces in one direction and equating to zero yields for the current I:

$$I = \frac{E_{RE} + E_{ES} - E_{RS}}{R_{RE} + R_{RS} + R_E + R_S + R_{ES}} \qquad \text{(Eq 1)}$$

Taken together, E_{ES} and R_S have negligible effect on current. The extracellular resistance, R_E, is usually in the range between 10^4 and 10^6 Ω because of variations in particular hard tissue structures, and to possible variations in membrane/hard tissue interfacial characteristics. The potentials E_{RE} and E_{RS} are characteristics of the metal-electrolyte combinations, and the resistances R_{RE} and R_{RS} are dependent on the polarization characteristics for the particular combinations.

Polarization is related to the corrosion products that form. For soluble or loosely adhered products, the contact resistances will not be changed significantly. However, for tenaciously adhering products with semiconducting or insulating electrical characteristics, the contact resistances will be largely affected. These resistances are the primary parameters affecting the magnitude of the generated current. This reasoning is directly in line with the mixed-potential theory for electrochemical corrosion (Ref 65). The corrosion current, I_{corr}, without ohmic resistance control is:

$$I_{corr} = \frac{\beta_a \beta_c}{(\beta_a + \beta_c) R_p} \qquad \text{(Eq 2)}$$

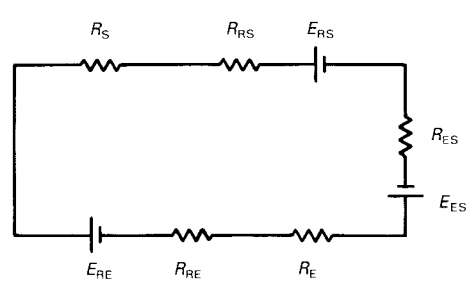

Fig. 11 Electrical schematic representing the equivalent circuit of a single loop shown in Fig. 10. Terms are defined in text.

where β_a and β_c are the Tafel slopes from the anodic and cathodic polarization curves, and R_p is the polarization resistance or the linear slope of the $\Delta E/\Delta I$ curve within ± 10 mV of the corrosion potential.

Nonisolated. For two restorations not in contact (Fig. 12), the extracellular fluid-saliva resistance, R_{ES}, determines the extent to which the current will be short circuited through the saliva/extracellular fluid interface. If R_{ES} is high, there is maximum interaction between the separated restorations (the currents are small, of the order of 1 to 10×10^{-9} A/cm^2 between an amalgam and a gold alloy restoration). As R_{RS} decreases, the current through the interface between saliva and extracellular fluids increases. The interaction between the separated restorations will then be minimized. Each restoration, though, will still generate its own current path loop (Ref 66).

Intraoral Electrochemical Properties. In a study comprising 115 people, the corrosion potentials from 243 restorations ranged between -0.55 and $+0.4$ V versus SCE. Amalgam restorations were the most active, followed by cobalt-chromium alloys and gold-base alloys. Variations in potential on different surfaces of the same restoration occurred routinely. This was likely due to the effects from abrasion on the occlusal surfaces and from the accumulation of plaque and debris on nonocclusal surfaces (Ref 67).

For noncontacting amalgam and gold alloy restorations (78 fillings in 66 people), the average currents flowing through the restorations due to saliva-bone fluid liquid junction cells were calculated from measured intraoral potential and resistance data to be 0.48 and 0.26 μA, respectively (Ref 12).

Using constant current pulses (1 to 10 μA) and measuring the corresponding potential changes, the intraoral polarization resistances for noncontacting amalgam restorations ranged between 50 and 300×10^3 Ω (Ref 68). With the use of linear polarization theory, corrosion currents are calculated to be 0.2 to 1.0 μA.

Restorations Making Intermittent or Continuous Contact

Intermittent Contact. A situation can occur in the mouth in which two alloy restorations, one in the upper arch and the other in the lower arch, come into contact intermittently by biting (Fig. 13). When the two restorations are in direct contact, a galvanic cell is generated with an associated galvanic current short-circuited between the two restorations. The external current path can take a number of directions, with the least resistance path controlling. Figure 13 shows two possible pathways, one entirely through extracellular fluids and the other partly through extracellular fluids and partly through saliva.

The current-time transients have been measured and are presented in Fig. 14. Upon first making contact, currents of the order of 10 μA and more occur and decrease rapidly within a matter of minutes. If, however, the restorations are open-circuited for a time interval and then again closed, the current level will again increase but not to the same magnitude as from the previous closure. The amount of recovery will increase as the time lapse between closure increases. This phenomenon is explained by the formation of protective surface films on the electrodes due to the passage of current. Upon making contact on succeeding occasions, the film offers additional resistance to the flow of current, even though the two restorations appear to be in direct intimate contact. The films dissipate with time, thus increasing the level of the initial current on recontacting restorations.

A similar situation can occur because of an alloy restoration contacting, for example, eating utensils or dental instruments during dental treatment. Again a short-circuited galvanic current is generated. The external circuit will be partly through saliva and partly through extracellular fluids.

Continuous Contact. Another situation in which metallic restorations in the mouth are capable of generating galvanic currents involves two dissimilar metallic restorations in continuous contact, as shown in Fig. 15. Most attention has been given to the combination of amalgam-gold alloy couples (Ref 52). Other situations

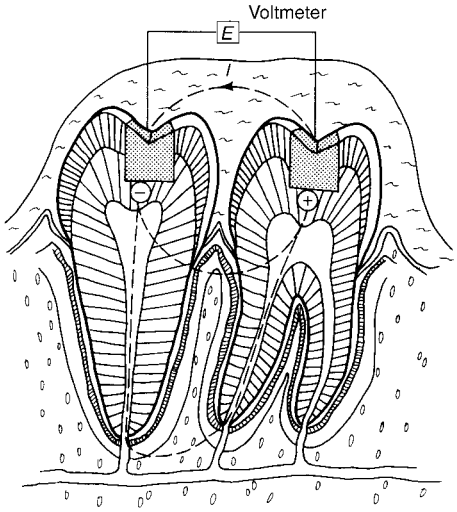

Fig. 12 Schematic of two nonisolated, noncontacting restorations. The alloy restoration on the left, which is an amalgam, is more active than the restoration on right, which is a gold-base alloy.

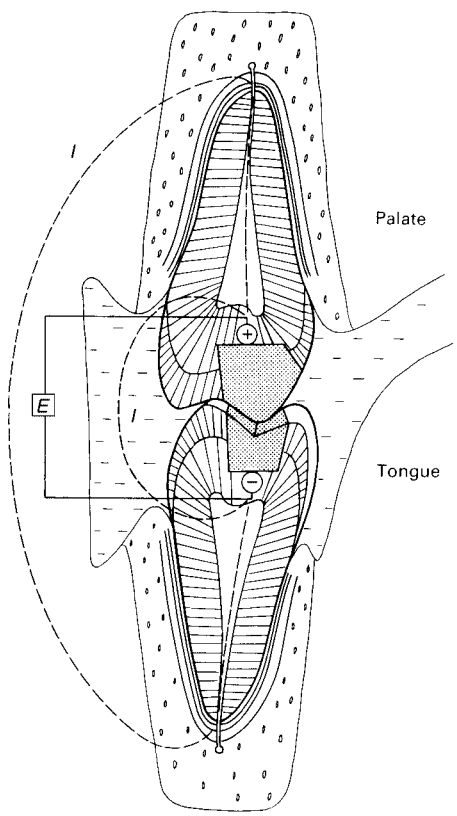

Fig. 13 Schematic of two restorations making intermittent contact due to biting. The restoration in the lower arch, which is an amalgam, is more active than the restoration in the upper arch, which is a gold-base alloy. Two possible current pathways are shown. An additional path very likely to occur would be directly through saliva between the two restorations.

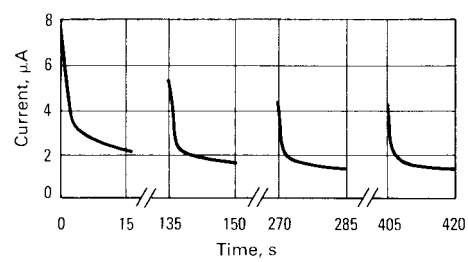

Fig. 14 Current-time responses between gold alloy and amalgam of the same cross-sectional areas. Short circuiting occurred for 15 s, followed by a 2 min delay before recontacting. Source: Ref 69

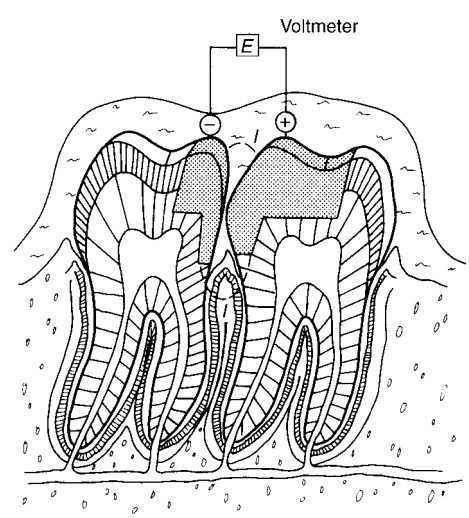

Fig. 15 Schematic of two adjacent restorations in continuous contact. Two possible current paths shown.

occur, for example, between two amalgam restorations (Ref 70)—one a conventional amalgam and the other a high-copper amalgam—and between two gold alloys with differences in noble metal content. Other situations have already been discussed. These include a stainless steel reinforced amalgam (Fig. 8a), an endodontically restored tooth with silver cones making contact with a gold crown (Fig. 8b), and an endodontically restored tooth with steel screwposts making contact with a gold crown (Fig. 8c). Soldered appliances are also examples of dissimilar metals making continuous contact. Any multiphase microstructures are situations for galvanic corrosion to occur. Multiphase microstructures occur extensively with dental alloys.

For the amalgam-gold alloy couple making direct contact, the amalgam is the anode and suffers corrosive attack; the gold alloy is the cathode. As with galvanic couples making intermittent contact, large galvanic currents occur on first contact and decrease rapidly with time. For silver-tin amalgams, the tin from the tin-mercury phase suffers corrosion attack. The freed mercury combines with the gold of the gold alloy to form a gold amalgam that is capable of producing surface discolorations on the gold alloy. In addition to becoming corroded, the amalgam is capable of being degraded in strength by the corrosion generated by the galvanic currents (Ref 70).

Currents calculated from polarization resistance and potential differences of various contacting dissimilar metallic restorations indicate most couples to pass 1 to 5 μA on first contact (Ref 67). However, amalgam-gold alloy couples indicate a greater percentage of currents in the ranges of 6 to 10 and 11 to 15 μA. All couples initially show a sharp decrease in current with time, followed by a gradual leveling off as zero current is approached. However, disruption of surface protective films can result in increases in current at later times.

Concentration Cells

Interior-Exterior Surfaces. Because the interior surfaces of restorations adjacent to the cavity walls are exposed to extracellular fluids and higher concentrations of Cl^- than the exterior surfaces exposed to saliva, the interior instead of the exterior surfaces are more susceptible to anodic attack from Cl^-. However, if the electrons generated by the anodic oxidations are not consumed by reductions, the oxidation reactions will cease. Because the extracellular fluids have low concentrations of dissolved oxygen, corrosion of the interior surfaces would likely cease if it were not for the accessibility of electrons to the exterior surfaces exposed to saliva having a supply of dissolved oxygen from contact with the atmosphere.

Corrosion that is perpetuated by electrochemical reactions occurring on adjacent or opposite surfaces of the same restoration constitutes an important pathway for the tarnishing and corrosion of dental alloys. This pathway is germane to amalgams as well as all types of restorations, including crowns and inlays that are cemented into the cavity preparation. In the mouth, cements are likely to become electrical conductors because the absorption of oral fluids permits the passage of ions.

Marginal Crevices. A second pathway can occur because of the seepage of salivary fluids into crevices or marginal openings formed between the restoration (especially with amalgams) and the cavity walls. The pathway is distinguished from the first in that the conditions developed in the crevice are due to diffusion and charge balances resulting from the salivary fluids instead of the extracellular fluids. Because of a lack of diffusion of the large O_2 molecule into the crevice, low O_2 concentrations result within the crevice. With time, the acidity within the crevice increases because of the accumulation of H^+ ions from the oral environment and from corrosive reactions occurring within the crevice. Chloride and other anion concentrations will also tend to increase within the crevice over time because of charge equalization. Therefore, this pathway results in conditions that are similar to the interior-exterior pathway.

Alloy Surface Characteristics. Porosities, differences in surface finish, pits, weak microstructural phases, and the deposition of organic matter can initiate corrosion by concentration cell effects. For example, gold-base alloys are known to become tarnished more easily when containing porosities and inhomogeneities (Ref 71). Rougher surface finishes of restorations generate increased corrosive conditions (Ref 72). Similarly, the pitting of base metal dental alloys of the stainless steel and nickel-chromium varieties occurs by concentration cell corrosion. Basically, the advancing pit front is free of O_2, but the surfaces of the alloy outside the pit have an ample supply of O_2 from the air. Because the anode-to-cathode surface area is very small, the corrosion occurring at the bottom of the pit is concentrated to a very small area, thus increasing intensity of the attack. Removal of only a small amount of metal has a large effect on advancing the pit front.

Amalgam γ_2 Phase. Deterioration of the weak, corrosion-prone tin-mercury phase (γ_2) in silver-tin amalgams has also been proposed to occur by concentration cell corrosion (Ref 66). In this model, partial removal of the γ_2 phase initially occurs by abrasion resulting from biting and chewing. After removal of the γ_2 phase has progressed to a sufficient depth, an occluded cell is formed between the bottom of the depression and the unabraded surface. Mass transport is restricted from and into the cell. The condition will approach conditions occurring in other types of concentration cells. In the present example, however, Sn^{2+} will be slowly released from the passivated γ_2 regions. The concentration of Sn^{2+} will slowly increase within the occluded cell and will be neutralized by an equivalent amount of Cl^- by migration from the bulk electrolyte.

Consumption of O_2 within the occluded cell will take place by its utilization in the consumption of electrons by cathodic depolarization. Replenishment of O_2 will be restricted, and the concentration of O_2 within the cell will become reduced. When the solubility product of stannous oxide (SnO) is exceeded, SnO precipitates and the H^+ concentration increases. At this point, activation of the γ_2 phase occurs. Dissolution of tin occurs freely. The Cl^- concentration within the cell continuously increases to maintain electrical neutrality. Galvanic coupling of the occluded cell to the external surface generates a galvanic cell by which the cathodic reduction of O_2 occurs. Corrosion of γ_2 tin within the cell continues. Under conditions of high acidity and high concentration of Cl^-, the formation of insoluble tin chloride hydroxide ($Sn(OH)Cl \cdot H_2O$) becomes thermodynamically possible.

Oral Corrosion Processes

Whether corrosion is occurring between microstructural phases of a single restoration, between components having different environmental concentrations, or between individual restorations of different compositions and making intermittent or continuous contact, the corrosion processes involved consist of oxidation and reduction. The dissolution of ions is involved with the anodic reaction, and the consumption of electrons is involved with the cathodic reaction. The slowest step in the complete chain of events controls the overall corrosion rate. Corrosion of alloys in the mouth can be viewed as being the result of corrosive and inhibiting factors (Ref 73). Some corrosive factors consist of Cl^- (in most instances), H^+, S^- (at times), O_2, microorganisms, and the clearance rate of corrosion products from the mouth, while some inhibiting factors consist of protein and glycoproteins (in most instances), CO_2/HCO_3^- buffering system, $PO_4^-/PO_4^{2-}/PO_4^{3-}$ buffering system, and salivary flow rate.

Corrosive Factors

Chloride. The effect of Cl^- on the deterioration of passivated surface films on stainless steel, nickel-chromium, and cobalt-chromium alloys is well known. The susceptibility to pitting attack is increased. Increased Cl^- content also increases the attack of corrosion-prone phases in amalgam, other base metal alloys, and the low noble metal content alloys. Because the Cl^- concentration in saliva is about seven times lower than that in the extracellular fluids, the corrosiveness of Cl^- in saliva is usually less. Figure 16 illustrates the effect of Cl^- concentration on the polarization of amalgam by comparing the cyclic voltammetry in deaerated artificial saliva to that in Ringer's solution.

Increases in Cl^- concentrations are also likely to occur in crevices, such as the interfaces between cavity walls and adjacent surfaces of restoration. The Cl^- concentration within crevices is expected to increase to preserve electrical neutrality from the increase in Sn^+ concentration resulting from the γ_2 tin and γ_1 corrosion (Ref 66).

Chloride is capable of generating numerous compounds as products of corrosion. Chloride combines with zinc, tin, copper, silver, and others contained in dental alloys. Some of the products formed include zinc chloride (ZnCl), stannous chloride ($SnCl_2$), stannic chloride ($SnCl_4$), SnCl compounds such as hydrated $SnOHCl \cdot H_2O$ and $Sn_4(OH)_6Cl_2$, copper chloride (CuCl), cupric chloride ($CuCl_2$), complex hydrated cupric chloride ($CuCl_2 \cdot 3Cu(OH)_2$), and silver chloride (AgCl). The solubilities are high for all compounds, except CuCl, AgCl, and the basic tin and copper chlorides. Many additional compounds are to be considered for a complete listing of all potential corrosion products that form from dental alloys. Certainly, the chlorides of indium, gallium, beryllium, iron, nickel, chromium, cobalt, and molybdenum should be included.

Hydrogen Ion. The pH in the mouth can vary from about 4.5 and lower to about 8. In addition to the normal variations in pH of saliva due to human factors (see the section "Oral Fluids" earlier in this article), increased acidity can also result from a number of additional factors, such as the operation of crevice corrosion conditions, the acid production by dental plaque, and the effects of food, drink, and atmospheric conditions. The operation of crevice conditions in amalgams can increase acidity to well below a pH of 4. For amalgams, this acidity is mostly the result of the oxidation of γ_2 and γ_1 tin in aqueous solution. Under these conditions, the freed H^+ will become the cathodic depolarizers. With this increased acidity, dissolution of the tooth structure is also likely to occur. Calcium and phosphorus are likely to be dissolved from enamel and dentin. Dental plaque acid is produced by the fermentation of carbohydrate by microorganisms (Ref 13, 14). Most of the fermentable carbohydrate responsible for acid production comes from the diet in the form of sugars or starchy foodstuffs.

Figure 17 shows a schematic Stephan pH test curve of plaque. Stephan showed that the pH for all plaques decrease in value following a sugar challenge (Ref 13). This means that the production of acid by fermentable carbohydrate is greater than the rate at which acid can be removed. As time proceeds, the pH again rises. For caries-free and caries-active individuals, the qualitative shapes of Stephan pH curves are similar; however, the relative position of the curve for caries-active individuals is shifted to values in pH of 4.5 and lower. Depending on the source of the sugar challenge, the pH minimum on the Stephan pH curves have been shown to remain for a number of hours (Ref 15). Even though no data are available to show the effect of plaque pH value on the tarnishing and corrosion of dental alloys, it follows from first principles that the reduction in pH will adversely affect tarnishing and corrosion resistance. Metallic restorations can become severely deposited with plaque and organic matter, as shown in Fig. 18.

Sulfide compounds, such as silver sulfide (Ag_2S), cuprous sulfide (Cu_2S), and cupric sulfide (CuS), have very low solubility product constants and often constitute the tarnished films on dental alloys. Mercury and tin sulfides may also be present when amalgams are considered. The formation of thin insoluble films occurs with very small amounts of formed corrosion products, especially on the higher noble metal content alloys. In spite of even microgram quantities of tarnishing products at times, surface discolorations can still occur and elicit unsatisfactory personal responses. Tarnishing products under these conditions almost always maintain biocompatibility with the alloy system. With the lower noble metal content alloys, however, increased quantities of corrosion products can form, and tarnishing and corrosion can become more involved.

The corrosion potentials for many dental alloys in sulfide-containing solutions are often lower than the standard reduction potentials for the formation of the metal sulfides—an indication that the metal sulfides are thermodynamically stable. In some instances, particularly with amalgams, dissolution rates increase with S^- concentrations. This is probably due to the increased solubility for some of the sulfides (for example, Sn_2S_3 with amalgams) to form complexes with other species. Dietary factors are the main source for increasing S^- levels in saliva. Some foods, such as eggs and fish, as well as some drinking waters, are high in sulfur. Smokers have higher SCN^- saliva concentrations than nonsmokers (Ref 76). Sulfate-reducing bacteria may also generate S^- in the mouth. Hydrogen sulfide that is produced in the crevicular fluid and periodontal pockets can be easily dissolved in oral fluids. Atmospheric pollutants often contain high levels of SO_2 and H_2S and may influence the concentrations of S^- in the oral fluids.

Dissolved oxygen participates in corrosion reactions by either depolarizing cathodic reactions or by reoxidizing disruptive passivated surface films on base metal alloys. The first case increases or perpetuates corrosion, while the second case reduces or inhibits corrosion. Oxygen depolarization occurs by the customary electrochemical redox reactions. Electrons from the anodic process are consumed by the depolarization process. For a typical restoration, the exterior surfaces are exposed to higher O_2 concentrations. Differential aeration conditions can become operative, with the outer surfaces cathodic to the anodic interior surfaces. In other situations, differential aeration cells are set up between the bottoms of pits and the surrounding surfaces. Other types of pores and porosities are also likely to generate concentration cells. In near-neutral solution that corresponds to saliva, the reaction $O_2 + 2H_2O + 4e^- \rightarrow 4OH^-$ occurs

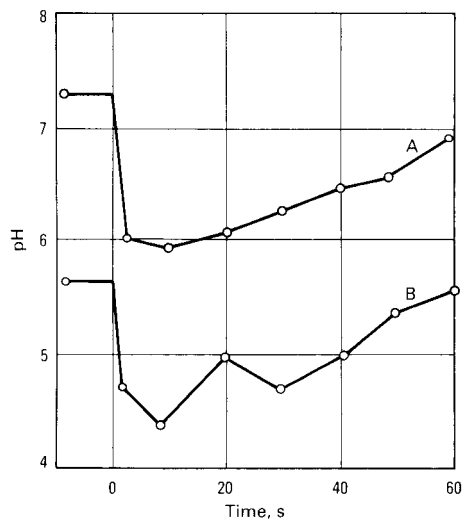

Fig. 17 pH versus time responses (Stephan curves) of plaque from caries-active (B) and caries-free (A) groups following a sugar challenge. Source: Ref 13

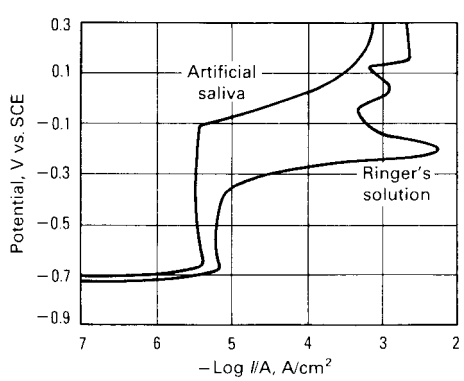

Fig. 16 Anodic polarization at 0.03 V/min of low-copper amalgam (Microalloy) in artificial saliva and Ringer's solution. Source: Ref 74

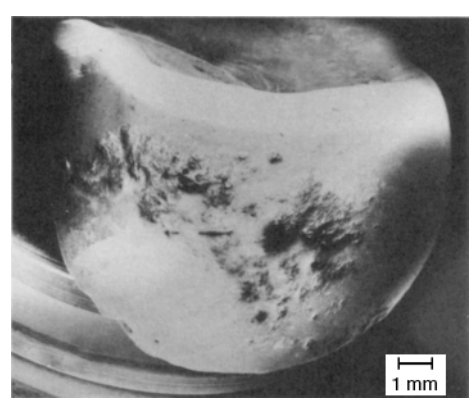

Fig. 18 Alloy restoration after intraoral usage showing the severity of plaque buildup that can occur. Source: Ref 75

most prevalently. If a driving force exists for metal oxidation, dissolution will be perpetuated on surfaces exposed to the lower O_2 concentration.

Oxygen is involved with numerous corrosion products formed on dental alloys. The tin from the γ_1 and γ_2 phases from silver-tin amalgams generates tin oxide products. These products passivate the amalgam at potentials less negative than about -0.7 V versus SCE, as indicated by the passive regions on the anodic polarization curves shown in Fig. 16. At more noble potentials, basic tin chlorides of the type $SnOHCl \cdot H_2O$ are formed, as indicated by the large current increases on the polarization curves. For copper-containing amalgams, basic copper chlorides of the type $CuCl_2 \cdot 3Cu\ (OH)_2$ form. Some additional products containing oxygen that are likely to occur with the corrosion of dental alloys include SnO_2, $Sn_4(OH)_6Cl_2$, Cu_2O, CuO, ZnO, $Zn(OH)_2$, and the oxides of chromium, nickel, cobalt, molybdenum, iron, titanium, and so on.

Oxygen is usually excluded from solutions during polarization testing with alloys. Dissolved O_2 interferes with the anodic processes. The generated anodic polarization curves obtained in O_2 containing solutions are usually cut off within the negative potential regions. For this reason, deaerated solutions are usually used to obtain entire anodic polarization curves. Passive breakdown potentials were observed to vary depending on whether aerated, dearated, or air-exposed solutions were used (Ref 77). However, within the O_2 concentration range likely to occur for surgical implants, the anodic polarization of type 316L stainless steel in Ringer's solution was independent of oxygen concentration (Ref 78).

Microorganisms. Two types of organisms—sulfate-reducing (*Bacteriodes corrodens*) and acid-producing (*Streptococcus mutans*) bacteria—have been discussed with the corrosion of dental alloys in the mouth (Ref 73). With regard to sulfate-reducing bacteria, depolarization of cathodic sites is thought to occur by removing H^+ from the metal surface. The hydrogen is used by the bacteria for the reduction of sulfate to sulfide, such as by the reaction $SO_4^- + 8H^+ \rightarrow S_2^- + 4H_2O$. In the case of acid--producing bacteria, the adsorbed microorganisms on the surface establish differential aeration conditions. As the dissolution of the metal occurs underneath the deposited microorganisms, the released acidic metabolic products, which include organic acids such as lactic, pyruvic, acetic, proprionic, and butyric, increase corrosion of the already-formed anodic sites. Because anodic areas are relatively small compared with the larger cathodic areas, corrosion can be severe.

The effects of dental plaque by-products from the fermentation of carbohydrates on the tarnishing and corrosion of dental alloys are probably more significant than the effect on alloy corrosion of only the microorganisms themselves.

Clearance Rate. The clearance of corrosion products from the mouth by the movement of saliva toward the back of the mouth and eventually by swallowing and replenishment affects the concentration of products in equilibrium with the metallic restorations. Therefore, a driving force for the continuation of the corrosion processes is maintained. Products of corrosion, like chemical species introduced through the diet, are cleared from the mouth by binding the exterior surfaces of the oral mucosa to the salivary glycoproteins and mucopolysaccharides lining. Detailed information on the binding ability of corroded metallic ions to proteins in human saliva can be found in Ref 40, 41, and 79.

Alloy Factors. Although the effects of alloy selection on tarnish and corrosion behavior are considered in more detail in the section "Tarnish and Corrosion under Simulated or Accelerated Conditions" later in this article, some of the important factors are mentioned here. Alloy composition and microstructure are probably the two most important factors. The corrosion resistance of dental alloys is the result of nobility in composition or the protectiveness of oxide films formed on base metal alloys. Multiphase microstructures are capable of exhibiting increased tarnish and corrosion because of the galvanic coupling of the individual components. The heat treatment state of cast alloys has an important influence on corrosion resistance (Ref 80). Surface state or finish also influence corrosion; furthermore, cast restorations with burnished margins are more susceptible to corrosion because of differences in surface cold-worked states.

Inhibiting Factors

Organics in the form of microorganisms and plaque usually have an accelerating effect on the tarnishing and corrosion of dental alloys (see the earlier sections "Effect of Saliva Composition on Alloy Tarnish and Corrosion" and "Oral Corrosion Processes"). Organics in the form of amino acids, protein, and glycoproteins have received mixed reports. For the amino acids, the building blocks of proteins, the passivation of copper was shown to be improved in Ringer's solution with added cysteine, while nickel became more corrosion prone (Ref 81). Alanine had little effect. For Ti-6Al-4V, the amino acids proline, glycine, tyrosine, and others that constitute many salivary proteins were again shown to have very little effect.

For the plasma proteins, which simulate the organic content in blood and which simulate dental and surgical implant applications more closely, additional evidence can be found implicating the effect of proteins on corrosion behavior. For example, the corrosion rates of cobalt and copper powders increased significantly when exposed to saline solutions with albumin and fibrinogen (Ref 82); however, for chromium and nickel powders, only slight increases occurred, and for molybdenum, decreases occurred. Corrosion of stainless steel by applied external currents was shown to be increased when conducted in saline with added calf's serum (Ref 83). For a copper-zinc alloy, the cyclic voltammetry was reported to be altered by addition of plasma proteins and plasma concentrations to a phosphated physiological saline solution (Ref 84). Albumin and γ-globulin generated increased passivation currents, while fibrinogen generated decreased critical current densities. The anodic polarizations prior to the onset of critical current densities were also shifted to more active behavior in the protein solutions. Finally, the pitting potential for aluminum increased slightly in human plasma, and current-time transients were shifted to lower values in plasma (Ref 85).

Carbon Dioxide/Bicarbonate Buffering System. The major buffering system in saliva is the CO_2/HCO_3^- system, which has been found to inhibit corrosion processes on dental alloys. Inhibition results from the deposition of such elements as copper, zinc, and calcium as carbonate films. Carbon dioxide, above all other gases, is contained most abundantly in saliva. Up to about 150 vol% (~3000 ppm) is contained in vigorously stimulated saliva. The equilibrium concentration of HCO_3^- in saliva is identified by the redox reaction:

$$CO_2(g) + H_2O \rightarrow H^+ + HCO_3^- \qquad \text{(Eq 3)}$$

and with its equilibrium constant pK equal to (Ref 49):

$$pK = 7.9 = -\log \frac{[(H^+)(HCO_3^-)]}{p_{CO_2}} \qquad \text{(Eq 4)}$$

At a pH = 7 and rearranging terms yields:

$$\frac{p_{CO_2}}{HCO_3^-} = 7.9 \qquad \text{(Eq 5)}$$

Equation 5 states that the partial pressure, p, of CO_2 in units of atmospheres is 7.9 times larger than the HCO_3^- concentration in mol/L. Therefore, for p_{CO_2} of the order of 0.07 atm, HCO_3^- concentrations of the order of 0.009 mol/L are formed. This shows that relatively large concentrations of HCO_3^- can be made available in saliva to form carbonates with cations released from corrosion reactions on dental alloys and with other cations found in the mouth, such as calcium.

Many of the different carbonates likely to form are insoluble in aqueous solution. The calcium carbonates are known for making waters hard. Compounds of this type being deposited as thin-film tarnish and corrosion products on dental alloys are very likely to interfere with the corrosion activity. Deposition over cathodic sites effectively increases corrosion resistance by increasing resistance to depolarization reactions. Because the films of carbonates are also likely to increase the contact resistances between electrodes and saliva, galvanic-corrosion processes are likely to change from purely corrosion control to at least partial ohmic control. Under

these conditions, local anodes and cathodes may change in order to maintain lower-resistance paths for both ionic and electronic conduction. For example, the *in vivo* tarnishing of several silver-palladium alloys was shown to be due to the galvanic coupling between microstructural phases located very close to each other on the alloy surface (Ref 86).

Phosphate Buffering System. A secondary buffering system in saliva, the $PO_4^-/PO_4^{2-}/PO_4^{3-}$ system, has also inhibited the corrosion of dental alloys. The progressive inhibition of amalgam corrosion activity in a chloride solution (10 millimolar NaCl) was shown to occur with increasing added phosphate concentrations (Ref 73). A 15 millimolar phosphate addition retarded the anodic polarization almost entirely, while concentrations of 10, 7, 5, and 1 millimolar generated anodic current peaks of about 2.5, 3.0, 3.5, and 6.0 $\mu A/mm^2$, respectively. The 10 millimolar NaCl solution, without phosphate, generated a continuous increase in current, to much larger values. No passivation occurred within the potential range used.

For tin in neutral phosphate solutions, a passive film forms by precipitation or by a nucleation and growth process (Ref 87). Tin phosphate, basic tin phosphate complexes, and tin hydroxides are formed.

Salivary Flow Rate. Increasing the salivary flow rate increases the concentration of most buffering species in saliva. This tends to inhibit corrosion. The organic content, the CO_2/HCO_3^- content, the $PO_4^-/PO_4^{2-}/PO_4^{3-}$ content, pH, and the Ca^{2+} content all increase with flow rate; however, only the increases in Cl^- concentration promote corrosion. Figure 9 shows the effect of flow rate on the concentration of a number of species.

Overview. Saliva acts as an ocean of anions, cations, nonelectrolytes, amino acids, proteins, carbohydrates, and lipids, flowing in waves against and into dental surfaces, with a diurnal tide and varying degrees of intensity (Ref 88). Whether tarnish and/or corrosion of dental metallic materials will occur cannot be categorically stated. It has been discussed that the degree to which dental alloy corrosion occurs in the mouth is dependent on the oral environmental conditions for each person. In addition to effects from the dental alloy itself, competition between corrosive and inhibitory factors of the oral environment will dictate whether corrosion will occur and to what extent. In addition to the aforementioned factors, still others have been isolated and should be included for a more complete assessment of the overall corrosiveness or protectiveness of the oral environment (Ref 73).

Nature of the Intraoral Surface

The composition and characterization of biofilms, corrosion products, and other debris that deposit on dental material surfaces are discussed in this section. As will be shown, the nature of these deposits is dependent on the substrate material (enamel, alloy, porcelain, and so on).

Acquired Pellicles

Characteristics. Most surfaces that come into contact with saliva, including metallic, polymeric, and ceramic dental materials, as well as enamel, interact almost instantaneously with proteins and glycoproteins to form a bacteria-free biofilm of the order of several nanometers in thickness (Ref 89–91). This most intimate layer of organic matter adsorbed to the substrate material is called the acquired pellicle. A fourier transform infrared spectroscopy spectra of the surface of a low-gold dental crown and bridge alloy after *in vivo* exposure is shown in Fig. 19. Detection for protein, carbohydrate, and lipid is indicated. Thicknesses of the films increase only slightly with longer exposure times. The pellicles, in contrast to enamel and most dental alloys, are for the most part acid insoluble, although an acid-soluble fraction also occurs. The films are diffusion barriers against acids, thus reducing the acid solubility of enamel and metallic materials and inhibiting, or at least reducing, the adherence of organisms (Ref 92, 93).

Composition. Chemical analysis of 2-h pellicles formed on enamel indicated abundant amounts of glycine, glutamic acid, and serine (Ref 94). Carbohydrate contents of similar pellicles formed to enamel were found to contain about 70% glucose, with a number of other sugars and small molecules. Acidic proline-rich phosphoproteins have also been identified from *in vivo* enamel pellicles (Ref 95). The proline-rich proteins constitute as much as about 37% of the total proteins in new pellicles within the first hour. However, there is a gradual degradation beginning after about 24 h that is reflected by the fact that the proline-rich protein content in aged pellicles is less than 0.1%.

Substrate Effects on Pellicle Composition. Chemical analysis of the pellicles formed on several plastics and glass showed that the amino acid content varied and was different from that formed on enamel (Ref 96). It was concluded that the chemical composition of the substrate has an important influence on the type of proteins that become adsorbed. For the pellicle formed on dentures, it was concluded that a specific mechanism was controlling the deposition of protein and that specific proteins seemed to be precursors in forming the film (Ref 97). Isoelectric focusing of the extracted proteins adsorbed from a human saliva preparation onto a number of different powder substrate compositions, including palladium, silver, copper, silver-copper, tin, silver-tin-copper alloy, bismuth, polymethyl methacrylate, porcelain, hydroxyapatite, and enamel, indicated that the same three to four proteins appeared to be involved with the adsorption process on all substrates regardless of composition (Ref 41). Therefore, from this study, substrate composition appeared not to affect the type of proteins becoming adsorbed.

Binding Mechanisms. The binding of salivary macromolecules to surfaces has been proposed to consist of electrostatic interactions between the charged groups in the molecule and the surface charges on the substrate (Ref 98). For enamel, only the hydroxyapatite, and not the organic matrix, contributes a surface charge for binding. Because the negatively charged phosphate group comprises about 90% of the surface area of hydroxyapatite, the phosphate group rather than the calcium ions will be the primary binding sites. The hydration layer contains soluble calcium and phosphate ions as well as soluble cations and anions. Because the salivary molecules adsorbed to enamel are mainly acidic, binding to the negatively charged

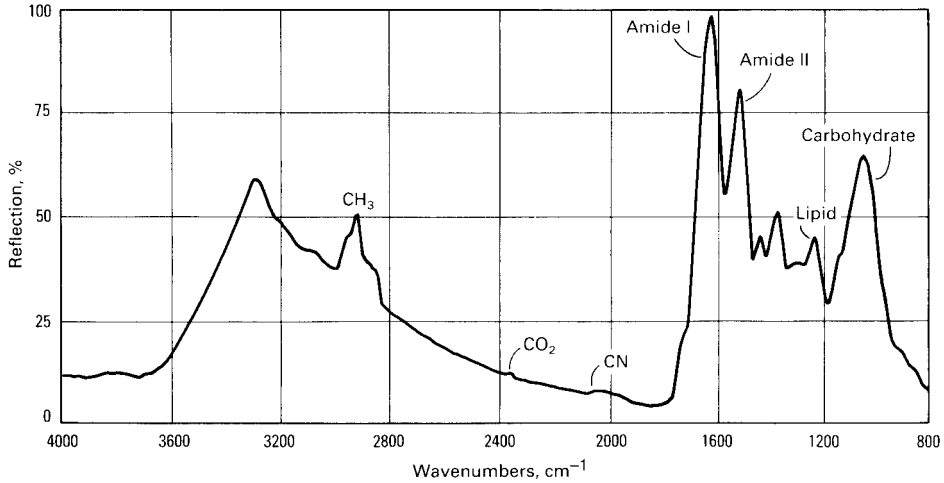

Fig. 19 Fourier transform infrared spectroscopy spectra from surface of a crown and bridge alloy (Midas) after several weeks of intraoral usage. Amide I and II are protein. Additional smaller peaks at 1375 and 1425 cm^{-1} are also protein.

phosphate group appears to occur through a divalent cation, such as calcium. Phosphorylated and sulfated acidic proteins show a high affinity for hydroxyapatite. A direct replacement of the protein phosphate group and the phosphate in hydroxyapatite is also likely (Ref 99).

Direct binding to the calcium surface ions in enamel will also occur, but will be limited because of the relatively small surface area fraction occupied by the calcium ions. Adsorption of salivary proteins to metals may again occur through a divalent cation. The negative charges in the acidic proteins are likely to be bound to the negative anodic surface sites on the metal surface by the bridging cation. Additional information on protein binding and analyses of variations in protein binding to a metal surface through differential scanning calorimetry can be found in Ref 100.

Plaque, Corrosion Products, and Other Debris

Integument. In addition to the thin acquired biofilms, aged pellicles contain microorganisms or plaque, mineralized products, corrosion products, and other debris all commonly referred to as dental calculus. Calculus, which is a byproduct of the reaction between microorganisms and calcification, may form in abundance in some environments. Calculus does not form directly onto teeth or other materials. It is deposited or adsorbed onto the acquired pellicle. The combined surface coating, including the adsorbed pellicle, plaque, and calculus, which includes organic matter and any released ions or corrosion products generated by the substrate, is often referred to as the integument.

Substrate Effects on Integument Characteristics. A study was made of the effect of the restorative material type on plaque composition (Ref 101). The carbohydrate/nitrogen ratios (CHO/N) were similar for amalgam, gold inlay, gold foil, and resin. Plaque analyzed from freshly placed restorations had CHO/N = 1; this value increased to 1.3 and 1.2 at 3 and 6 months, respectively, and decreased to 0.5 at 1 year and for old restorations. It was proposed that the variation in plaque carbohydrate content with the age of the restoration was due to corrosion or to the absorption of impurities into surface porosities and pits. These mechanisms are supported by the data generated with silicate restorations. This was the only material to show significant differences in CHO/N. The CHO/N was 1.0 at 1 year. This suggests that the carbohydrate is metabolized less efficiently by the silicate. It is known that silicate restorations leach fluoride with time. Therefore, the fluoride acts as an enzyme inhibitor.

The thicknesses of the integuments formed in the mouth vary and may depend on the substrate material. For example, sputtering times in Auger electron spectroscopy (AES) depth profiling required only 0.3 min to reach the amalgam substrate, while 2.4 min was required to reach the gold alloy substrate (Ref 91). Carbon, nitrogen, and oxygen were distributed in much the same manner as films formed on different substrates. The main difference between the integuments formed on the amalgam and on the gold alloy was the presence of tin ions with the amalgam and the presence of copper ions with the gold alloy. The release of substrate ions is likely to interact with the attachment of microorganisms and therefore with the metabolism of plaque.

Substrate Corrosion. Corrosion reactions involve diffusion of ions—whether cations from oxidations or dissolved O_2 and H^+ for reductions—through the formed integument. The surface coating has the ability to act as a diffusion barrier to the movement of ions. Released ions are likely to become complexed, or bound, to the proteins and glycoproteins constituting the integument and free native proteins in the bulk saliva, provided diffusion is not restricted by the integument. Insoluble corrosion products of the oxides, chlorides, sulfides, carbonates, phosphates, and so on have the capability of being deposited at the alloy/film interface or becoming an integral part of the integument. Soluble products, in addition, may be released into the bulk saliva.

For one dental restorative alloy, it was shown that the polarization resistance of the alloy increased with protein concentration, while at the same time, the concentration of soluble species in solution also increased (Ref 63). This situation was explained by the increased effect of proteins in solubilizing corrosion products. Energy-dispersive spectroscopy (EDS) spectra of the corroded surfaces showed reduced peak intensities for chlorine and sulfur on surfaces exposed to the proteins. Therefore, even though the severity of corrosion is less in protein-containing solutions, increased levels of soluble products are still generated.

***In Vivo* Tarnished Film Compositions.** Auger thin-film analysis of the surfaces of dental alloys with varying compositions and after functioning in the mouth indicated that the tarnished films were due to chemical reactions between alloy and inorganic species and to the adsorption and deposition of organic matter (Ref 43). Carbon was the dominant nonalloying element by about six times, followed by oxygen, calcium, nitrogen, chlorine, sulfur, magnesium, silicon, phosphorus, aluminum, sodium, and tin. Of the elements from the alloy itself, copper was dominant. In a microprobe analysis of *in vivo* discolorations on gold alloys, both silver sulfides and copper sulfides were detected, depending on the composition of the alloy. Sulfur was found isolated and carbon was present in greatest quantities (Ref 102).

Intraoral (In Vivo) versus Simulated (In Vitro) Exposures

Need for Laboratory Testing. The tarnish and corrosion behavior of dental alloys under actual oral environmental conditions is required. However, except for selected clinical trials, the initial testing of new and improved alloys for tarnish and corrosion resistance is usually carried out under laboratory conditions in either simulated or accelerated tests. This is so because of:

- The possible human exposure to harmful species
- The variability in the oral environmental conditions from person to person and even with the same person from location to location and with time
- As a result of the variability in the oral environment, the inability to follow the effects on tarnish and corrosion from changes in parameters in alloys and in solution

Most laboratory tests use an artificial saliva or a physiological saline solution, such as Ringer's solution (Table 3), diluted Ringer's solution, various concentrations of NaCl, and various concentrations of Na_2S. The main deficiencies with these solutions is that the nonelectrolytes, including the proteins, glycoproteins, and microorganisms, are not included. This fails to produce the pellicle and integuments on laboratory samples that otherwise would have formed on all intraoral surfaces.

In spite of these shortcomings, for the most part, the inorganic salt solutions have become indicators for the aggressiveness of the oral environment. However, the inability to correlate *in vivo* to *in vitro* behaviors in some instances is likely because of the failure to account for the shortcomings (Ref 86).

The use of solutions with higher-than-normal concentrations accelerates the tarnish and corrosion processes. For example, 3200 immersions of 15 s/min duration in a 5% Na_2S solution with a Tuccillo and Nielsen tarnishing apparatus (Ref 103) is estimated to simulate 12 months of actual in-service use (Ref 104). Ringer's and 1% NaCl solutions, which contain about seven times the Cl^- concentration of human saliva, are used in anodic polarization tests to amplify peaks in current behavior (Ref 60, 61). Corrosion of conventional amalgams in Ringer's or 1% NaCl generates products that are morphologically similar to those from retrieved amalgams after intraoral use (Ref 105, 106).

A comparison of the tarnishing of three gold alloys, both *in vivo* and *in vitro,* indicated that the cyclic immersions in a 5%Na_2S-air environment predicted with considerable reliability the relative susceptibility for the alloys to tarnish (Ref 107). The tarnishing of 81 gold-silver-palladium alloys also indicated accelerated laboratory exposures in Na_2S solution simulated *in vivo* use (Ref 108). *In vivo* and *in vitro* (Na_2S solutions) tarnishing of gold alloys in Na_2S solutions has shown the same microstructural constituents to be attacked (Ref 109, 110). Silver-and copper-rich lamellae were the constituents exhibiting sulfide deposits.

Artificial Solutions in Corrosion and Tarnish Testing. As already indicated, the interior surfaces of restorations are exposed to the

interstitial fluids and the exterior surfaces to the salivary fluids. A physiological saline solution such as Ringer's, which contains a Cl^- concentration of about seven times larger than artificial saliva, is therefore more appropriate for simulating *in vivo* interior surfaces in laboratory testing methodologies. The O_2 content should be reduced to simulate *in vivo* levels in dentin. The use of Ringer's and even higher Cl^- concentrations is appropriate for the testing of corrosion that may occur within marginal crevices of restorations because crevices can become chloride-rich and acidified. However, applying these results to the corrosion occurring on exterior surfaces of restorations may not be appropriate, even when considering that the increased Cl^- corrosion with Ringer's solution would be an even more stringent test and that the results would correspond to maximum corrosion conditions.

An artificial saliva is more appropriate for testing the corrosion of the exterior surfaces of restorations. The artificial saliva should take into account most of the species contained in saliva and not just a selected few that have been known to affect alloy corrosion. The artificial saliva should include the capabilities for generating organic films on the surfaces, even though their effects in isolated tests may prove unimportant. In order to simulate oral environment conditions, the tarnishing of the exterior surfaces of restorations, an artificial saliva incorporating sulfide is appropriate. Even though the normal sulfide concentrations contained in saliva are within low ranges, accumulations of sulfide can occur along and within crevices to justify the use of higher than normal concentrations. However, the sulfur peak intensities detected with secondary ion mass spectroscopy (SIMS) on alloy surfaces exposed to low levels of sulfide solutions were similar to those from solutions containing higher sulfide concentrations. However, the alloy surface color changes responded more to higher sulfide concentrations.

Classification and Characterization of Dental Alloys

As indicated in the introduction to this article, a wide range of dental alloys exist. This selection reviews the following types of alloys available for dental applications:

- Direct filling alloys
- Crown and bridge alloys
- Partial denture alloys
- Porcelain fused to metal alloys
- Wrought wire alloys
- Soldering alloys
- Implant alloys

The effects of composition and microstructure on the corrosion of each alloy group are discussed in this section. Additional information on tarnishing and corrosion behavior of these alloys is discussed later in the section "Tarnish and Corrosion under Simulated or Accelerated Conditions" in this article.

Direct Filling Alloys

Amalgams. Two types of amalgams are used: low copper (referred to as conventional) and high copper. The alloy particles of the low-copper type are all of the single-particle variety, whereas the high copper type can also be of the dispersed particle variety.

Amalgams are produced by combining mercury with alloy particles by a process referred to as trituration. About 42 to 50% Hg is initially triturated with the high-copper types, while increased quantities of mercury are used with the low-copper types. High-speed mechanical amalgamators achieve mixing in a matter of seconds. The plastic amalgam mass after trituration is inserted into the cavity by a process of condensation. This is accomplished by pressing small amalgam increments together until the entire filling is formed. For amalgams using excess mercury during trituration, the excess mercury is condensed to the top of the setting amalgams mass and scraped away. American National Standards Institute (ANSI)/American Dental Association (ADA) Specification No. 1 Alloy for Dental Amalgam details standard requirements for chemical composition, physical properties, mass, foreign material, and loss of mercury for alloys used in the preparation of dental amalgam (Ref 111).

Low-Copper Conventional Amalgams. The alloy particles with the low-copper type are basically Ag_3Sn, the γ phase of the Ag-Sn system, even though smaller amounts of the β phase, a phase richer in silver, may also be present. Copper can be added in amounts up to about 5 wt% and zinc up to 1 to 2%. About 2 to 4% Cu is soluble in Ag_3Sn, while the additional copper usually precipitates as Cu_3Sn, the ε phase of the Cu-Sn system, although amounts of Cu_6Sn_5, the η' phase, may also occur. The low-copper particles are mostly lathe cut irregular, although spherical atomized particles are also used. The amalgamation reaction for a low-copper amalgam is:

$$\begin{aligned} &Ag_3Sn\text{-}Cu_3Sn\text{-}Zn + Hg \rightarrow \\ &\quad Ag_{22}SnHg_{27} + Sn_8Hg + \\ &\quad Ag_3Sn\text{-}Cu_3Sn\text{-}Zn \text{ (unreacted)} \end{aligned} \qquad \text{(Eq 6)}$$

In Eq 6, Ag_3Sn with Cu_3Sn and zinc react with mercury to form two major reaction products of $Ag_{22}SnHg_{27}$ (the γ phase of the Ag-Hg system with dissolved tin and referred to as the γ_1 amalgam phase) and Sn_8Hg (the γ phase of the Sn-Hg system and referred to as the γ_2 amalgam phase) (Ref 112). Unreacted Ag_3Sn with Cu_3Sn and zinc particles are held together in a γ_1 matrix with γ_2 interspersed within the matrix. Typical distributions of the phases range up to about 30 wt% for γ, 60 to 80% for γ_1, 5 to 30% for γ_2, and up to about 3% for ε (Ref 113). Very minimal η' may also form. Zinc is generally distributed uniformly throughout material. Porosities are in all amalgam structures. As high as 6 to 7 vol% occur with some systems (Ref 114). Interconnection of the γ_2 phase throughout the bulk may also occur (Ref 115). Transformation of the γAg-Hg (γ_1 amalgam phase) to the βAg-Hg phase (β_1 amalgam phase) can also occur with aging (Ref 116). However, because of the dissolved tin in the γ_1 structure, stability is increased. Figure 20 presents the microstructure of a polished low-copper amalgam showing the γ, γ_1, and γ_2 phases and some porosity.

High-Copper Amalgams. The alloy particles with the high-copper dispersed-phase type are blends of conventional particles with basically spherical silver-copper eutectic particles in the proportion of about 3 to 1, respectively. The dispersed particles can be composed of a variety of silver-copper compositions, with other alloying elements, and combined in varying proportions with the conventional particles.

The alloy particles with the single-particle high copper are compositions that can contain up to 30% Cu and more. The particles are mostly atomized into spherical shape.

The setting reaction for high-copper dispersed phase amalgam is:

$$\begin{aligned} &Ag_3Sn\text{-}Cu_3Sn\text{-}Zn + Ag\text{-}Sn + Hg \rightarrow \\ &\quad Ag_{22}SnHg_{27} + Cu_6Sn_5 + \\ &\quad Ag_3Sn\text{-}Cu_3Sn\text{-}Zn \text{ (unreacted)} + \\ &\quad Ag\text{-}Cu \text{ (unreacted)} \end{aligned} \qquad \text{(Eq 7)}$$

and for high-copper single-particle amalgam is:

$$\begin{aligned} &Ag_3Sn\text{-}Cu_3Sn\text{-}Zn \rightarrow \\ &\quad Ag_{22}SnHg_{27} + Cu_6Sn_5 + \\ &\quad Ag_3Sn\text{-}Cu_3Sn\text{-}Zn \text{ (unreacted)} \end{aligned} \qquad \text{(Eq 8)}$$

For dispersed-phase amalgam, γ initially reacts with mercury to form γ_1 and γ_2 phases, as with the low-copper amalgam. However, an additional reaction occurs between γ_2 and the silver-copper particles to form η' and additional γ_1. The η' phase forms reaction rings around the dispersed particles as well as islands of reaction

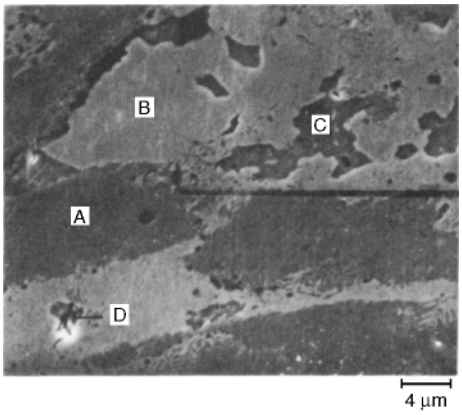

Fig. 20 SEM micrograph of polished, etched, and partially repolished low-copper amalgam (minimax). A, γ; B, γ_1; C, γ_2; D, porosity

phase within γ_1 matrix. Figures 21 and 22 present the microstructure of a dispersed-phase amalgam and EDS x-ray mapping for silver, mercury, tin, and copper, respectively.

For single-particle high-copper amalgam, reaction of the initially formed γ_2 phase occurs with the ε phase of the original alloy particles instead of with a dispersed particle to form the η' phase again. The γ_1 phase is likely to become tin enriched. Reaction zones around the original alloy particles, as well as products within the matrix, occur.

Figure 23 shows the microstructure of a polished, etched, and slightly repolished high-copper single-particle amalgam that shows primarily the distribution of the η' phase. The elimination of γ_2 phase and the subsequent formation of ε phase are time dependent and are dependent on the amalgam system (Ref 117). For fast-reacting amalgams, formation of η' may be complete within hours, while for slower-reacting systems, η' may continue to form for months. The single-particle high-copper amalgams contain higher percentages of the η' phase and lower percentages of the γ_2 phase, although all high-copper amalgams contain minimal γ_2 relative to conventional amalgams. Porosities with the high-copper amalgams can be up to approximately 5 vol% and with a smaller size distribution than with the conventional type (Ref 114). The γ_1 to β_1 transformation can also occur to a limited extent. With the high-copper amalgams, both indium (5%) and palladium (0.5%) containing amalgams add specific characteristics to the amalgams and have gained limited use.

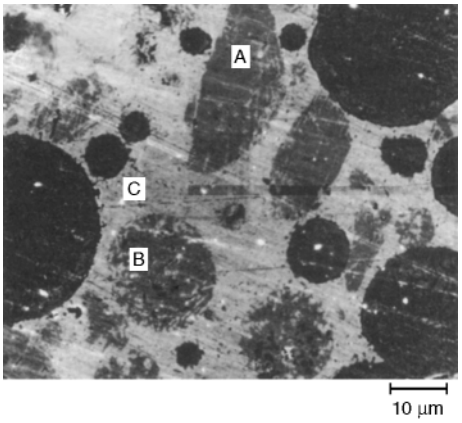

Fig. 21 SEM micrograph of polished, etched, and partially repolished high-copper dispersed-phase amalgam (Cupralloy). A, γ; B, Ag-Cu; C, γ_1. See also Fig. 22.

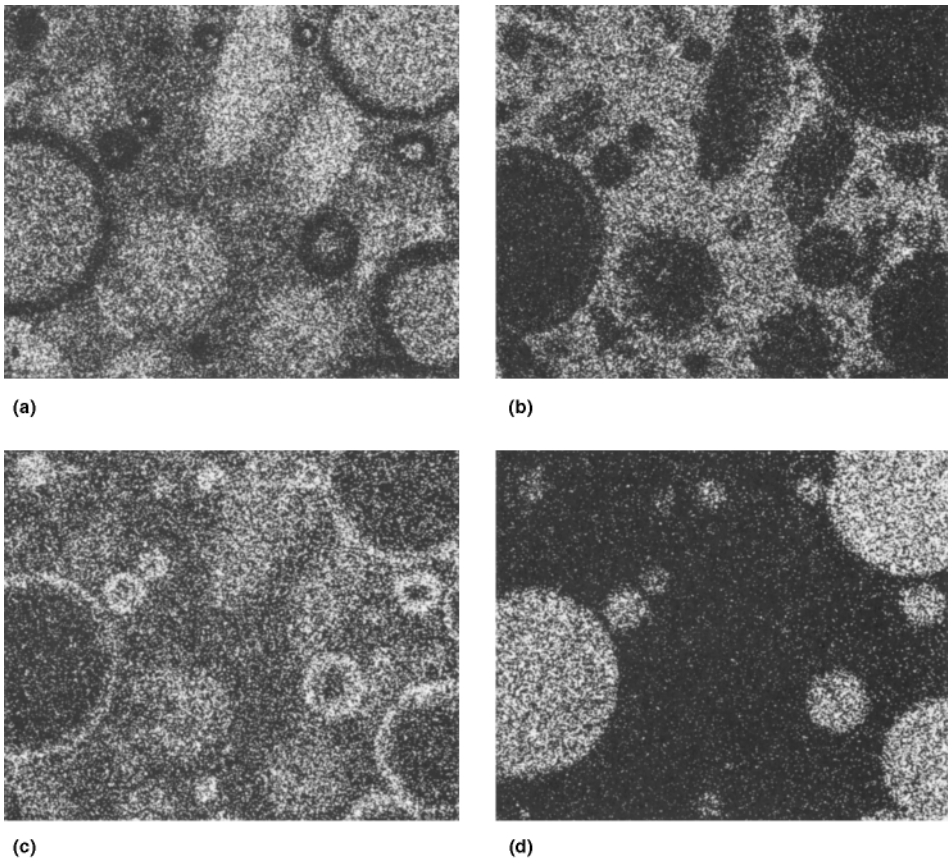

Fig. 22 Elemental maps obtained by energy-dispersive spectroscopy of the high-copper amalgam shown in Fig. 21. (a) Energy-dispersive spectroscopy (EDS) mapping for silver. (b) EDS mapping for mercury. (c) EDS mapping for tin. (d) EDS mapping for copper

Crown and Bridge and Partial Denture Alloys

Noble Dental Alloys. Noble metals have traditionally been used as dental casting alloys for their relative inertness in the oral environment. The metals that are considered to be noble differ depending on the source; however, typically, for dental applications, the noble metals are gold and the platinum-group metals (platinum, palladium, iridium, ruthenium, osmium, and rhodium). Because the alloying of silver with specific amounts of iridium can make it resistant to tarnish and corrosion, many also consider silver to be a noble metal (Ref 118). Historically, the noble dental casting alloys have consisted of alloys with greater than 75 wt% Au and metals of the platinum group, as indicated in the *Composition* requirement section of the 1966 edition of ANSI/ADA Specification No. 5 for "Dental Casting Gold Alloy" (Ref 119). This requirement was based on a belief that to attain acceptable corrosion and tarnish resistance in the oral cavity, dental casting alloys had to comprise at least this minimum percentage of noble metals. This belief was reflected by the fact that before 1969, over 95% of the fixed dental prostheses sold in the United States were made of alloys with a minimum of 75 wt% Au and other noble metals; however, in this same year, the United States government ended its support on the price of gold, placing it on the free market, and by the early eighties, the price of gold had increased from around $35 per ounce to over $400 per ounce (Ref 120). This created an impetus for the development of alternative alloys that used less gold and other noble metals. Eventually, advances in metallurgy yielded dental casting alloys with gold contents of less than 50 wt% that could exhibit acceptable corrosion and tarnish behavior in the oral environment (Ref 118). The clinical success and widespread use of these lower-cost alloys in dentistry prompted the revision of ANSI/ADA Specification No. 5 in 1989 (Ref 121). The revised

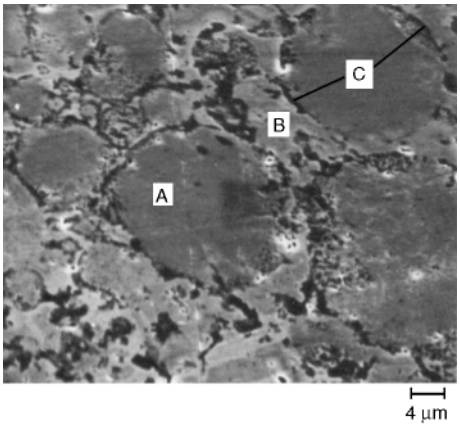

Fig. 23 SEM micrograph of polished, etched, and partially repolished high-copper amalgam (Sybraloy). A, alloy particles; B, γ_1; C, η'

specification dropped the compositional requirements, removed the word "gold" from the title, and suggested both a corrosion and tarnish test, which then became requirements in a further revision in 1998 (Ref 122). For the purpose of dental procedure codes, the ADA classifies "high noble" and "noble" dental casting alloys as follows (Ref 123):

- *High noble*: noble metal content (gold and metals of the platinum group) $\geq$60 wt% and gold $\geq$40 wt%.
- *Noble*: noble metal content (gold and metals of the platinum group) $\geq$25 wt%.
- *Gold-base*: must contain $\geq$40 wt% Au and gold must be the major element of the alloy.

This classification system is also supported by the Identalloy Council, which is a group (formed in 1986) comprising the major dental materials manufacturers. Table 4 shows the compositions of some common gold-base dental alloys.

The high noble dental alloys for cast appliances are primarily based on the gold-silver-copper ternary, with additions of palladium, platinum, and zinc, as well as grain-refining elements, such as rubidium and iridium. For the most part, the properties of the high noble dental alloys follow similar patterns as those shown by the gold-silver-copper ternary alloys, although the additional alloying elements in the dental alloys have significant effects on properties. Because the high noble alloys have relatively small liquidus-solidus gaps, casting segregations, inhomogeneities, and coring effects are not major problems. Microstructurally, single-phase structures predominate because compositions fall within the single-phase region of the Au-Ag-Cu system. Grain refinement by the noble metal additions of ruthenium and iridium decreases grain sizes 20 to 50 μm (0.8 to 2 mils) and increases strengths and elongations by about 30 and 15%, respectively (Ref 124).

The primary hardening mechanism in gold-base dental alloys is by disorder-order superlattice transformations of the Au-Cu system. The ordered domains of the Au-Cu system also extend into the ternary phase Au-Ag-Cu regions. Typically, heat treatment times and temperatures are 15 to 30 min at 350 to 375 °C (660 to 705 °F). Often, it is adequate to bench cool the casting in the investment after casting to gain hardness. Because of the complexity of the dental gold alloy compositions, the exact hardening mechanisms depend on the particular composition of the alloys. Table 5 presents a schematic representation of the age-hardening mechanisms and related microstructures occurring in gold dental alloys. Included are representations for high-gold alloys (HG), low-gold alloys (LG), gold-silver-palladium-base alloys (GSP), and 18 karat and 14 karat gold alloys. Five types of phase transformations are found (Ref 125):

- The formation of the AuCu I ordered platelets and twinning characterized by a stair-step fashion
- The formation of the AuCu II superlattice with periodic antiphase domain structure
- The precipitation of the PdCu superlattice with face-centered tetragonal structure analogous to the AuCu I
- Spinodal decomposition giving rise to a modulated structure
- The formation of the lamellae structure developed from grain boundaries by discontinuous precipitation

The noble metal alloys comprise a wide variety of compositions. Gold-, palladium-, silver-, and copper-base alloys are used. Platinum and zinc contents are usually held to several wt% maximum, if present. Microstructurally, the low-gold-content casting alloys are complex, and examination of phase diagrams of either the Au-Ag-Cu or Ag-Pd-Cu ternary systems indicates that the liquidus-solidus gaps between the various phases can be large (Ref 124). Therefore, coring and casting segregations occur upon solidification during casting. The alloys are characterized by dendritic structures combined with additional phases located within interdendritic positions. Both silver- and copper-rich segregations occur. The presence of gold, platinum, zinc, and other alloying elements further complicates the structures.

The addition of palladium and zinc to the Au-Ag-Cu alloy systems makes heat treatments to single-phase structures difficult. In silver-rich phases, the solubility limit for palladium and zinc is only about 1 to 2% at 500 °C (930 °F), while for copper-rich phases, solubilities are much higher—of the order of 10%. Therefore, precipitation of palladium- and zinc-rich phases occurs. Differences also occur in the gold contents between the phases with the copper-rich phases having the higher contents (Ref 126).

Silver-palladium-base alloys with additions of copper, gold, and zinc are also complex and contain multiple phases. Microstructurally these alloys are characterized by silver-rich matrices interspersed with Pd-Cu-Zn enriched compounds.

The hardening mechanisms associated with some of these noble alloys are shown in Table 5. In addition to the gold-copper disorder-order transformations, ordering due to the palladium-copper superlattices is also usually involved because of replacement of some of the gold by palladium.

Table 4 Compositions, yield strengths, and percent elongation for some common gold-base alloys

	Heat treatment		YS, MPa (ksi)		Elongation, %	
Composition, wt%	Annealed	Hardened	Annealed	Hardened	Annealed	Hardened
Au 83.4, Ag 11.5, Cu 5.0, Pd<1.0, Ir<1.0	A2	...	162 (3)	...	36	...
Au 83.0, Ag 12.0, Cu 4.0, Pd 0.95, Ir 0.05	AC	...	125 (18)	...	33	...
Au 77, Ag 13.54, Cu 7.95, Pd 1.00	A1	...	221 (32)	...	37.5	...
Au 77.0, Ag 13.63, Cu 7.87, Pd 0.95, Zn 0.5, Ir 0.05	AC	...	233 (34)	...	50	...
Au 76.8, Ag 12.8, Cu 8.3, Pd<0.10, Zn+In+In<1.0	A3	...	263 (38)	...	37	...
Au 74.5, Ag 11.0, Cu 10.45, Pd 3.5, Zn 0.5, Ir 0.05	A7	...	325 (47)	...	26	...
Au 74.0, Ag 12.0, Cu 9.0, Pd 3.8, Zn+In+Ir<1.0	A4	...	283 (41)	...	32	...
Au 68.75, Ag 12.4, Cu 12.34, Pd 3.35, Pt 2.9	A1	Hd1	328 (48)	568 (82)	36	12
Au 68.75, Ag 12.4, Cu 12.35, Pd 3.3, Pt 2.9, In 0.25, Ir 0.05	A7	Hd3	393 (57)	569 (83)	32	15
Au 68.3, Ag 10.0, Cu 13.8, Pd 3.6, Pt 2.9, Zn 1.1, In Ir<1.0	A6	Hd2	369 (54)	643 (93)	32	8
Au 66.5, Ag 14.50, Cu 14.49, Pd 3.50, Zn 1.0	A1	Hd1	384 (56)	700 (102)	36	7
Au 60, Ag 26.7, Cu 8.80, Pd 3.75	A1	...	249 (36)	...	41	...
Au 60, Ag 22, Cu 14, Pd 3.75	A1	Hd1	358 (52)	644 (93)	37.5	4
Au 58, Ag 27, Cu 10.49, Pd 3.25	A1	...	296 (43)	...	39	...
Au 56, Ag 25, Cu 13.75, Pd 4.00	A1	Hd1	343 (50)	602 (87)	40	6
Au 50.0, Ag 35.0, Cu 9.5, Pd 3.5, In 2.0, Ir<1.0	A5	...	270 (39)	...	32	...
Au 46, Ag 39.5, Cu 7.49, Pd 6.00, Zn 1.00	A1	...	268 (38)	...	28	...
Au 42.00, Ag 25.85, Cu 22.05, Pd 9.09	A1	Hd1	437 (63)	747 (108)	26	4.5

Key to abbreviations: YS, 0.2% offset yield strength; AC, as cast; A1, annealed at 704 °C (1299 °F) for 15 min and water quenched (wq); A2, annealed at 700 °C (1290 °F) for 10 min and wq; A3, annealed at 700 °C (1290 °F) for 30 min and wq; A4, annealed at 705 °C (1301 °F) for 15 min and wq; A5, annealed at 675 °C (1245 °F) for 15 min and wq; A6, annealed at 675 °C (1245 °F) for 10 min and wq; A7, annealed at 700 °C (1290 °F) for 15 min and wq; Hd1, hardened at 315 °C (600 °F) for 25 min and air cooled (ac); Hd2, hardened at 345 °C (655 °F) for 30 min and ac; Hd3, hardened at 350 °C (660 °F) for 15 min and ac

Base Metal Alloys. Predominantly base metal dental casting alloys are classified by the ADA, according to their noble metal content, as follows: Predominantly base—noble metal content (gold and metals of the platinum group) $\leq$25 wt%. A significant amount of the base metal alloys for metal cast crowns and bridges are composed of nickel-chromium alloys, although stainless steels are also used, particularly outside of the United States. Nickel-chromium alloys are also used for the construction of partial dentures; however, cobalt-chromium alloys far exceed any other alloy for use in this application. Titanium alloys are also gaining popularity for dental applications.

Nickel-Chromium Alloys. The primary alloying element with the nickel-base alloys is chromium between about 10 and 20 wt%: Molybdenum up to about 10%; manganese and aluminum up to about 4% each; and silicon, beryllium, copper, and iron up to several percent each can also be added. The carbon contents range between about 0.05 and 0.4%. Elements such as gallium, titanium, niobium, tin, and cobalt can also be added. Because of differences in properties required for crown and bridge applications versus partial denture applications, minor modifications in compositions occur between nickel-chromium alloys intended for the two applications. This is reflected by the fact that crown and bridge nickel-chromium alloys contain higher percentages of iron, very minimal or no aluminum and carbon, and copper additions (Ref 127).

Chromium and molybdenum are added for corrosion resistance. In order to be effective, these elements must not be concentrated along grain boundaries. Chromium contents below about 10% deplete the interior of the grains leading to corrosion. Molybdenum protects against concentration cell corrosion, such as pitting and crevice corrosion, and is also a solid-solution hardener. Thus, in 1993, the German Federal Health Department recommended a minimum amount of chromium and molybdenum of 20 wt% and 4 wt%, respectively, for dental surgery materials (Ref 128). Manganese and silicon are reducing agents, while aluminum also improves corrosion resistance and improves strength through its formation of intermetallic compounds with nickel. Silicon, like beryllium and gallium, lowers the melting temperature. Beryllium is also a solid-solution hardener and improves castability. Niobium, like molybdenum and iron, affects the coefficient of thermal expansion. Gallium is a stabilizer and improves corrosion resistance. The oxide-forming elements and the elements promoting good bond strength to porcelain are discussed later in the section "Porcelain Fused to Metal (PFM) Alloys" in this article.

Cobalt-Chromium Alloys. ASTM F 75 "Standard Specification for Cobalt-28 Chromium-6 Molybdenum Alloy Castings and Casting Alloy for Surgical Implants" sets the compositional requirements for chromium, molybdenum, and carbon, in wt%, as follows: 27.00 to 30.00% for chromium, 5.00 to 7.00% for molybdenum, and a maximum of 0.35% for carbon (Ref 129). Small additions of other elements, such as silicon and manganese at maximum values of 1%, iron at a maximum of 0.75%, and nickel at a maximum of 0.50%, are also sometimes present, with the balance of the alloy being cobalt. This composition forms the basis for two additional generalized compositions. The first includes a group of alloys that has been developed from the aforementioned basic composition but with each modified by the addition of one or more elements in order to obtain a particular range of properties (Ref 130). Some of these modifying elements include gallium, zirconium, boron, tungsten, niobium, tantalum, and titanium.

Table 5 Hardening mechanisms for some dental alloys

The hatched areas represent the hardness peaks on aging of (9/5)°C+ 32 °F.

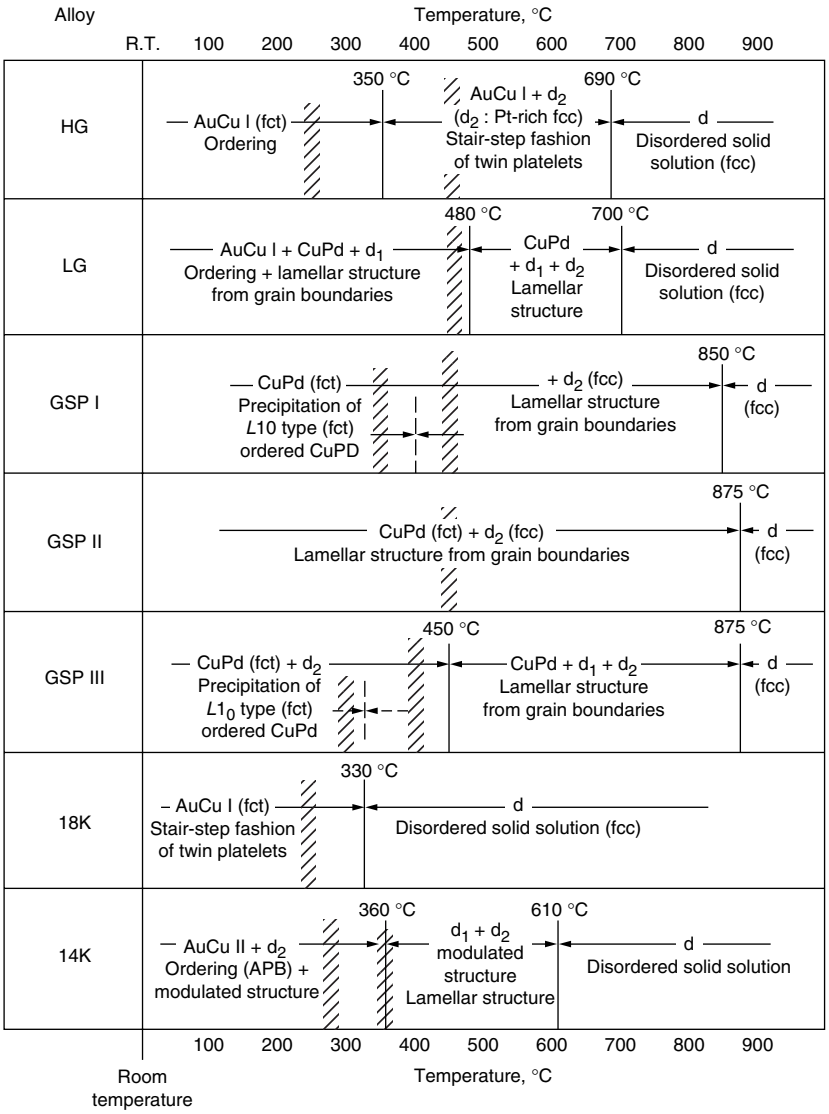

Alloy	Composition, wt%				
	Au	Pt	Pd	Ag	Cu
HG	68	11	6	6	9
LG	30	. . .	22	29	18
GSP-I	20.0	. . .	25.2	44.9	9.9
GSP-II	12.0	. . .	28.0	48.8	11.2
GSP-III	10.0	. . .	25.4	50.0	12.8
18K	75.0	. . .	. . .	8.7	16.3
14K	58.3	. . .	. . .	14.6	27.1

HG, high-gold; LG, low-gold, GSP, gold-silver-palladium. Source: Ref 125

The second generalized composition includes replacement-type alloys, with a major portion of the cobalt replaced by nickel and/or iron. The resulting composition is a cross between cobalt-base alloys and stainless steels. The effects of the individual elements on the properties of the alloys are similar to those already discussed for the nickel-chromium alloys.

Even though chromium is just one of the alloying elements in cobalt-chromium-molybdenum alloys, many studies have attributed the passivating behavior of the films that cover these alloys to the oxides of chromium (Ref 131–135). For example, using electron spectroscopy for chemical analysis (ESCA), Storp and Holm determined that a chromium-rich oxide layer had formed on a Vitallium implant (28% Cr, 6% Mo, Mn + Ni + Fe + W <2%, balance Co) that had been immersed in water, with the chromium that was present being in the trivalent form (Ref 132). Chromium (III) oxide, Cr_2O_3, is known to be a metal deficit (oxygen excess) oxide, or *p*-type semiconductor, under most conditions (Ref 136–140). This is significant because generally for *p*-type semiconductors, oxide growth occurs at the oxide/ambient interface, as a result of outward cation diffusion (Ref 137). Thus, oxide growth occurs at the oxide/electrolyte surface, which makes it feasible to image this oxide growth. With this in mind, in-situ electrochemical atomic force microscopy (AFM) has been performed on a cast cobalt-chromium-molybdenum alloy, relating its electrochemical behavior with its oxide structure (Ref 141, 142).

In general, cobalt-chromium alloys are hardened principally by carbide formation, and it is known that the variance in carbon composition has a great effect on carbide content. An increase in carbon from 0.05 to 0.30% will increase the carbide content from less than 2 to 5% to between 5 and 15% by volume, which will substantially increase the hardness of the alloy (Ref 143). A number of carbides have been detected in dental cobalt-chromium alloys (Ref 144), with MC, M_6C, and $M_{23}C_6$ being the most prominent.

Molybdenum is added to cobalt-chromium alloys as a grain refiner to produce finer grains upon casting and forging, resulting in a material with greater mechanical properties (Ref 145). Molybdenum is also added as a hardening agent, an oxide former, and to increase crevice and pitting corrosion resistance.

The scanning electron micrographs (SEMs) in Fig. 24 show an ASTM F 75 cast cobalt-chromium-molybdenum alloy with a carbon content of 0.22 wt% that was subjected to a homogenizing anneal (Ref 142). The grains range from approximately 50 to 500 μm (2 to 20 mils) in size, and the alloy contains both intragranular (at interdendritic sites) and intergranular carbide distributions, with a variety of shapes and sizes. However, thermomechanical processing of cobalt-chromium-molybdenum alloys can have a drastic effect on the microstructure, as discussed later in the section "Cast, Wrought, and Forged Cobalt-Chromium Alloys."

Titanium-Base Alloys. The first alloy to be successfully cast had a composition of 82Ti-13Cu-4.5Ni with a melting temperature of 1330 °C (2426 °F). The introduction of an argon/electric arc vertical centrifugal casting machine and a vacuum-argon electric arc pressure casting machine made the casting of the higher melting point titanium alloys achievable. Pure titanium and Ti-6Al-4V have been successfully cast by these latter methods (Ref 146).

Copper-aluminum alloys are also used as dental restorative materials. Compositions include the copper base, with about 10 to 20% Al, and up to approximately 10% iron, manganese, and nickel. The as-cast etched structures are dendritic.

Factors Related to Casting. Many factors determine the castability of dental alloys. Some of these factors include the casting temperature and surface tension of the molten alloy as well as many variables associated with the casting technique, some of which include wax pattern preparation, position of the pattern in the casting ring, techniques used in alloy heating, and centrifugal casting force. Some factors affecting casting accuracy include the thermal contraction of the alloy as a result of going from liquid to room temperature, the effectiveness of investment material to compensate for the thermal contraction of the alloy, anisotropic contractions, and the roughness of the casting.

Casting porosity is another important factor in the casting process. Although casting technique variables affect porosity contents, alloy composition can also affect porosity. One way in which composition affects porosity is the generation of internal shrinkage pores between microstructural phases in complex multiphase alloys. This microporosity weakens alloys, makes finishing and polishing more difficult, and is a prime factor in tarnishing. Palladium in alloys is susceptible to occluding gases from the melt. Therefore, palladium-containing alloys have the potential for becoming affected mechanically through embrittlement.

Porcelain Fused to Metal (PFM) Alloys

Stringent demands are placed on the alloy system meant to be used as a substrate for the baking on or firing of a porcelain veneer. The thermal expansion coefficients of alloy and porcelain must be matched so that the porcelain will not crack and break away from the alloy as the temperature is cooled from firing temperature to room temperature. Thermal expansion coefficients of porcelains are in the range of 14×10^{-6} to 15×10^{-6} in./in.°C. Selection of an alloy with a slightly larger coefficient by about 0.05% is recommended so that the alloy will be under slight compression.

The alloy must have a high melting point so that it can withstand the firing temperatures involved with the porcelain. However, the temperature must not be excessively high so that conventional dental equipment can still be used. A temperature of 1300 to 1350 °C (2370 to 2460 °F) is about maximum. The porcelain firing procedures require an alloy with high hardness, strength, and modulus so that thin sections of the alloy substrate can support the porcelain, especially at the firing temperatures.

High mechanical properties are also required for resisting sag of long span bridge unit assemblies during firing. The alloy should also have the ability to absorb the thermal contraction stresses due to any mismatch in expansion coefficients as well as occlusal stresses without plastic deformation. Therefore, too high of a modulus for a material with an insufficient yield strength is contraindicated, although too high of an elastic deformation is also contraindicated. High bond strengths are required so that the porcelain veneers remain attached to the alloy. The alloy system must also be chemically compatible with the porcelain. Alloying elements must not discolor porcelain yet must have tarnish and corrosion resistance to the fluids in the oral environment.

In order to promote and form high bond strengths between porcelain and alloys, the alloy must have the ability to form soluble oxides that are compatible with the porcelain. At the

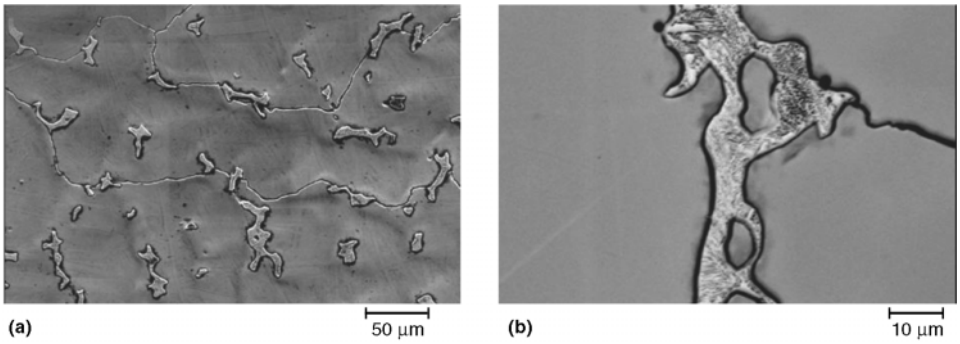

Fig. 24 SEM micrographs showing the microstructure of an ASTM F 75 cast cobalt-chromium-molybdenum alloy that was subjected to a homogenizing anneal. (a) SEM in the secondary electron mode showing both intragranular and intergranular carbide distribution. 350×. (b) SEM in the backscattered electron mode showing a large intergranular carbide. 1500×. The samples were polished to a 0.05 μm (0.002 mils) alumina finish and electrolytically etched in 2% HCl at 3.5 V for 6 s. Source: Ref 142

firing temperature, the porcelain should spread or wet the surface of the alloy. Therefore, both mechanical and chemical interactions are involved in this process. In order to promote chemical interactions, specific oxide-forming elements, such as tin, indium, or gallium, are added to the alloy in low concentrations. The addition of iron, nickel, cobalt, copper, and zinc provide the means for hardening.

The fabrication of the PFM restoration consists of a complex set of processes. After casting, the alloy substrate is subjected to a preoxidation heat treatment to achieve the optimum surface oxides that are important for porcelain bonding. As many as three or more different porcelain firings follow. These include a thin opaque layer adjacent to the alloy, followed by body porcelain layers, including both dentin and enamel porcelain buildups. The opaque layer should mask the color of the alloy from interfering with the appearance of the porcelain. The body porcelain layers build up the restoration to the desired occlusion. The alloy-porcelain systems are slowly cooled from firing temperatures to accommodate dimensional changes occurring in both alloy and porcelain. Therefore, the alloy substrates are subjected to a number of temperature cycles during processing that affect their microstructure and properties. The slow cooling cycles also permit the formation of the compounds important for hardening of alloys.

Noble Metal PFM Alloys. The evolution of alloys for the PFM restoration has generated at least four different noble alloy systems. These are classified as gold-platinum-palladium, gold-palladium with and without silver, silver-palladium, and high-palladium content alloys (Ref 124, 147–149).

Gold-Platinum-Palladium PFM alloys. The compositions of alloys included within this group are in the range of 80 to 90% Au, 5 to 15% Pt, 0 to 10% Pd, and 0 to 5% Ag, along with about 1% each of tin and indium. Other additions may include up to about 1% each of iron, cobalt, zinc, and copper. Platinum and palladium additions increase melting temperature and decrease thermal expansion coefficients, with platinum having the added effect of hardening the alloy. Iron is the principal hardening agent. Iron promotes the formation of an ordered iron-platinum type intermetallic phase that forms between 850 and 1050 °C (1560 and 1920 °F) on cooling from the firing temperature (Ref 124). The ordered phase is finely dispersed throughout the matrix. Iron, along with tin and indium, promotes bonding to porcelain by diffusing into the porcelain up to about 60 μm (2 mils) at the firing temperature. Tin and indium also promote solid-solution strengthening. Alloys within this group range in color from light yellow to yellow.

Even though these alloys have many advantages, their high cost and low sag resistances have necessitated the development of additional alloy systems. Unless they are used in thick sections, for example, 3×3 mm (0.12×0.12 in.), plastic deformation of long spans will occur during firing.

Gold-Palladium and Gold-Palladium-Silver PFM Alloys. Gold-palladium with and without silver alloys were developed as alternatives to the costly gold-platinum-palladium alloys. The Au-Pd-Ag system was one of the first alternative systems. Up to 15% Ag and 30% Pd replaced all of the platinum and a large fraction of the gold from the Au-Pt-Pd system, which resulted in substantial cost savings. The gold-palladium-silver alloys possessed better mechanical properties for the PFM restoration. Because gold-palladium, gold-silver, and palladium-silver are all solid-solution alloys, the ternary Au-Pd-Ag system also forms a series of solid-solution alloys over the entire compositional ranges. Therefore, the matrices of the gold-palladium-silver dental alloys are single phase. Up to 5% Sn is added, which hardens the alloy by forming compounds with palladium that are dispersed throughout the matrix, and it serves as an oxide former and bonding agent with porcelain. Because platinum was avoided, there was no need to incorporate iron for hardening.

A major shortcoming of the Au-Pd-Ag PFM alloys was the ability of silver from the alloys to vaporize, diffuse, and combine with the porcelain at the firing temperature. This resulted in color changes, mostly greenish, along the alloy-porcelain margin, with sodium-containing porcelains being more susceptible to changes in color.

The development of the silver-free gold-palladium alloys eliminated the discoloration of the porcelain. Their compositions cover a wide range: 50 to 85% Au, 10 to 40% Pd, 0 to 5% Sn, and 0 to 5% In, along with possible additions from zinc, gallium, and other elements. The alloy matrix is based on the Au-Pd binary system, which is of the solid-solution type. Hardening is due to Pd-(In, Sn, Ga, Zn) complexes that disperse throughout the matrix. Microstructurally, a fine network of gold-rich regions are entwined by second-phase particles of Pd-(Sn, In, Ga, Zn). Their color is only a pale yellow, unlike some of the deeper yellow gold-platinum-palladium alloys. However, about a 30 to 40% cost savings is obtained. Their mechanical properties are superior, which means good sag resistance at the firing temperatures. The only disadvantage with these alloys is their lower thermal expansion coefficients when used with some of the higher-expanding porcelains.

Some gold-palladium alloys have up to 5% Ag, which is much lower than the 15% contents used with the original gold-palladium-silver alloys. The lower silver concentrations result in better thermal expansion matches with porcelain and the elimination of porcelain discoloration.

Palladium-Silver PFM Alloys. These alloys were developed out of the need to reduce the cost of the PFM restoration even more than from those fabricated from gold-palladium alloys. Compositions range from 50 to 60% Pd, 25 to 35% Ag, 5 to 10% Sn, 0 to 5% In, and up to 2% Zn.

The microstrutures of the alloys are based on the Pd-Ag solid-solution system. Instead of using copper to harden the alloys, hardening occurs through compounds formed between palladium and tin, indium, zinc, and others. Hardening rates are high, which indicates nondiffusional reactions. It is likely that hardening occurs by ordering processes that form by spinodal decomposition (Ref 124). Oxides are imparted to the alloy surface because of the oxide-forming ability of indium, tin, and zinc alloying additions. This promotes high bond strengths. The mechanical properties of the palladium-silver alloys, along with the high-palladium alloys discussed subsequently, are superior to those of any other system, excluding the nickel-chromium alloys. As with the gold-palladium-silver alloys, the chief shortcoming of the palladium-silver PFM alloys is the ability of silver to discolor porcelains during firing. In order to overcome this problem, various methods have been used, including coupling agents composed of porcelains or colloidal gold.

High-Palladium PFM. The compositions of these alloys are 75 to 85% Pd with 0 to 15% Cu, 0 to 10% Ga, 0 to 8% In, 0 to 5% Co, 0 to 5% Sn, and 0 to 2% Au. The alloys are based on either the Pd-Cu-Ga or the Pd-Co-Ga ternary systems. Regardless of the high copper contents, these alloys do not induce porcelain discoloration and bonding problems. Many of these alloys have better workability than other types of PFM alloys, while retaining high hardnesses. The hardness is dependent on the formation of intermetallic compounds with palladium on cooling from the firing temperature. Because of their oxidizer content, the alloys form strong bonds with porcelain. Oxides form with palladium and the alloying additives. However, palladium oxide (PdO) forms only during heating and cooling because of the relatively low decomposition temperature for the oxide.

The oxide-forming ability of the added oxidizers is dependent on alloy composition, temperature, and time. Indium, gallium, and cobalt oxidize preferentially, while copper and tin show nonpreferential oxidation. Cobalt suppressed the oxidation for copper and tin in one alloy system (Ref 150).

Base metal PFM alloys are primarily composed of the nickel-chromium alloys. Cobalt-chromium alloys are also used, but they constitute only a very small percentage of base metal use for PFM.

The nickel-chromium PFM alloys are very similar, if not the same, as the compositions of the nickel-chromium alloys used for partial dentures, which are discussed earlier in this article. One distinction in the compositions, however, is the absence of carbon with the PFM compositions (Ref 127).

The mechanical properties of the nickel-chromium alloys are excellent for the PFM restoration. The high strengths, moduli, yield strengths, and hardnesses are used to advantage

with PFM and partial dentures. Thinner alloy sections can be made from nickel-chromium alloys than from the noble metal alloys. The flexibilities of long span partial denture frameworks are only one-half those for the high gold-content alloys. Additionally, the sag resistances of the nickel-chromium alloys at the porcelain firing temperatures are superior to all of the noble metal alloys.

The bond strengths are seriously impaired by nonadherent or loosely attached oxides. A properly attached oxide is characterized by minute protrusions on the underside of the oxide layer at the alloy/oxide interface that extends into the alloy. For alloys containing additional microstructural phases, larger peg-shaped protrusions also occur on the underside of the oxide layer, improving oxide adherence (Ref 151). The oxide layer on nickel-chromium alloys contains nickel oxide (NiO) on the exterior of the oxide scale, chromium oxide (Cr_2O_3) at the interior covering the alloy, and nickel-chromium oxide ($NiCr_2O_3$) in between. The relative amounts of the oxides depend on the chromium concentration and alloying elements in the alloy, as well as temperature, time of oxidation, and pO_2 in atmosphere.

The bond strengths between alloy and porcelain are significantly affected by minor alloying elements. The additional alloying elements of molybdenum, aluminum, silicon, boron, titanium, beryllium, and manganese also form oxides of their own. An aluminum content of 5% is necessary for aluminum oxide (Al_2O_3) to form, while 3% Si is required to form silicon dioxide (SiO_2), which increases in concentration as the alloy/oxide interface is approached. Manganese forms manganese oxide (MnO) and manganese chromite ($MnCr_2O_4$), and these are mainly concentrated at the outermost part of the oxide. Even though molybdenum oxide (MoO) volatizes above 600 °C (1110 °F), molybdenum is still found in the oxide layer close to the alloy/oxide interface with alloys containing more than 3% Mo. Beryllium, which improves the adherence of the oxide layer to the alloy, is also found concentrated near the alloy/oxide interface.

The cobalt-chromium PFM alloys typically comprise nickel, tungsten, and molybdenum as major alloying elements. Tungsten and molybdenum are high-temperature strengtheners, and, therefore, increase sag resistance. Tantalum and ruthenium can also be added in minor amounts. The carbon is also reduced or eliminated with PFM alloys (Ref 127). The carbon monoxide gases generated during firing of porcelain are likely to cause porosities in the interface and in the porcelain.

Wrought Alloys for Wires

Property Requirements with Orthodontic Biomechanics. Orthodontic wires (frequently used round sizes are 0.3 to 0.7 mm, or 0.012 to 0.028 in., in diameter) constitute a large percentage of the wrought alloys used in dentistry. The orthodontic wires most commonly used include stainless steels, cobalt-chromium-nickel alloys, nickel-titanium alloys, and β-titanium alloys. Note that gold-base wires are used on a very limited basis (formerly, they were used more extensively). The stainless steel and cobalt-chromium-nickel wires have been used extensively with conventional orthodontic biomechanics. That is, the ability to move teeth was based to a large extent on the stiffnesses of the wire appliances. Materials with high yield strength to modulus of elasticity ratios were required. However, the nickel-titanium and β-titanium alloys take advantage of relatively lower yield strength to modulus of elasticity ratios. This is because even though slopes for the stress-strain curves of these alloys are low, the released energies (area under the stress-strain curve) can still be large, as a result of greater deflections. Certified orthodontic wires comply with the property requirements of ANSI/ADA Specification No. 32, "Orthodontic Wires," which covers base metal wires for orthodontics (Ref 152).

Stainless Steel and Cobalt-Chromium-Nickel Wires. The stainless steels used are usually the austenitic 18-8 type (approximately 18% chromium and 8% nickel by weight), although precipitation-hardening type steels have also been used. The springback of the 18-8 wires can be improved by a stress-relief heat treatment. For instance, heat treatment of the as-received drawn wires at 400 °C (750 °F) treatment for 10 min generates significant improvements in springback (Ref 153). The cobalt-chromium-nickel wires also generally include nickel and iron as other major alloying elements. Aluminum, silicon, gallium, and copper are not added to the cobalt-chromium-nickel wires, as with the PFM cobalt-chromium alloys, because bonding agents with porcelain are not needed. Mechanical properties are controlled primarily through the addition of carbon, which affects carbide formation. Although the operator has some control over the mechanical properties of the cobalt-chromium-nickel wires through heat treatments, these wires are supplied in different temper designations from soft to semiresilient to resilient (Elgiloy is one of the commonly used cobalt-chromium-nickel alloys).

Nickel-Titanium and β-Titanium Wires. The elasticity effect of nickel-titanium (generically referred to as Nitinol) is one of its most important characteristics. Nickel-titanium wires can almost be bent back on themselves without taking a permanent set. Even greater deformations, by as much as 1.6 times, can be achieved with superelastic nickel-titanium alloys (Ref 154). Nickel-titanium orthodontic alloys are primarily composed of the intermetallic compound NiTi. The alloy is tough, resilient, and has a low modulus of elasticity. Cobalt is sometimes added to nickel-titanium wires in order to obtain critical temperatures that are useful for the shape memory effect of the alloys. Furthermore, copper and chromium ranging from 5 to 6% and 0.2 to 0.5% by weight, respectively, have been added to superelastic nickel-titanium wires to obtain shape memory at temperatures between 27 and 40 °C (81 and 104 °F); however, an in-vitro study in simulated physiologic media showed that these alloy additions did not affect the corrosion resistance of the wires (Ref 154).

Alpha-titanium (hexagonal close-packed structure) is the stable form of titanium at room temperature. By adding alloying elements to the high-temperature form of β-titanium (body-centered cubic structure), the β phase can also exist at room temperature, but in the metastable condition. The β stabilizers include molybdenum, vanadium, cobalt, tantalum, manganese, iron, chromium, nickel, cobalt, and copper. Beta-titanium is strengthened by cold working or by precipitating the phase. A variety of heat treatments can be used to alter the properties of the wires (Ref 155).

Soldering Alloys

Composition and Applications. Gold-base and silver-base solder alloys are used for the joining of separate alloy components (Table 6). High fusing temperature base alloy solders are also used for the joining of nickel-chromium and other alloys. In many cases, the term *brazing* would be more appropriate, but the term is seldom used in dentistry (technically, brazing is performed at temperatures exceeding 425 °C, or 800 °F, and soldering is performed at temperatures below this value). The gold-containing solders are used almost exclusively in bridgework because of their superior tarnish and corrosion resistance. The use of non-noble metal containing silver-base solders is limited mainly to the joining of stainless steel and cobalt-chromium wires in orthodontic appliances because of the impermanence of the appliances.

The joining by soldering of small units to form a large one-piece partial denture is employed in some processing techniques. This is done to prevent framework distortions that may occur with large one-piece castings. The salvaging of large, poorly fitting castings by sectioning, repositioning, and soldering the pieces together also takes place. For PFM restorations, soldering is carried out either prior to or after the porcelain has been baked onto the alloy substrate. Presoldering uses high fusing temperature solders, while postsoldering uses lower fusing temperature solders.

Gold-base solders are most often rated according to their fineness, that is, the gold content in weight percent related to a proportional number

Table 6 Compositions of some dental solders

	Composition, wt%						
Type	Au	Pd	Ag	Cu	Sn	In	Zn
Silver	...	...	52.6	22.2	7.1	...	14.1
Gold	45.0	...	20.6	28.4	4.3	...	2.9
Gold	63.0	2.7	19.0	8.6	...	6.5	...

of units contained in 1000. Conventional gold-base crown and bridge alloys are seldom soldered together with solders having less than a 600 to 650 fineness. The soldering of gold-base wire clasps to cobalt-chromium partial dentures is another application for the higher-fineness solders. However, with the use of the low-gold-content crown and bridge alloys, lower-fineness solders are used. The lower-fineness solders are also occasionally used to solder the cobalt-chromium-nickel wires. The gold-base solders usually do not contain platinum or palladium, which increases melting temperatures. The important requirement to be satisfied during soldering is that the solders melt and flow at temperatures below the melting ranges of the parts to be joined.

The compositions of gold-base solders are largely gold-silver-copper alloys to which small amounts of other elements, such as zinc, tin, and indium, have been added to control melting temperatures and flow during melting. The silver-base solders are basically silver-copper-zinc alloys to which smaller amounts of tin have been added. The higher-fusing solders, to be used with the high-fusing alloys, are usually specially formulated for a particular alloy composition because not all alloys have good soldering characteristics.

Microstructure of Solder-Alloy Joints. The microstructural appearance of the gold alloy-solder joints provides information as to their quality. A thin, distinct, continuous demarcation between the solder alloy and the casting alloy should exist, indicating that the solder has flown freely over the surface and that no mutual diffusion between the alloys has occurred. The junction region should be free of isolated and demarcated domains, indicative of the formation of new alloy phases. Obviously, porosity is to be avoided. However, microporosity among the phases in solder may be unavoidable. As with the cooling that occurs with all alloys, differences in the thermal expansion coefficient among phases can generate microporosity. The presence of a distinct layer of columnar dendrites within the solder, starting at the solder/alloy interface and projecting into the solder bulk, is assurance that there has been no tendency of the alloy surface to melt (Ref 156). The solidified solder tends to match the grain size of the parent alloy by epitaxial nucleation of the solder by the casting alloy. The microstructural characteristics of low-gold-content casting alloys interfaced by soldering affect the microstructural characteristics of the solidified solder (Ref 156).

Microstructurally, a silver-base solder is multiphasal. Both silver- and copper-zinc-rich areas occur, which is in contrast to some of the higher-fineness gold-base solders that are single phase.

Implant Alloys

Applications and Compositions. Dental implants, which are used for supporting and attaching crowns, bridges, and partial and full dentures, can be of the endosseous and subperiosteal types. The endosseous implants pass into or through the mandibular or maxillary arch bones, while the subperiosteal implants are positioned directly on top of or below the mandibular or maxillary bones, respectively. Endosseous implants are usually selected for size and type from implants already made, while the subperiosteal implants are usually custom made for the particular case. Therefore, both cast and wrought forms of implants are used. The alloys used for dental implants are similar in composition to the alloys mentioned previously for use with crowns and bridges and partial dentures. These include stainless steel, cobalt-chromium, and titanium and its alloys (Ref 28, 127).

Cast, Wrought, and Forged Cobalt-Chromium Alloys. In addition to castings, cobalt-chromium alloys for surgical implants can also be obtained in the wrought and forged condition. ASTM F 1537 and F 799 for wrought and forged cobalt-chromium-molybdenum alloys, respectively, specify both low- and high-carbon alloys, along with a dispersion-strengthened alloy (Ref 157, 158). The low-carbon and dispersion-strengthened alloys have a maximum carbon content of 0.14 wt%, while the high-carbon alloy has a minimum and maximum carbon content of 0.15 and 0.35 wt%, respectively. In general, the wrought and forged cobalt-chromium-molybolenum alloys exhibit superior mechanical properties to the cast form (ASTM F 75 of the alloy.

The scanning electron micrographs in Fig. 25 show the varied microstructures of five different cobalt-chromium-molybdenum (Ref 142) at the same magnification: an ASTM F 75 cast alloy, two wrought high-carbon alloys, a forged

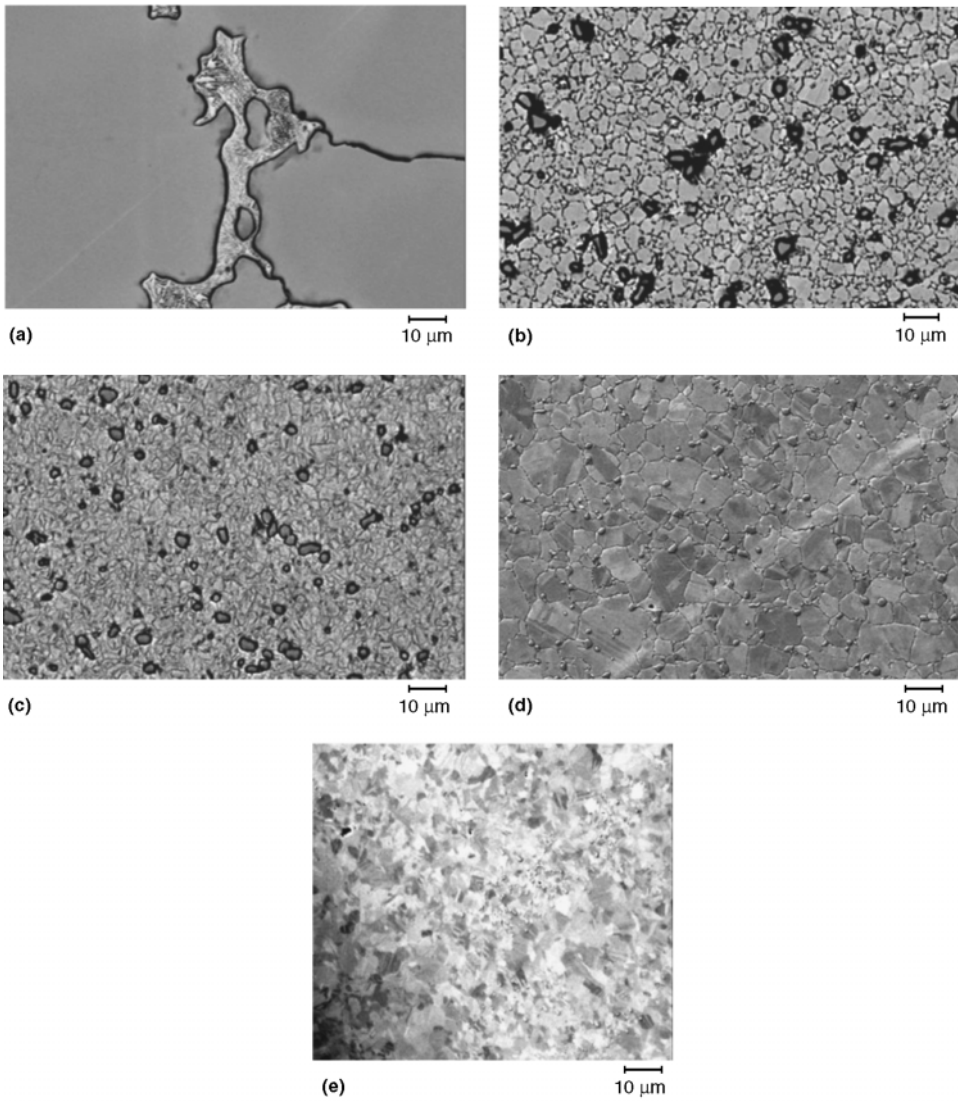

Fig. 25 SEM micrographs in the backscattered electron mode showing the varied microstructures of five different types of cobalt-chromium-molybdenum alloys at a magnification of 1000×. The samples were polished to a 0.05 μm (0.002 mils) finish and electrolytically etched in 2% HCl at 3.5 V for 6 s. (a) ASTM F 75 cast alloy. (b) Wrought high-carbon alloy. (c) Wrought high-carbon alloy in the aged condition. (d) Forged high-carbon alloy. (e) Forged low-carbon alloy. See text for further microstructural details. Source: Ref 142

high-carbon alloy, and a forged low-carbon alloy. The wrought high-carbon and forged high-carbon alloys have a carbon content of 0.24 wt%; the cast alloy has a carbon content of 0.22 wt%; and the forged low-carbon alloy has a carbon content of 0.05 wt%. Figures 25(b) and (c) show the wrought alloys exhibit much smaller grain sizes (about 2 to 8 μm, or 0.08 to 0.3 mils) than the cast alloy (previously described in the section "Cobalt-Chromium Alloys") and are covered by small (2 to 5 μm, or 0.08 to 0.2 mils), mostly spheroidized carbides. The wrought alloys were produced by hot-isostatic pressing powder particles and then hot rolling into a finished product. Generally, this forming operation results in a structure that has fewer voids (low porosity), greater ductility, and finer grains of greater uniformity than the original cast structure (Ref 159). The alloy in Fig. 25(c) was also aged at 730 °C (1350 °F) for 15 h. The aging of the wrought high-carbon alloy resulted in small equiaxed grains and seemed to cause the agglomeration of some of the carbides and the formation of much smaller intergranular precipitates. It is known that the aging of cobalt-chromium-molybdenum alloys produces carbide precipitation along slip lines, twin boundaries, and stacking faults upon quenching, further increasing the hardness of the alloy (Ref 160).

The single-blow forged and water-quenched, high-carbon alloy shown in Figure 25(d) also exhibits much finer grains (2 to 20 μm, or 0.08 to 0.8 mils, in size) than the cast alloy. It is covered with carbides of a semirounded morphology ranging from about 1 to 4 μm (0.04 to 0.2 mils) in size (the majority of which are located in grain boundaries) and small intergranular precipitates. In contrast, the single-blow forged and water-quenched, low-carbon alloy shown in Fig. 25(e) exhibits a highly deformed and twinned structure that contains relatively few dispersed carbides, which are less than 1 μm (0.04 mils) in size.

Modified cobalt-chromium alloys containing higher nickel contents are also used for dental implants. One wrought alloy included in this category is MP35N (35Co-35Ni-20Cr-10Mo). Microstructurally, the alloy takes the character of cobalt-chromium alloys. However, no carbides are formed because carbon has not been added to the alloy.

Porous Surfaces. Alloy powders of the same composition as the implants have been sintered onto the surfaces of the implants for generating bone ingrowth to obtain better retention between the implant and the bone.

Tarnish and Corrosion under Simulated or Accelerated Conditions

Low-Copper Amalgams. The Sn_8Hg (γ_2) phase shown in Fig. 20 is electrochemically the most active phase in conventional amalgam. Upon exposure to an electrolyte, the tin oxide (SnO)/tin couple becomes operative. The formed SnO may or may not protect the γ_2 phase from further corrosion. Depending on environmental conditions, the tin from the γ_2 phase will either be protected by a film of SnO or consumed by additional corrosion reactions.

In the case of an artificial saliva, the γ_2-tin becomes protected. This is shown in Fig. 26 on the anodic polarization curve as the current peak at about −0.7 V versus SCE, which relates in potential to the SnO/Sn couple. With increasing potential, the film protects the amalgam, as shown by the presence of a limiting or passivating current. The film will remain passivating until the potential of another redox reaction is reached that is controlling and nonpassivating. For instance, in a Cl^- solution, this is the situation that occurs when the corrosion potential for the amalgam approaches and surpasses the redox potential for a reaction that produces $SnOCl \cdot H_2O$.

If this condition is satisfied, the SnO passivating film is no longer thermodynamically favorable; therefore, it begins to break down and dissociate, exposing freely corroding γ_2-tin to the electrolyte. Likewise, nonprotective products of the form $SnOHCl \cdot H_2O$ precipitate. This is represented on the polarization curve in Fig. 26 as the sharp increase in current at about −0.1 V versus SCE. As a result of the interconnection of the γ_2 phase, the interior γ_2 can also become corroded. Figure 27 shows the devastating effect that corrosion of the γ_2 phase has on the microstructure of a conventional amalgam, while Fig. 28 shows typical tin-containing products that precipitate on the surface.

High-Copper Amalgams. Corrosion of high-copper amalgams by γ_2-phase corrosion will not occur because of its almost complete absence from the microstructure. Although possessing better corrosion resistance than the γ_2-phase, the Cu_6Sn_5 (η') phase will be the least-resistant phase in the microstructure (Fig. 21, 22). Upon exposure to solution, any corrodible tin within the material first forms a protective SnO film indicated on the anodic polarization curve in Fig. 26 as the small current peak at about −0.7 V. Upon attaining a steady-state corrosion potential in chloride solution, high-copper amalgam is likely to surpass redox potentials for couples of $CuCl_2$/Cu, $Cu(OH)_2$, Cu_2O/Cu, and $CuCl_2 \cdot 3Cu(OH)_2$/Cu. Under these conditions, both soluble and insoluble corrosion products will form. This is indicated on the polarization curve as a small anodic current peak at about −0.25 V.

Microstructurally, if the copper from the η' phase becomes exhausted by corrosion, copper corrosion from the silver-copper and γ particles may also follow. Freed by copper corrosion, tin also becomes corroded. Corrosion of the γ_1-tin decreases the stability of the η_1 phase, which is likely to be transformed into the β_1 phase. Unlike low-copper amalgam, the interior of high-copper amalgam, which demonstrates a lack of interconnection between any of the phases, is not likely to become affected by corrosion. Figure 29 shows a corroded high-copper dispersed-phase amalgam, emphasizing the reaction zones of the η' phase, the interior of the silver-copper particles, the γ particles, and the matrix.

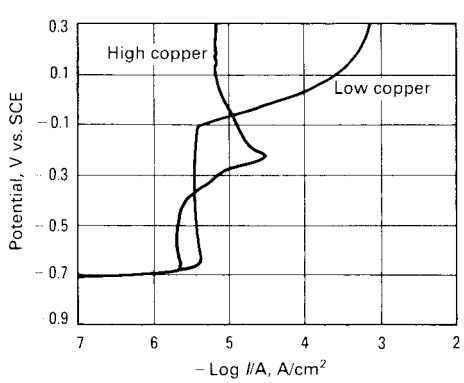

Fig. 26 Anodic polarization at 0.03 V/min of both low (Microalloy) and high (Sybraloy) copper amalgams in artificial saliva. Source: Ref 74

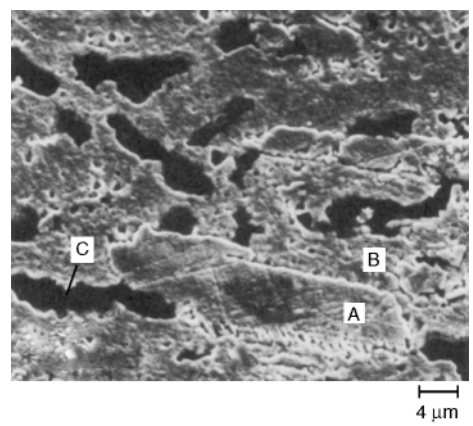

Fig. 27 SEM micrograph of corroded (10 μA/cm²) low-copper amalgam (New True Dentalloy) in 0.2% NaCl after removal of corrosion products by ultrasonics. A, alloy particles; B, matrix; C, regions formerly occupied by γ_2 phase

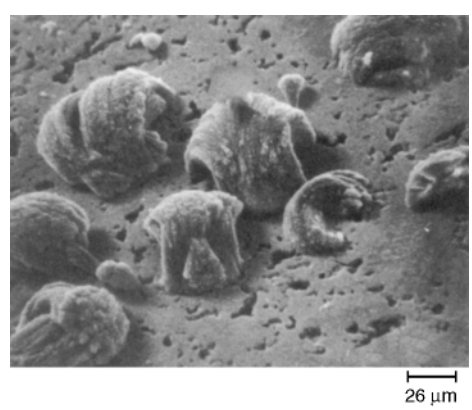

Fig. 28 SEM micrograph of low-copper amalgam (New True Dentalloy) after immersion in artificial saliva. The clumps of corrosion products contain tin.

Tarnish of Gold Alloys. Because tarnish is by definition the surface discoloration of a metallic material by the formation of a thin film or corrosion product, the quantification of dental alloy tarnish by assessing color changes on surfaces is most appropriate. By determining the color of an alloy before and after exposure to a test solution, the degree of discoloration can be obtained by quantitative colorimetry techniques, which are described in Ref 161 to 167. The use of quantitative colorimetry in conjunction with SIMS for determining the effects of alloy nobility (in at.%) and sulfide concentration on color changes in gold crown and bridge alloys is detailed in Ref 168.

Effect of Microstructure on Tarnishing Behavior. The devastating effect of microgalvanic coupling on tarnishing behavior is shown by a comparison of solid-solution annealed (750 °C, or 1380 °F) and as-cast structures (Fig. 30). The as-cast alloys, composed of two-phase structures, consistently showed greater color change or tarnish (Ref 164).

Single-phase, as-cast gold-silver-copper alloys with gold contents between 50 and 84 wt% were observed microstructurally to tarnish in Na_2S solutions by localized microgalvanic cells. The characteristics of the various tarnished surfaces included a uniformly speckled appearance, dendritic attack, matrix attack, grain-boundary dependent attack, and grain-boundary attack. Silver-rich areas discolored preferentially because of the operation of the silver-rich areas as anodes and the surrounding copper-rich areas as cathodes. The uniformly speckled appearance occurred with high-silver, low-copper contents, while the grain orientation dependent appearance occurred with low-silver, high-copper contents. The dendritic and matrix attack occurred with alloys containing intermediate silver and copper contents (Ref 103).

For gold-silver-copper-palladium alloys with gold contents between 35 and 73 wt%, the tarnishability in oxygenated 2% Na_2S has been shown to be affected by altering the microstructure through heat treatment. Tarnishing occurred on multiphase structures annealed at 500 °C (930 °F) but did not occur on single-phase structures annealed at 700 °C (1290 °F). Silver-, copper-, and palladium-rich phases were precipitated. Some alloys, though, showed only silver- and copper-rich phases. In these cases, the palladium tended to follow the copper-rich phase. Splitting of the matrix into thin lamellae of alternating silver and copper enrichments also occurred. The silver-rich phases in all materials were attacked by the sulfide and were responsible for the tarnish. Age hardening by AuCu(I)-ordered precipitates increased the tendency of the silver-rich lamellae to tarnish (Ref 169).

In sulfide solutions, silver sulfide (Ag_2S) is the principle product of tarnish, although copper sulfides (Cu_2S and CuS) also form. These products are produced by the operation of microgalvanic cells set up between silver-rich and copper-rich lamellae. The addition of palladium to gold-silver-copper alloys considerably reduces the rate of tarnishing by slowing down the formation of a layer of silver and copper sulfides on the surface. This has been shown to be due to the enrichment of palladium and gold on the surface of the alloy when exposed to the atmosphere prior to sulfide exposure (Ref 170). The rate of diffusion from the bulk to the surface is hindered by the palladium enrichment. The active sites on the alloy surface for the sulfidation reaction are selectively blocked by the palladium atoms (Ref 170).

Effect of the Silver/Copper Ratio. The silver/copper ratio is an important aspect affecting the tarnish and corrosion resistance of gold dental alloys. A comparison was made of three gold alloys, with similar noble metal contents, but different Ag/Cu ratios (based on wt%) of 41/7.4, 10.3/37.9, and 9.8/37.7 (Ref 169). Polarization tests of the three alloys in a sulfide solution showed that the alloy with a Ag/Cu ratio of 41/7.4 exhibited increases in current density up to 10 $\mu A/cm^2$ at -0.3 V, while the other two alloys exhibited current densities of ~1 $\mu A/cm^2$ extending to positive potentials. Therefore, high silver contents relative to low copper contents in low-gold alloys can have detrimental effects on tarnishing and corrosion. For some low-gold alloys, the best resistance to tarnishing has been obtained by using Ag/Co ratios between 1.2 and 1.4 and a palladium content of 9 wt%.

Effect of the Palladium/Gold Ratio. Increasing the palladium content in gold alloys increases the tarnish resistance. However, in gold-silver-copper-palladium alloys, this effect is greater. The palladium/gold ratio is just as important as the silver/copper ratio. In gold-silver-copper alloys without palladium, the degree of tarnish (subjective test: 0 = least and 8 = most) was evaluated to be between 6.5 and 8 for all silver/copper ratios (1 : 3, 1 : 2, 2 : 3, 1 : 1, 3 : 2, 2 : 1, 3 : 1) (Ref 108). However, in alloys having palladium/gold ratios of 1 : 12, the degree of tarnish diminished to between 2 and 3.

Tarnishing and Corrosion Compared. Figure 31 shows reflection loss versus nobility and weight loss versus nobility for 15 gold alloys. Tarnishing was by immersion for 3 days in 0.1 *M* Na_2S, while corrosion was by immersion for seven days in aerated 0.1 *M* lactic acid plus 0.1 *M* NaCl at 37 °C. As is evident, a number of alloys that appear not to have been affected by corrosion are, however, largely affected by tarnishing (Ref 171).

Corrosion of Gold Alloys. Electrochemical polarization has been applied to the corrosion evaluation of gold dental alloys. Very small current peaks on the anodic polarization curves for some gold alloys in artificial saliva have been detected and interpreted to be due to the dissolution of alloying components (Ref 172).

A comparison of the anodic polarization of noble alloys in artificial saliva with and without sulfide indicated that without sulfide the electrochemistry is governed mainly by chloride ions. The alloys passivate in a state with very low current densities, which makes detection of differences among the alloys difficult. With sulfide added to the artificial saliva, a preferential sulfidation of the less noble alloy component is induced. The sulfidation is characterized by a critical potential and limiting current density, both of which may be dependent on composition (Ref 173).

The corrosion susceptibilities for silver and copper in various gold alloys were quantified by an analysis of both forward and reverse polarization scans (Ref 174). Both silver and copper demonstrated characteristic current peaks. The heights of the current peaks were taken to be a measure of the amount of corrodible silver and copper in the alloys. In a similar technique, the

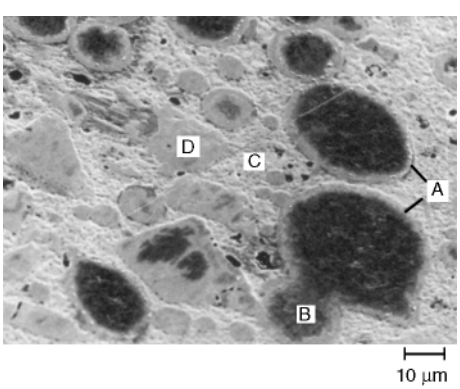

Fig. 29 SEM micrograph of corroded (5 $\mu A/cm^2/d$) high-copper amalgam (cluster) in 0.2% NaCl solution. Note the definition of the γ' rings (A), Ag-Cu particles (B), matrix (C), and η' particles (D).

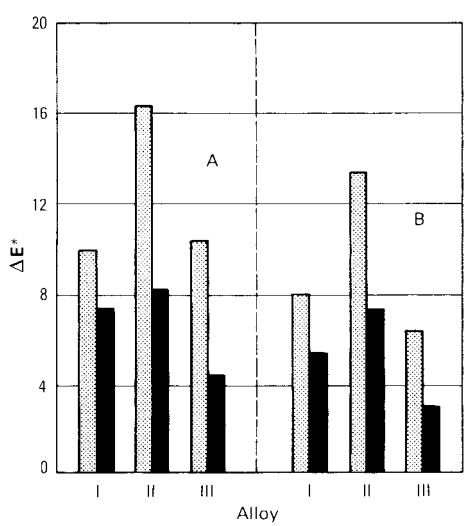

Fig. 30 Color change vector ΔE^* for three low-gold alloys (I, Miracast; II, Sunrise; III, Tiffany) in both the as-cast (left bar for each alloy) and solutionized at 750 °C (1380 °F) (right bar for each alloy) conditions after exposure for 3 days to artificial saliva (A) or 0.5% Na_2S solution (B). Source: Ref 164

integrated current from the polarization curves within a potential range of −0.3 V to+0.3 V versus SCE was taken to be a measure for the corrodible species (Ref 175). Figure 32 shows a plot of the nobility of eight as-cast gold alloys versus their integrated anodic currents.

Silver-Palladium Alloys. Silver is prone to tarnishing by sulfur and is prone to corrosion by chloride. The addition of palladium to silver generates alloys with much better resistance to tarnishing and silver corrosion. In 1/7 diluted Ringer's solution and 0.1% NaCl, alloys with more than 40% Pd showed passive anodic polarization behavior (Ref 176). In sulfur-saturated air, the amount of sulfur deposited onto the surfaces of silver-palladium alloys was minimal for compositions with ≥40 wt% Pd (Ref 173). In artificial saliva, two transitions in the corrosion currents occurred with palladium content. The first occurred at about 22% Pd, where the current decreased from 6 to 1 μA. The second transition occurred at about 29% Pd, where the current decreased to about 0.4 μA and then remained fairly constant throughout the rest of the compositional range (Ref 177). Figure 33 shows the color range vectors for the pure metals and alloys from the Ag-Pd system after tarnishing in artificial saliva with 0.5% Na_2S. The compositions 50Pd-50Ag and 75Pd-25Ag showed the best tarnish resistance (Ref 178).

Corrosion behavior and tarnishing behavior usually must be viewed independently. That is, corrosion is not an indicator for tarnishing, and vice versa. Alloy nobility dominates corrosion behavior, while alloy nobility, composition, and microstructure (in conjunction with environment) influence tarnishing behavior.

Microstructurally, the silver-palladium alloys tarnish by chlorides and/or sulfides becoming deposited over the silver-rich matrix, while the palladium-rich precipitates display resistance to chlorides and sulfides. Furthermore, microstructurally, the alloys are generally composed of a corrosion-resistant copper- and palladium-rich phase and a nonresistant silver-rich phase. Increased tarnish and corrosion of this silver-rich phase component can occur as a result of microgalvanic coupling (Ref 179). Manipulation of the microstructural features through heat treatments can produce structures with varying proportions of the tarnish-resistant and tarnish-prone phases. For example, age hardening has been shown to increase the proportion of the tarnish- and corrosion-prone phases (Ref 180, 181).

High-Palladium PFM Alloys. Alloys with up to 80 wt% Pd and additions of copper, gallium, tin, indium, gold, and others have been shown to exhibit good saline corrosion resistance in the potential range and Cl^- ion concentration associated with oral use. For example, anodic polarization tests showed passive behavior until breakdown occurred, which was at potential magnitudes well above those occurring intraorally (Ref 182).

Nickel-Chromium Alloys. The tarnish resistance and corrosion resistance of these alloys result from balancing the composition with regard to the passivating elements chromium, molybdenum, manganese, and silicon. Alloys containing increased amounts of molybdenum and manganese have shown to exhibit increased passivation; however, increasing the chromium content too much (more than 20%) can precipitate an additional phase and alter the corrosion resistance. By using polarization methods, three different behaviors were observed with 12 nickel-chromium alloys with varying compositions in deaerated and aerated artificial saliva (Ref 183). Some alloys were constantly passive, others were either active/passive or passive according to the aeration condition of the electrolyte, and still others (<16% Cr without molybdenum) were constantly active and corroding.

Corrosion potentials for nickel-chromium alloys in artificial saliva were low, ranging between about −0.2 V and −0.8 V versus SCE. Breakdown potentials varied, depending on composition. For alloys with less than 16% Cr and no molybdenum, breakdown potentials as low as −0.2 V occurred. For compositions with higher chromium contents and with molybdenum and various manganese contents, breakdown potentials as high as +0.6 V also occurred.

Pitting attack occurs with these alloys because they rely on protective surface oxide films for

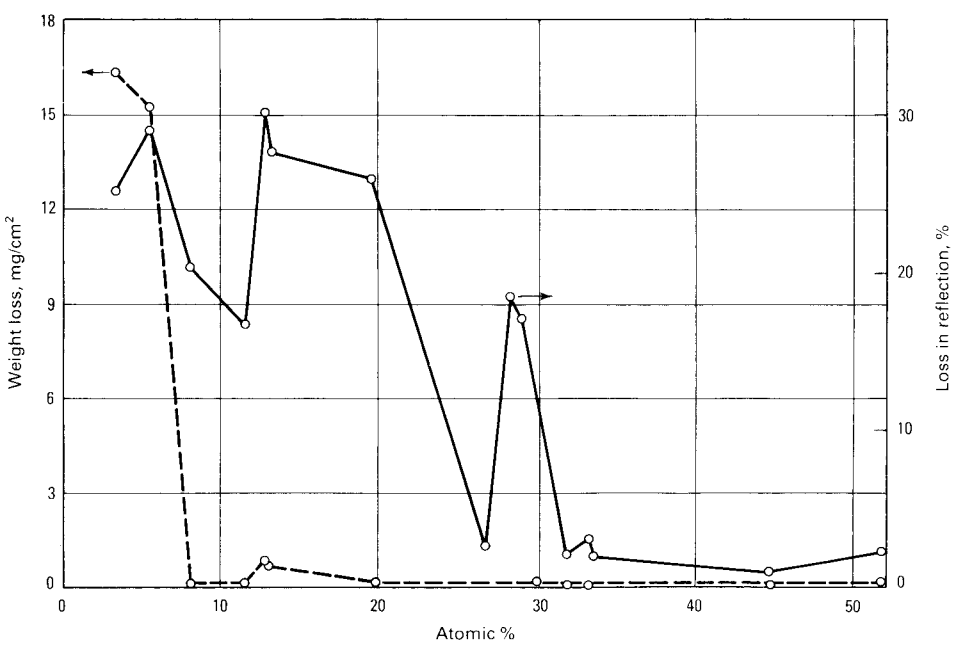

Fig. 31 Effect of nobility (in atomic percent) on tarnish (percent loss in reflection after 3 days in 0.1% Na_2S) and corrosion (weight loss after 7 days in aerated 0.1 *M* lactic acid plus 0.1 *M* NaCl at 37 °C, or 99 °F) of 15 gold alloys. Source: Ref 171

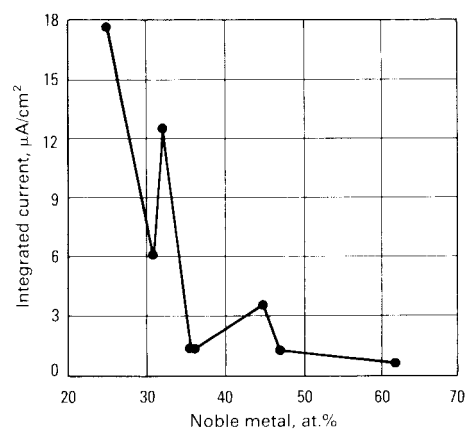

Fig. 32 Integrated anodic currents between −0.3 V vs. saturated calomel electrode (SCE) and+0.3 V (at 0.06 V/min) for eight gold alloys in deaerated 1% NaCl plotted against the atomic nobility. Source: Ref 164

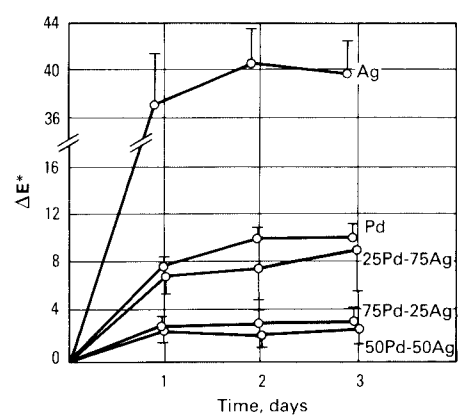

Fig. 33 Color change vector **ΔE*** for pure silver, palladium, and three Ag-Pd binary compositions after exposure to Na_2S solutions. Source: Ref 178

imparting protection. From electrochemical and immersion tests, the resistance of nickel-chromium alloys to pitting attack was found to be good in solutions with Cl^- concentrations equivalent to that found in saliva. Only at higher Cl^- concentrations are pitting and tarnishing likely to occur (Ref 184).

Cobalt-Chromium Alloys. Compared with the nickel-chromium alloys, the cobalt-chromium alloys for partial denture and implant prosthesis exhibit superior tarnish and corrosion resistance. Figure 34 shows the polarization curve for the cast cobalt-chromium-molybdenum alloy shown in Fig. 25(a). The alloy was tested at a scan rate of approximately 1.5 mV/s (1.8 V/h) in aerated physiologic phosphate buffered saline (PBS) that was heated and held at a temperature of 37 ± 1 °C (99 ± 2 °F) with a pH of 7.4 ± 0.2 (Ref 142, 185). From this curve, the breakdown potential (E_b), protection potential (E_p), zero current potential (E_{zcp}), and passive current density (J_p) can be determined. Table 7 lists the mean values of these parameters for the five different types of cobalt-chromium-molybdenum alloys shown in Fig. 25. A one-way analysis of variance test revealed no statistical differences between the groups for any of the parameters listed in Table 7 at the p (probability of occurence) <0.05 level.

In Fig. 34, the potential at which the up and down scans intersect is the protection potential, E_p. Below this potential, existing pits will not grow (Ref 186). The magnitude of the hysterisis between the up and down scans is $E_b - E_p$, which is considered to be a measure of the degree of pitting (Ref 134, 186, 187). Thus, $E_b - E_p$ is used to characterize the susceptibility of an alloy to pitting or crevice corrosion. Consequently, from Table 7, it can be seen that the different cobalt-chromium-molybdenum alloys did not show a significant difference in their susceptibility to pitting or crevice corrosion.

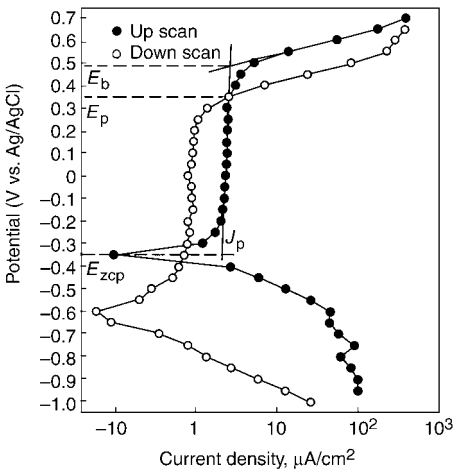

Fig. 34 Polarization curve for cast cobalt-chromium-molybdenum alloy shown in Fig. 25(a). The alloy was tested at a scan rate of about 1.5 mV/s (1.8 V/h) in aerated physiologic phosphate buffered saline (PBS) that was heated and held at a temperature of 37 ± 1 °C (99 ± 2 °F) with a pH of 7.4 ± 0.2. The sample was scanned from −1000 to +700 mV vs. Ag/AgCl and back down to −1000 mV vs. Ag/AgCl. Source: Ref 142

Table 7 also lists the results of impedance spectroscopy tests performed on the five different types of cobalt-chromium-molybdenum alloys shown in Fig. 25 (Ref 142, 185). The test solution and conditions were the same as for the polarization tests described previously. Impedance spectrums were collected every 50 mV, starting at −1000 mV, up to +700 mV, and back down to −1000 mV versus. Ag/AgCl, for a total of 68 impedance spectrums. The average maximum early resistance (R_e) and polarization resistance (R_p) values for each alloy group are displayed in Table 7, along with the average minimum capacitance (C) values (note that analysis of the impedance values indicated that the R_p values were controlled by the rate of the corrosion process, as opposed to being controlled by charge transfer resistance, and the R_e values were a combination of the solution resistance and the oxide film resistance). One-way analysis of variance tests were performed on the impedance values in Table 7 and the results did not indicate any significant differences between the alloy groups for any of the parameters at the $p<0.05$ level. Thus, the similar passive electrochemical behavior of the five different cobalt-chromium-molybdenum alloy groups, as shown by the results of the impedance and polarization tests in Table 7, suggests that the oxide films covering them were not significantly altered by changes in carbon content and processing.

However, studies have shown that carbide content and grain size are both factors that may affect the corrosion resistance of cobalt-chromium-molybdenum alloys. For instance, Placko *et al.* investigated cobalt-chromium-molybdenum alloy porous coatings with four different microstructures (Ref 188). They observed that, for accelerated anodic corrosion experiments, an increase in carbide content correlated with an increase in severity of the preferential attack of the areas surrounding carbides, which was most likely attributable to the phenomenon of sensitization (a depletion of the chromium in the material matrix surrounding carbides). Furthermore, it was also noted that as grain size decreased for the microstructures, localized attack of the grain boundaries increased.

On the other hand, research by Devine and Wulff found that the crevice corrosion resistance for cast cobalt-chromium-molybdenum alloy was not as great as for the wrought material (Ref 189). They ascribed this finding to the greater chemical homogeneity of the wrought cobalt-chromium-molybdenum alloy, as determined by electron microprobe measurements. Also, optical micrographs comparing the cast with the wrought material showed the wrought material to possess a finer grain size and a more uniform and finer distribution of carbides.

In spite of the excellent corrosion resistance of cobalt-chromium alloys, allergic reactions to cobalt, chromium, and nickel contained in appliances made from these alloys are known to have occurred (see the section "Allergic Hypersensitive Reactions" in this article).

Titanium Alloys. The anodic polarization for pure titanium and its alloys indicates passivities over at least several volts in overvoltage (Ref 77, 190). This demonstrates the tenacity and protectiveness of the titanium oxide films formed on these materials.

With regard to the casting titanium alloys for crown and bridgework and partial dentures, good corrosion resistance is still preserved (Ref 191). However, a point of concern is the higher percentages of alloying elements in the titanium casting alloys, with the potential for elucidating diminished chemical stabilities.

Wrought Orthodontic Wires. A comparison of their anodic polarization curves (Fig. 35) shows that both β-titanium and cobalt-chromium-nickel (Elgiloy) exhibit resistance to corrosion in artificial saliva, within the

Table 7 Polarization and impedance data for five different cobalt-chromium-molybdenum alloys shown in Fig. 25 and described in the section "Cost, wrought, and Forged Cobalt-Chromium Alloys"

	Alloy				
Property	Cast	WHC	WHCA	FHC	FLC
Polarization data(a)(b)					
E_b, mV	497 (2.9)	505 (8.7)	502 (7.6)	497 (6.4)	507 (6.4)
E_p, mV	354 (10.8)	356 (12.8)	359 (16.2)	355 (10.8)	346 (18.3)
E_b-E_p, mV	143 (9.0)	149 (5.3)	142 (22.5)	142 (13.8)	161 (21.8)
E_{zcp}, mV	−366 (29.3)	−341 (12–5)	−313 (32.7)	−357 (80.4)	−400 (51.5)
J_p, μA/cm^2	2.03 (0.45)	2.13 (0.31)	1.80 (0.10)	2.40 (0.40)	2.07 (0.58)
Impedance data(a)					
Minimum C, μF/cm^2	6.63 (2.50)	3.64 (0.33)	4.15 (1.83)	4.75 (1.71)	2.45 (0.35)
Maximum R_e, Ω · cm^2	231 (21)	273 (39)	243 (31)	272 (30)	324 (55)
Maximum R_p, kΩ · cm^2	6.47 (0.89)	7.24 (0.82)	7.59 (0.94)	7.99 (0.38)	8.27 (0.38)

(a) The data are the mean for $N = 3$ number of samples with the standard deviation in parenthesis. (b) The potentials, E, are relative to the Ag/AgCl reference electrode. Key to abbreviations: WHC, wrought high carbon; WHCA, wrought high carbon+ aged; FHC, forged high carbon; FLC, forged high carbon; E_b, breakdown potential; E_p, protection potential; E_{zcp}, zero current potential; J_p, passive current density; C, capacitance; R_e, early resistance; R_p, polarization resistance. Source: Ref 142

potential ranges employed (+0.8 V vs. SCE) in the study. With the nickel-titanium and stainless steel wires, breakdown occurred at +0.2 and 0.05 V versus SCE, respectively. The nickel-titanium and stainless steel wires also exhibited current increases upon potential reversals at + 0.8 V versus SCE, an indication of their susceptibility to pitting corrosion. Breakdown potentials differed by as much as 0.6 V between different brands of stainless steel wires. Variations in the polarization characteristics of stainless steel have been related to microstructure (Ref 77) and to surface preparation and finish (Ref 78). It has been shown that the resistance to pitting is decreased with increasing cold deformation for stainless steel in a NaCl solution; the pitting potential decreased by over 300 mV as the degree of cold deformation increased from 0 to 50% (Ref 193). Microstructurally, nickel-titanium wires have been observed to suffer pitting attack and selective dissolution of nickel after polarization tests (Ref 193). Furthermore, it has been shown that the dissolution of nickel can take place at sites of surface damage on nickel-titanium wires, which can be a concern to nickel-sensitive patients (Ref 154).

Silver and Gold Solders. A corroded stainless steel-silver soldered joint is shown in Fig. 36. Microstructurally, silver solders are composed of two phases: silver- and copper-zinc rich segregations (Ref 194). The copper-zinc regions are the least resistant to corrosion. These solders corrode by microgalvanic coupling, either by cells set up between the two microstructural phases, or between the solder and the parts they join. Figure 37 shows the copper-zinc phase of a silver solder attacked by corrosion.

Figure 38 shows the polarization curves for both silver and gold (450 fine) solders in 0.16 *M* NaCl. The silver solder demonstrates active behavior. Zinc, tin, copper, and even silver products can be precipitated or become dissolved in solution. The polarization curve for gold solder indicates activity by the sharp current density peak at + 0.25 V versus SCE. Because the solder contains silver, copper, and zinc, in addition to gold, this peak is probably due to the corrosion of one of these elements. Figure 39 shows the gold solder after the polarization test. Corrosion has delineated the basic microstructure of the solder alloy. Chlorine was detected with the white appearing phase.

Silver-Indium Alloys. These alloys rely on the unusual properties of indium oxide for providing tarnish and corrosion control. Small amounts of noble metals, such as palladium, may also be added in an attempt to improve corrosion resistance. Anodic polarization of a silver-indium alloy in artificial saliva indicated only a very narrow potential range of about 0.1 V of reduced current densities. The tarnish resistance of these alloys appears to be acceptable, but the long-term corrosion resistance has yet to be established (Ref 195).

Copper-Aluminum Alloys. A comparison of the released copper in human saliva from a dental copper-aluminum alloy to that from a high-copper amalgam is shown in Fig. 40. The amalgam released more copper over a 45 day interval. No aluminum, iron, manganese, or nickel was detected. Figures 41(a) to (c) show micrographs from an in vivo restoration of various magnifications. Large amounts of organic matter were adsorbed onto the surface, as well as light powdery corrosion products composed of copper oxides.

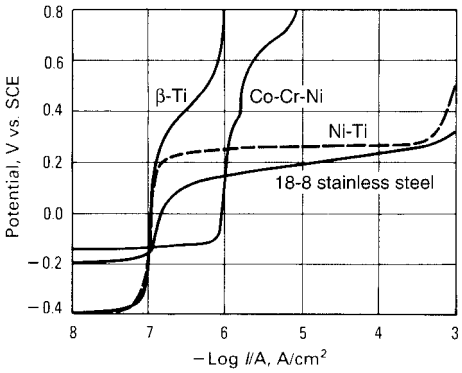

Fig. 35 Anodic polarization at 0.03 V/min of four orthodontic wires in artificial saliva. Source: Ref 192

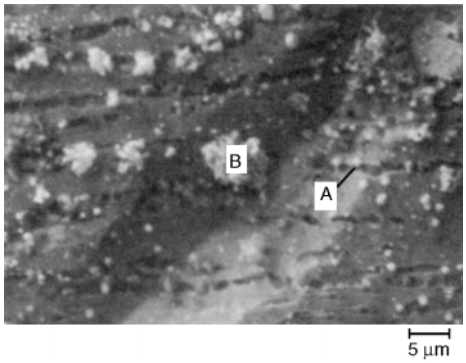

Fig. 37 SEM micrograph of a corroded silver solder in 1% NaCl (held at −0.05 V vs. SCE) showing the destruction of the copper-zinc-rich phase (A) and the accumulation of products (B) that contain copper, zinc, and chlorine. Source: Ref 194

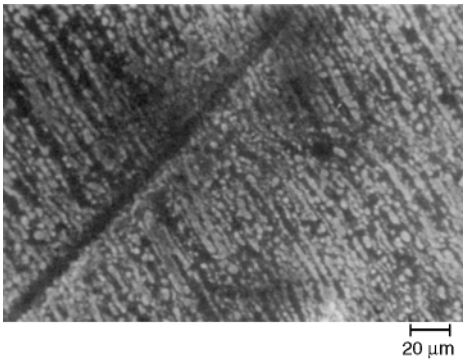

Fig. 39 SEM micrograph of a corroded (polarized to+ 0.5 V vs. SCE) gold solder (450 solder) in 1% NaCl. The light areas contain chlorine. Source: Ref 194

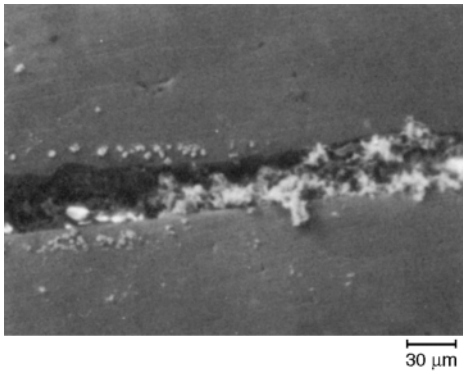

Fig. 36 SEM micrograph of a corroded stainless steel-silver soldered joint after immersion in a 1% H_2O_2 solution. Source: Ref 194

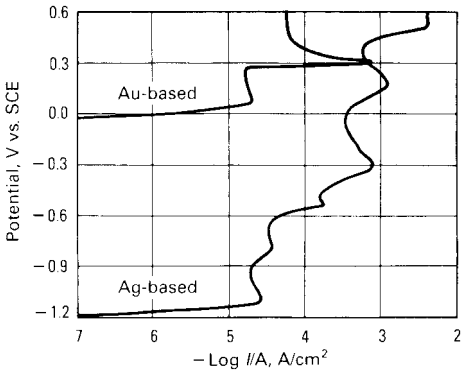

Fig. 38 Anodic polarization at 0.03 V/min of silver and gold (450 fine) solders in 1% NaCl solution. Source: Ref 194

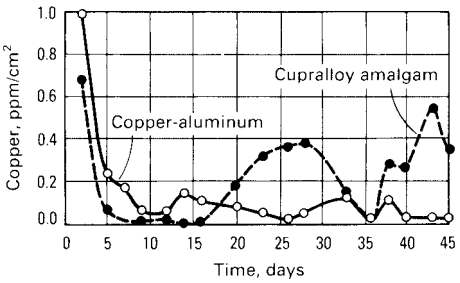

Fig. 40 Released copper into human saliva from a copper-aluminum crown and bridge alloy (MS) and a high-copper amalgam (Cupralloy) plotted against time for up to 45 days. Source: Ref 75

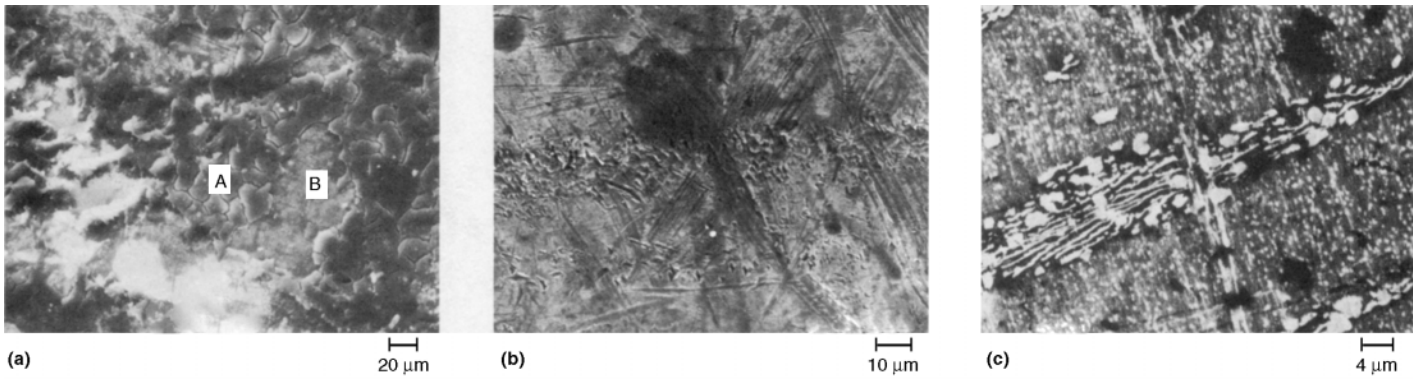

Fig. 41 SEM micrographs of the copper-aluminum restoration shown in Fig. 18 at higher magnifications. In (a), both accumulated plaque (A) and corrosion products (B) occur. (b) Higher-magnification view of the areas identified by (B) contain copper. The light-appearing areas are probably copper oxides. (c) Still higher magnification of the products shown in (b). Here the copper oxides are deposited over the dark copper-rich microstructural phase. Source: Ref 75

ACKNOWLEDGMENT

This article was adapted from Herbert J. Mueller, Tarnish and Corrosion of Dental Alloys, *Corrosion,* Vol 13, *ASM Handbook,* 1987, pages 1336–1366.

REFERENCES

1. *Dental Technician, Prosthetic,* Navpers 10685 c, U.S. Naval Dental School, Bureau of Naval Personnel, 1965, p 256
2. G. Ravasini, Clinical Procedures for Partial Crowns, Inlays, Onlays, and Pontics, *An Atlas,* Quintessence Publishing, Hanover Park, IL 1985, p 136
3. K.L. Stewart, K.D. Rudd, and W.A. Kuebker, *Clinical Removable Partial Dentures,* C.V. Mosby, 1983, p 31, 230, 494
4. T.M. Graber and B.F. Swain, *Orthodontics: Current Principles and Techniques,* C.V. Mosby, 1985, p 385
5. D.C. Smith and D.F. Williams, *Biocompatibility of Dental Materials,* Vol 1–4, CRC Press, 1982
6. *Workshop on Biocompatibility of Metals in Dentistry, Conf. Proc.,* American Dental Association, 1984
7. *An International Workshop: Biocompatibility, Toxicity and Hypersensitivity to Alloy Systems Used in Dentistry, Proc.,* The University of Michigan School of Dentistry, 1985
8. D.C. Smith, The Biocompatibility of Dental Materials, *Biocompatibility of Dental Materials,* Vol I, D.C. Smith and D.F. Williams, Ed., CRC Press, 1982, p 11
9. D.C. Smith, Tissue Reaction to Noble and Base Metal Alloys, *Biocompatibility of Dental Materials,* Vol IV, D.C. Smith and D.F. Williams, Ed., CRC Press, 1982, p 55
10. A. Halse, Metal in Dentinal Tubles beneath Amalgam Fillings in Human Teeth, *Arch. Oral Biol.,* Vol 20, 1975, p 87–88
11. K. Arvidson and R. Wroblewski, Migration of Metallic Ions from Screwposts into Dentin and Surrounding Tissues, *Scand. J. Dent. Res.,* Vol 86, 1978, p 200–203
12. W. Schriever and L.E. Diamond, Electromotive Forces and Electric Currents Caused by Metallic Dental Fillings, *J. Dent. Res.,* Vol 31, 1952, p 205–229
13. I. Kleinberg, Etiology of Dental Caries, *J. Can. Dent. Assn.,* Vol 12, 1979, p 661–668
14. I.D. Mandel, Dental Caries, *Am. Sci.,* Vol 67, 1979, p 680–688
15. M.E. Jensen, Telemetric Methods Using Ion-specific Electrodes, *Adv. Dent. Res.,* Vol. 1, 1987, p 92–98
16. E. Hals and A. Halse, Electron Probe Microanalysis of Secondary Carious Lesions Associated with Silver Amalgam Fillings, *Acta Odontol. Scand.,* Vol 33, 1975, p 149–160
17. N. Kurosahi and T. Fusayama, Penetration of Elements from Amalgam into Dentin, *J. Dent. Res.,* Vol 52, 1973, p 309–317
18. L.W.J. van der Linden and J. van Aken, The Origin of Localized Increased Radiopacity in the Dentin, *Oral Surg.,* Vol 35, 1973, p 862–871
19. B.L. Dahl, Hypersensitivity to Dental Materials, *Biocompatibility of Dental Materials,* Vol I, D.C. Smith and D.F. Williams, Ed., CRC Press, 1982, p 177–185
20. E.W. Mitchell, Summary and Recommendations to the Workshop, *Workshop on Biocompatibility of Metals in Dentistry, Conf. Proc.,* American Dental Association, 1984
21. J. Vilaplana, C. Romaguera, and F. Grimalt, Occupational and Non-Occupational Allergic Contact Dermatitis from Beryllium, *Contact Dermatitis,* Vol 26 (No. 5), 1992, p 295–298
22. A.L. Haberman, M. Pratt, and F.J. Storrs, Contact Dermatitis from Beryllium in Dental Alloys, *Contact Dermatitis,* Vol 23 (No. 3), 1993, p 157–162
23. Preventing Adverse Health Effects from Exposure to Beryllium in Dental Laboratories OSHA Hazard Information Bulletin, HIB 02-04-19 (rev. 5-14-02), Available at www.osha.gov/dts/hib/hib_data/hib20020419.pdf. U.S. Department of Labor, Occupational Safety and Health Administration, Washington, DC, 2002
24. Proper Use of Beryllium-Containing Alloys *JADA,* Vol 134, April 2003, p 476–478
25. "Resolution 6 on Beryllium in Dental Alloys," Brussels, Belgium, CEN/TC 055 Dentistry, Feb 26, 2002
26. M. Bergan and O. Ginstrup, Dissolution Rate of Cadmium from Dental Gold Solder Alloys, *Acta Odontol Scand.,* Vol 33, 1975, p 199–210
27. D.R. Zielke, J.M. Brady, and C.E. del Rio, Corrosion of Silver Cones in Bone: A Scanning Electron Microscope and Microprobe Analysis, *J. Endo.,* Vol 1, 1975, p 356–360
28. R.A. James, Host Response to Dental Implant Devices, *Biocompatibility of Dental Materials,* Vol IV, D.C. Smith and D.F. Williams, Ed., CRC Press, 1982, p 163–195
29. J.R. Natiella, Local Tissue Reaction/Carcinogenesis, *International Workshop on Bicompatibility, Toxicity, and Hypersensitivity to Alloy Systems Used in Dentistry, Section 6, Conference Proceedings,* University of Michigan School of Dentistry, 1985
30. R.S. Mateer and C.D. Reitz, Corrosion of Amalgam Restorations, *J. Dent. Res.,* Vol 49, 1970, p 399–407
31. M. Berge, N.R. Gjerdet, and E.S. Erichsen, Corrosion of Silver Soldered Orthodontic Wires, *Acta Odontol. Scand.,* Vol 40, 1982, p 75–79
32. B. Angmar-Mansson, K.-A. Omnell, and J. Rud, Root Fractures due to Corrosion, *Odontol. Revy.,* Vol 20, 1969, p 245–256

33. D.C. Mears, Metals in Medicine and Surgery, *Int. Met. Rev.,* Vol 22 (No. 218), 1977, p 119–155
34. P.L. Altman, *Blood and Other Body Fluids, Analysis and Compilation,* Washington, DC, Federation of American Societies for Experimental Biology, 1961
35. J.R. Cahoon and L.D. Hill, Evaluation of a Precipitation Hardened Wrought Cobalt-Nickel-Chromium-Titanium Alloy for Surgical Implants, *J. Biomed. Mater. Res.,* Vol 12, 1978, p 805–821
36. T.C. Ruck and J.F. Fulton, *Medical Physiology and Biophysics,* 18th ed., W.B. Saunders, 1960
37. C. Dawes, The Effects of Flow Rate and Duration of Stimulation of the Concentrations of Protein and the Main Electrolytes in Human Parotid Saliva, *Arch. Oral Biol.,* Vol 14, 1969, p 277–294
38. C.M. Carey, M. Spencer, R.J. Gove, and F.C. Eichmiller, Fluoride Release from a Resin-Modified Glass-Ionomer Cement in a Continuous-Flow System: Effect of pH, *J. Dent. Res.,* Vol 82, 2003, p 829–832
39. H.C. McCann, Inorganic Components of Salivary Secretions, *Art and Science of Dental Caries Research,* R.S. Harris, Ed., Academic Press, 1968, p 55–73
40. H.J. Mueller, Binding of Corroded Ions to Human Saliva, *Biomaterials,* Vol 6, 1985, p 146–149
41. H.J. Mueller, Characterization of the Acquired Biofilms on Materials Exposed to Human Saliva, *Proteins at Interfaces,* T.A. Horbett and J. Brash, Ed., *Advances in Chemistry Series,* American Chemical Society, 1987
42. S.A. Ellison, The Identification of Salivary Components, Saliva and Dental Caries, I. Kleinberg, S.A. Ellison, and I.D. Mandell, Ed., *Sp. Supp. Microbiol,* Abst., 1979, p 13–29
43. C.E. Ingersoll, Characterization of Tarnish, *J. Dent. Res.,* Vol 55, 1976, IADR No. 144
44. K. Barton, Chapter 2, in *Protection against Atmospheric Corrosion,* John Wiley & Sons, 1973
45. I.C. Schoonover and W. Souder, Corrosion of Dental Alloys, *J. Am. Dent. Assoc.,* Vol 28, 1941, p 1278–1291
46. J.C. Muhler and H.M. Swenson, Preparation of Synthetic Saliva from Direct Analysis of Human Saliva, *J. Dent. Res.,* Vol 26, 1947, p 474
47. D.A. Carter, T.K. Ross, and D.C. Smith, Some Corrosion Studies on Silver-Tin Amalgams, *Br. Corros. J.,* Vol 2, 1967, p 199–205
48. G. Tani and F. Zucci, Electrochemical Evaluation of the Corrosion Resistance of the Commonly Used Metals in Dental Prosthesis, *Minerva. Stomat.,* Vol 16, 1967, p 710–713
49. J.M. Meyer and J.N. Nally, Influence of Artificial Salivas on the Corrosion of Dental Alloys, *J. Dent. Res.,* Vol 54, 1975, IADR No. 76
50. B.W. Darvell, The Development of an Artificial Saliva for In-Vitro Amalgam Corrosion Studies, *J. Oral Rehab.,* Vol 5, 1978, p 41–49
51. M.L. Swartz, R.W. Phillips, and M.D. El Tannir, Tarnish of Certain Dental Alloys, *J. Dent. Res.,* Vol 37, 1958, p 837–847
52. F. Fusayama, T. Katayori, and S. Nomoto, Corrosion of Gold and Amalgam Placed in Contact with Each Other, *J. Dent. Res.,* Vol 42, 1963, p 1183–1197
53. C.E. Guthrow, L.B. Johnson, and K.R. Lawless, Corrosion of Dental Amalgam and Its Component Phases, *J. Dent. Res.,* Vol 46, 1967, p 1372–1381
54. F.V. Wald and F.H. Cocks, Investigation of Copper-Manganesse-Nickel Alloys for Dental Purposes, *J. Dent. Res.,* Vol 50, 1971, p 44–59
55. M. Marek and R.F. Hockman, Corrosion Behavior of Amalgam Electrode in Artificial Saliva, *J. Dent. Res.,* Vol 51, 1972, IADR No. 63
56. J. Brugirard, R. Bargain, J.C. Dupuy, H. Mazille, and G. Monnier, Study of the Electrochemical Behavior of Gold Dental Alloys, *J. Dent. Res.,* Vol 52, 1973, p 828–836
57. M. Marek and E. Topfl, Electrolytes for Corrosion Testing of Dental Alloys, *J. Dent. Res.,* Vol 65, 1986, IADR No. 1192
58. N.K. Sarkar and E.H. Greener, In Vitro Corrosion of Dental Amalgam, *J. Dent. Res.,* Vol 50, 1971, IADR No.13
59. G.F. Finkelstein and E.H. Greener, In Vitro Polarization of Dental Amalgam in Human Saliva, *J. Oral. Rehab.,* Vol 4, p 355–368
60. G.F. Finkelstein and E.H. Greener, Role of Mucin and Albumin in Saline Polarization of Dental Amalgam, *J. Oral Rehab.,* Vol 5, 1978, p 95–110
61. H. Do Duc, P. Tissot, and J.-M. Meyer, Potential Sweep and Intensiostatic Pulse Studies of Sn, Sn_8Hg, and Dental Amalgam in Chloride Solution, *J. Oral Rehab.,* Vol 6, 1979, p 189–197
62. R.I. Holland, Effect of Pellicle on Galvanic Corrosion of Amalgam, Scand. *J. Dent. Res.,* Vol 92, 1984, p 93–96
63. H.J. Mueller, The Effects of a Human Salivary Dialysate upon Ionic Release and Electrochemical Corrosion of a Cu-Al Alloy, *J. Electrochem. Soc.,* Vol 134, 187, p 555–580
64. A. Schulman, H.A.B. Linke, and T.K. Vaidyanathan, Tarnish of Dental Alloys by Oral Microorganisms, *J. Dent. Res.,* Vol 63, 1984, IADR No. 55
65. M. Stern and E.D. Weisert, Experimental Observation on the Relation between Polarization Resistance and Corrosion Rate, *Proc. ASTM,* Vol 59, 1959, p 1280–1291
66. M. Marek, The Corrosion of Dental Materials, *Corrosion: Aqueous Processes and Passive Films,* Vol 23, *Treatise on Materials Science,* J.C. Scully, Ed., Academic Press, 1983, p 331–394
67. M. Bergman, O. Ginstrup, and B. Nilsson, Potentials of and Currents between Dental Metallic Restorations, *Scand. J. Dent. Res.,* Vol 90, 1982, p 404–408
68. K. Nilner, P.-O. Glantz, B. Zoger, On Intraoral Potential and Polarization Measurements of Metallic Restorations, *Acta Odontol Scand.,* Vol 40, 1982, p 275–281
69. J.M. Mumford, Electrolytic Action in the Mouth and Its Relationship to Pain, *J. Dent. Res.,* Vol 36, 1957, p 632–640
70. C.P. Wang Chen and E.H. Greener, A Galvanic Study of Different Amalgams, *J. Oral Rehab.,* Vol 4, 1977, p 23–27
71. R. Soremark, G. Freedman, J. Goldin, and L. Gettleman, Structure and Microdistribution of Gold Alloys, *J. Dent. Res.,* Vol 45, 1966, p 1723–1735
72. D.B. Boyer, K. Chan, and C.W. Svare, The Effect of Finishing on the Anodic Polarization of High-Copper Amalgams, *J. Oral Rehab.,* Vol 5, 1978, p 223–228
73. G. Palaghias, Oral Corrosion Inhibition Processes, *Swed. Dent. J.,* Supp 30, 1985
74. H.J. Mueller and A. Edahl, The Effect of Exposure Conditions upon the Release of Soluble Copper and Tin from Dental Amalgams, *Biomaterials,* Vol 5, 1984, p 194–200
75. H.J. Mueller and R.M. Barrie, Intraoral Corrosion of Copper-Aluminum Alloys, *J. Dent. Res.,* Vol 64, 1985, IADR No. 1753
76. G.N. Jenkins, *The Physiology and Biochemistry of the Mouth,* 4th ed., Blackwell, 1978, p 284–359
77. H.J. Mueller and E.H. Greener, Polarization Resistance of Surgical Materials in Ringer's Solution, *J. Biomed. Mater. Res.,* Vol 4, 1970, p 29–41
78. E.J. Sutow, S.R. Pollack, and E. Korostoff, An In Vitro Investigation of the Anodic Polarization and Capacitance Behavior of 316-L Stainless Steel, *J. Biomed. Mater. Res.,* Vol 10, 1976, p 671–693
79. H.J. Mueller, The Binding of Corroded Metallic Ions to Salivary-Type Proteins, *Biomaterials,* Vol 4, 1983, p 66–72
80. J.R. Strub, C. Eyer, and N.K. Sarkar, Microstructure and Corrosion of a Low-Gold Casting Alloy, *J. Dent. Res.,* Vol 63, 1984, IADR No. 793
81. C.W. Svare, G. Belton, and E. Korostoff, The Role of Organics in Metallic Passivation, *J. Biomed. Mater. Res.,* Vol 4, 1970, p 457–467
82. G.C.F. Clark and D.F. Williams, The Effects of Proteins on Metallic Passivation, *J. Biomed. Mater. Res.,* Vol 16, 1982, p 125–134
83. S.A. Brown and K. Merritt, Electrochemical Corrosion in Saline and Serum,

J. Biomed. Mater. Res., Vol 14, 1980, p 173–175

84. H.J. Mueller, The Effect of Electrical Signals upon the Adsorption of Plasma Proteins to a High Cu Alloy, *Biomaterials: Interfacial Phenomena and Applications,* S.L. Cooper and N.A. Peppas, Ed., ACS monograph series 199, American Chemical Society, 1982
85. R.C. Salvarezza, M.E.L. de Mele, H.H. Videla, and F.R. Goni, Electrochemical Behavior of Aluminum in Human Plasma, *J. Biomed. Mater. Res.,* Vol 19, 1985, p 1073–1084
86. H. Hero and L. Niemi, Tarnishing In Vivo of Ag-Pd-Cu-Zn, *J. Dent. Res.,* Vol 65, 1986, p 1303–1307
87. H. Do Duc and P. Tissot, Rotating Disc and Ring Disc Electrode Studies of Tin in Neutral Phosphate Solution, *Corros. Sci.,* Vol 19, 1979, p 191–197
88. I.D. Mandel, Relation of Saliva and Plaque to Caries, *J. Dent. Res.,* Vol 53, 1974, p 246
89. T. Ericson, K.M. Pruitt, H. Arwin, and I. Lunstrom, Ellipsometric Studies of Film Formation on Tooth Enamel and Hydrophilic Silicon Surfaces, *Acta Odontol. Scand.,* Vol 40, 1982, p 197–201
90. R.E. Baier and P.-O. Glantz, Characterization of Oral In Vivo Films Formed on Different Types of Solid Surfaces, *Acta Odontol. Scand.,* Vol 36, 1978, p 289–301
91. K. Skjorland, Auger Analysis of Integuments Formed on Different Dental Filling Materials In Vivo, *Acta Odontol. Scand.,* Vol 40, 1982, p 129–134
92. C.M. Carey, G.L. Vogel, and L.C. Chow, Permselectivity of Sound and Carious Human Dental Enamel as Measured by Membrane Potential, *J. Dent. Res.,* Vol 70, 1991, p 1479–1485
93. G.L. Vogel, Y. Mao, C.M. Carey, and L.C. Chow, Changes in Permselectivity of Human Teeth during Caries Attack, *J. Dent. Res.,* Vol 76, 1997, p 673–681
94. K. Hannesson Eggen and G. Rolla, Gel Filtration, Ion Exchange Chromatography and Chemical Analysis of Macromolecules Present in Acquired Enamel Pellicle (2-hr), *Scand. J. Dent. Res.,* Vol 90, 1982, p 182–188
95. A. Bennick, G. Chau, R. Goodlin, S. Abrams, D. Tustian, and G. Mandapallimatam, The Role of Human Salivary Acidic Proline-Rich Proteins in the Formation of Acquired Dental Pellicle In Vivo and Their Fate after Adsorption to the Human Enamel Surface, *Arch. Oral Biol.,* Vol 28, 1983, p 19–27
96. T. Sonju and P.-O. Glantz, Chemical Composition of Salivary Integuments Formed In Vitro on Solids with Some Established Surface Characteristics, *Arch. Oral Biol.,* Vol 20, 1975, p 687–691
97. D.I. Hay, The Adsorption of Salivary Proteins by Hydroxyapatite and Enamel, *Arch. Oral Biol.,* Vol 12, 1967, p 937–946
98. G. Rolla, Formation of Dental Integuments—Basic Chemical Considerations, *Swed. Dent. J.,* Vol 1, 1977, p 241–251
99. A.C. Juriaanse, M. Booij, J. Arends, and J.J. Ten Bosch, The Adsorption In Vivo of Purified Salivary Proteins on Bovine Dental Enamel, *Arch. Oral Biol.,* Vol 26, 1981, p 91–96
100. H.J. Mueller, Differential Scanning Calorimetry of Adsorbed Protein Films, *Trans. of the 13th Annual Meeting Society of the Biomaterials,* 1987
101. R.D. Norman, R.V. Mehra, and M.L. Schwartz, The Effects of Restorative Materials on Plaque Composition, *J. Dent. Res.,* Vol 50, 1971, IADR No. 162
102. J.J. Tuccillo and J.P. Nielsen, Microprobe Analysis of an In Vivo Discoloration, *J. Prosthet. Dent.,* Vol 31, 1974, p 285–289
103. J.J. Tuccillo and J.P. Nielsen, Observation of Onset of Sulfide Tarnish on Gold-Base Alloys, *J. Prosthet. Dent.,* Vol 25, 1971, p 629–637
104. R.P. Lubovich, R.E. Kovarik, and D.L. Kinser, A Quantitative and Subjective Characterization of Tarnishing in Low-Gold Alloys, *J. Prosthet. Dent.,* Vol 42, 1979, p 534–538
105. G.W. Marshall, N.K. Sarkar, and E.H. Greener, Detection of Oxygen in Corrosion Products of Dental Amalgam, *J. Dent. Res.,* Vol 54, 1975, p 904
106. H. Otani, W.A. Jesser, and H.G.F. Wilsdorf, The In Vivo and the In Vitro Corrosion Products of Dental Amalgam, *J. Biomed. Mater. Res.,* Vol 7, 1973, p 523–539
107. A.B. Burse, M.L. Swartz, R.W. Phillips, and R.W. Oykema, Comparison of the In Vivo and In Vitro Tarnish of Three Gold Alloys, *J. Biomed. Mater. Res.,* Vol 6, 1972, p 267–277
108. B.R. Laing, S.H. Bernier, Z. Giday, and K. Asgar, Tarnish and Corrosion of Noble Metal Alloys, *J. Prosthet. Dent.,* Vol 48, 1982, p 245–252
109. H. Hero and J. Valderhaug, Tarnishing In Vivo and In Vitro of a Low-Gold Alloy Related to Its Structure, *J. Dent. Res.,* Vol 64, 1985, p 139–143
110. H. Hero and R.B. Jorgensen, Tarnishing of a Low-Gold Alloy in Different Structural States, *J. Dent. Res.,* Vol 62, p 371–376
111. American National Standards Institute/American Dental Association "Specification No. 1 Alloy for Dental Amalgam," American Dental Association, Chicago, IL, 2003
112. D.B. Mahler and J.D. Adey, Microprobe Analysis of Three High Copper Amalgams, *J. Dent. Res.,* Vol 63, 1984, p 921–925
113. J.W. Edie, D.B. Boyer, and K.C. Chjan, Estimation of the Phase Distribution in Dental Amalgams with Electron Microprobe, *J. Dent. Res.,* Vol 57, 1978, p 277–282
114. J. Leitao, Surface Roughness and Porosity of Dental Amalgam, *Acta Odontol. Scand.,* Vol 40, 1982, p 9–16
115. R.W. Bryant, Gamma-2 Phase in Conventional Amalgam-Discrete Clumps or Continuous Network—A Review, *Aust. Dent. J.,* Vol 29, 1984, p 163–167
116. L.B. Johnson, X-Ray Diffraction Evidence for the Presence of β(Ag-Hg) in Dental Amalgam, *J. Biomed. Mater. Res.,* Vol 1, 1967, p 285–297
117. S.J. Marshall and G.W. Marshall, Jr., Time-Dependent Phase Changes in Cu-Rich Amalgams, *J. Biomed. Mater. Res.,* Vol 13, 1979, p 395–406
118. R. W. Phillips, *Skinner's Science of Dental Materials,* W.B. Saunders Company, 1982
119. "American Dental Association Specification No. 5 for Dental Casting Gold Alloy," American Dental Association, Chicago, IL
120. R.G. Craig, *Restorative Dental Materials,* Mosby *Inc.,* 1997
121. American National Standards Institute/American Dental Association "Specification No. 5 Dental Casting Alloys," American Dental Association Council on Scientific Affairs, Chicago, IL, 1989
122. American National Standards Institute/American Dental Association "Specification No. 5 Dental Casting Alloys," American Dental Association Council on Scientific Affairs, Chicago, IL, 1998
123. Classification System for Cast Alloys, *American Dental Assoc.,* Vol 109, Nov 1984, p766
124. R.M. German, Precious-Metal Dental Casting Alloys, *Int. Met. Rev.,* Vol 27, 1982, p 260–288
125. K. Yasuda and K. Hisatsune, The Development of Dental Alloys Conserving Precious Metals: Improving Corrosion Resistance by Controlled Aging, *Int. Dent. J.,* Vol 33, 1983
126. H. Hero, Tarnishing and Structures of Some Annealed Dental Low-Gold Alloys, *J. Dent. Res.,* Vol 63, 1984, p 926–931
127. R.G. Craig (Chm), Section One Report, in *International Workshop on Biocompatibility, Toxicity, and Hypersensitivity to Alloy Systems Used in Dentistry, Conf. Proc.,* University of Michigan School of Dentistry, 1985
128. D. Scharnweber, Degradation (In Vitro-In Vivo Corrosion) *Metals as Biomaterials*. J.A. Helsen and H.J. Breme, Ed., John Wiley & Sons, 1998, p 101–152
129. "Standard Specification for Cobalt-28 Chromium-6 Molybdenum Alloy Castings and Casting Alloy for Surgical Implants (UNS R30075)," F 75, *Annual Book of ASTM Standards,* ASTM International, Vol 13.01, 2001
130. K. Asgar and F.C. Allan, Microstructure and Physical Properties of Alloys of Partial Denture Castings, *J. Dent. Res.,* Vol 47, 1968, p 189–197

131. P. Kovacs, *In Vitro Studies on the Electrochemical Behavior of Pure Metals Used in Orthopaedic Implant Alloys, Extended Abstracts of the Electrochemical Society Meeting* (Phoenix, AZ), The Electrochemical Society, Oct 13–17, 1991
132. S. Storp and R. Holm, ESCA Investigation of the Oxide Layers on Some Cr Containing Alloys, *Surf. Sci.,* Vol 68, 1977, p 10–19
133. J. Ohnsorge and R. Holm, Surface Investigations of Oxide Layers on Cobalt-Chromium Alloyed Orthopedic Implants Using ESCA Technique, *Med. Progr. Technol.,* 5, 1978, p 171–177
134. J.J. Jacobs, R.M. Latanison, et al., The Effect of Porous Coating Processing on the Corrosion Behavior of Cast Co-Cr-Mo Surgical Implant Alloys, *Orthopaedic Res.,* Vol 8, p 874–882
135. J. Hubrecht, Electrochemical Impedance Spectroscopy as a Surface Analytical Technique for Biomaterials, *Metals as Biomaterials*, J.A. Helsen and H.J. Breme, Ed., Chichester, England, John Wiley & Sons, Ltd., 1998
136. O. Kubaschewski and B.E. Hopkins, *Oxidation of Metals and Alloys*, London, Butterworth and Co., 1962
137. M. Fontana and N. Greene, *Corrosion Engineering,* McGraw-Hill, 1967
138. P. Kofstad, *Nonstoichiometry, Diffusion, and Electrical Conductivity in Binary Metal Oxides,* John Wiley & Sons, Inc., 1972
139. Jones, D.A. *Principles and Prevention of Corrosion,* Macmillan Publishing Company, New York, 1992
140. M. Metikos-Hukovic and M. Ceraj-Ceric, p-Type and n-Type Behavior of Chromium Oxide as a Function of the Applied Potential, *J. Electrochem. Soc.,* Vol 134 (No. 9), Sept 1987, p 2193–2197
141. S.J. Megremis and J.L. Gilbert, *In-Situ Electrochemical Atomic Force Microscopy of a Cast Co-Cr-Mo Alloy with Simultaneous Impedance Analysis, Transactions of the Society for Biomaterials,* Saint Paul, MN, April 2001
142. S.J. Megremis, The Mechanical, Electrochemical, and Morphological Characteristics of Passivating Oxide Films Covering Co-Cr-Mo Alloys: A Study of Five Microstructures, *Biomedical Engineering,* Northwestern University, Evanston, IL, Dec 2001
143. R.A. Poggie, "A Review of the Effects of Design, Contact Stress, and Materials on the Wear of Metal-on-Metal Hip Prostheses," *Alternative Bearing Surfaces in Total Joint Replacements,* J. Jacobs and T.L. Craig, Ed., ASTM STP 1346, 1998, p 47–54
144. K. Asgar and F.A. Peyton, Effect of Microstructure on the Physical Properties of Cobalt-Base Alloys, *J. Dent. Res.,* Vol 40, 1961, p 63–72
145. J.B. Park and R.S. Lakes, *Biomaterials: An Introduction,* Plenum Press, 1992
146. M. Taira, J.B. Moser, and E.H. Greener, Mechanical Properties of Cast Ti Alloys for Dental Uses, *J. Dent. Res.,* Vol 65, 1986, IADR No. 603
147. J.F. Bates and A.G. Knapton, Metal and Alloys in Dentistry, *Int. Met. Rev.,* Vol 22 (No. 215), 1977, p 39–60
148. R.L. Bertolotti, Selection of Alloys for Today's Crown and Fixed Partial Denture Restorations, *J. Am. Dent. Assoc.,* Vol 108, 1984, p 959–966
149. J.J. Tuccillo, Compositional and Functional Characteristics of Precious Metal Alloys for Dental Restorations, *Alternatives to Gold Alloys in Dentistry,* Con. Proc., T.M. Valega, Ed., DHEW Publication (NIH) 77-1227, Department of Health, Education, and Welfare, 1977
150. M.M.A. Vrijhoef, Oxidation of Two High-Palladium PFM Alloys, *Dent. Mater.,* Vol 1, 1985, p 214–218
151. J.R. Mackert, Jr., E.E. Parry, and C.W. Fairhurst, Oxide Metal Interface Morphology Related to Oxide Adherence, *J. Dent. Res.,* Vol 63, 1984, IADR No. 405
152. American National Standards Institute/American Dental Association "Specification No. 32 for Orthodontic Wires," American Dental Association, Chicago, IL, 2000
153. M.R. Marcotte, Optimum Time and Temperature for Stress Relief Heat Treatment of Stainless Steel Wire, *J. Dent. Res.,* Vol 52, 1973, p 1171–1175
154. W.J. O'Brien, *Dental Materials and Their Selection,* Quintessence Publishing Co., Inc., Hanover, IL, 2002
155. A.J. Goldberg and C.J. Burstone, an Evaluation of Beta-Stabilized Titanium Alloys for Use in Orthodontic Appliances, *J. Dent. Res.,* Vol 57, 1978, p 593–600
156. C.E. Janus, D.F. Taylor, and G.A. Holland, A Microstructural Study of Soldered Connectors of Low-Gold Casting Alloys, *J. Prosthet. Dent.,* Vol 50, 1983, p 657–663
157. "Standard Specification for Wrought Cobalt-28Chromium-6Molybdenum Alloys for Surgical Implants (UNS R31537, UNS R31538, UNS R31539)," F 1537, *Annual Book of ASTM Standards,* ASTM International, Vol 13.01, 2000
158. "Standard Specification for Cobalt-28 Chromium-6 Molybdenum Alloy Forgings for Surgical Implants (UNS R31537, R31538, R31539)," F 799, *Annual Book of ASTM Standards,* ASTM International, Vol 13.01, 2002
159. K.C. Ludema, R.M. Caddell, et al., *Manufacturing Engineering: Economics and Processes,* Prentice-Hall, 1987
160. H.S. Dobbs and J.L.M. Robertson, Heat Treatment of Cast Co-Cr-Mo for Orthopaedic Implant Use, *J. Mater. Sci.,* Vol 18, 1983, p 391–401
161. L. Gettleman, C. Amman, and N.K. Sarkar, Quantitative In Vivo and In Vitro Measurement of Tarnish, *J. Dent. Res.,* Vol 58, 1979, IADR No. 969
162. R.M. German, M.M. Guzowski, and D.C. Wright, Color and Color Stability as Alloy Design Criterion, *Jom,* Vol 32, 1980, p 20–27
163. D.J.L. Treacy and R.M. German, Chemical Stability of Gold Dental Alloys, *Gold Bull.,* Vol 17, 1984, p 46–54
164. P.P. Coroso, Jr., R.M. German, and H.D. Simmons, Jr., Tarnish Evaluation of Gold-Based Dental Alloys, *J. Dent. Res.,* Vol 64, 1965
165. R.M. German, The Role of Microstructure in the Tarnish of Low Gold Alloys, *Metallography,* Vol 14, 1981, p 253–266
166. R.M. German, D.C. Wright, and R.F. Gallant, In Vitro Tarnish Measurements on Fixed Prosthodontic Alloys, *J. Prosthet. Dent.,* Vol 47, 1982, p 399–406
167. D.C. Wright and R.M. German, Quantification of Color and Tarnish Resistance of Dental Alloys, *J. Dent. Res.,* Vol 58A, 1979, IADR No. 975
168. H.J. Mueller, SIMS and Colorimetry of In-Vitro Sulfided Crown and Bridge Alloys, *Fifth International Symposium on New Spectroscopic Methods for Biomedical Research,* Battelle Laboratories and University of Washington, 1986
169. H. Hero, Tarnishing and Structures of Some Annealed Dental Low-Gold Alloys, *J. Dent. Res.,* Vol 63, 1984, p 926–931
170. E. Suoninen and H. Hero, Effect of Palladium on Sulfide Tarnishing of Noble Metal Alloys, *J. Biomed. Mater. Res.,* Vol 19, 1985, p 917–934
171. R. Kropp, Application of Corrosion and Tarnish Tests to Different Dental Alloys, *J. Dent. Res.,* Vol 65, 1986, IADR No. 197
172. J. Brugirard, Baigain, J.C. Dupuy, H. Mazille, and G. Monnier, Study of the Electrochemical Behavior of Gold Dental Alloys, *J. Dent. Res.,* 1973, p 838–836
173. W. Popp, H. Kaiser, H. Kaesche, W. Bramer, and F. Sperner, Electrochemical Behavior of Noble Metal Dental Alloys in Different Artificial Saliva Solutions, *Proc. of the 8th International Congress of Metallic Corrosion,* Vol 1, DECHEMA, 1981, p 76–81
174. N.K. Sarkar, R.A. Fuys, and J.W. Stanford, The Chloride Corrosion Behavior of Silver-Base Casting Alloys, *J. Dent. Res.,* Vol 58, 1979, p 1572–1577
175. D.C. Wright, R.M. German, and R.F. Gallant, Copper and Silver Corrosion Activity in Crown and Bridge Alloys, *J. Dent. Res.,* Vol 60, 1981, p 809–814
176. T.K. Vaidyanathan and A. Prasad, In Vitro Corrosion and Tarnish Analysis of Ag-Pd Binary System, *J. Dent. Res.,* Vol 60, 1981, p 707–715
177. N. Ishizaki, Corrosion Resistance of Ag-Pd Alloy System in Artificial Saliva: An

Electrochemical Study, *J. Osaka Dent. Univ.,* Vol 3, 1969, p 121–133

178. L.A. O'Brien and R.M. German, Compositional Effects on Pd-Ag Dental Alloys, *J. Dent. Res.,* Vol 63, 1984, IADR No. 44
179. N.K. Sarkar, R.A. Fuys, and J.W. Stanford, The Chloride Behavior of Silver-Base Casting Alloys, *J. Dent. Res.,* Vol 58, 1979, p 1572–1577
180. L. Niemi and R.I. Holland, Tarnish and Corrosion of a Commercial Dental Ag-Pd-Cu-Au Casting Alloy, *J. Dent. Res.,* Vol 63, 1984, p 1014–1018
181. L. Niemi and H. Hero, Structure, Corrosion, and Tarnishing of Ag-Pd-Cu Alloys, *J. Dent. Res.,* Vol 64, 1985, p 1163–1169
182. P.R. Mezger, M.M.A. Vrijhoef, and E.H. Greener, Corrosion Resistance of Three High-Palladium Alloys, *Dent. Mater.,* Vol 1, 1985, p 177–180
183. J.M. Meyer, Corrosion Resistance of Ni-Cr Dental Casting Alloys, *Corros. Sci.,* Vol 17, 1977, p 971–982
184. R.J. Hodges, The Corrosion Resistance of Gold and Base Metal Alloys, *Alternatives to Gold Alloys in Dentistry,* T.M. Valega, Ed., DHEW Publication (NIH) 77-1227, Department of Health, Education, and Welfare, 1977
185. S.J. Megremis and J.L. Gilbert, Step-Polarization Impedance Spectroscopy of Five Different Co-Cr-Mo Alloys, *Sixth World Biomaterials Congress Transactions* (Kamuela, HI), Society for Biomaterials, 2000
186. J.R. Cahoon, R. Bandyopadhya, et al., The Concept of Protection Potential Applied to the Corrosion of Metallic Orthopedic Implants, *J. Biomed, Mater. Res.,* Vol 9, 1975, p. 259–264
187. B.C. Syrett and S.S. Wing, Pitting Resistance of New and Conventional Orthopedic Implant Materials: Effect of Metallurgical Condition, *Corrosion,* Vol 34 (No. 4), 1978, p 138–145
188. H.E. Placko, S.A. Brown, et al., Effects of Microstructure on the Corrosion Behavior of CoCr Porous Coatings on Orthopedic Implants, *J. Biomed. Mater. Res.,* Vol 39, 1998, p 292–299
189. T.M. Devine and J. Wulff, Cast vs Wrought Cobalt-Chromium Surgical Implant Alloys, *J. Biomed. Mater. Rest.,* Vol 9, 1975, p 151–167
190. N.K. Sarkar and E.H. Greener, In Vitro Corrosion Resistance of New Dental Alloys, *Biomater. Med. Dev. Art. Org.,* Vol 1, 1973, p 121–129
191. R.M. Waterstrat, N.W. Rupp, and O. Franklin, Production of a Cast Titanium-Base Partial Denture, *J. Dent. Res.,* Vol 57A, 1978, IADR No. 717
192. H.J. Mueller and C.P. Chen, Properties of a Fe-Cr-Mo Wire, *J. Dent.,* Vol 11, 1983, p 121–128
193. N.K. Sarkar, W. Redmond, B. Schwaninger, and A.J. Goldberg, The Chloride Corrosion Behavior of Four Orthodontic Wires, *J. Oral Rehab.,* Vol 10, 1983, p 121–128
194. H.J. Mueller, Silver and Gold Solders—Analysis due to Corrosion, *Quint. Int.,* Vol 37, 1981, p 327–337
195. D.L. Johnson, V.W. Rinne, and L.L. Bleich, Polarization-Corrosion Behavior of Commercial Gold- and Silver-Base Casting Alloys in Fusayama Solution, *J. Dent. Res.,* Vol 62, 1983, p 1221–1225